2011

Synthesis, biological and photophysical studies of novel compounds for cancer therapy

Edith Khavwajira Amuhaya
Louisiana State University and Agricultural and Mechanical College, khavwajira@yahoo.com

SYNTHESIS, BIOLOGICAL AND PHOTOPHYSICAL STUDIES OF NOVEL COMPOUNDS FOR CANCER THERAPY

A Dissertation

Submitted to the Graduate Faculty of the
Louisiana State University and
Agricultural and Mechanical College
in partial fulfillment of the
requirements for the degree of
Doctor of Philosophy

In

The Department of Chemistry

by
Edith Khavwajira Amuhaya
B.S. University of Nairobi, 2005
May 2011

DEDICATION

This dissertation is dedicated to my husband, Sam, and our daughter Emma. Sam, words cannot begin to express the love and gratitude I have for you. You have been a source of inspiration to me. Thank you for your patience, for encouraging me every step of the way, and for all the sacrifices you made so that I could fulfill my dream. To our daughter Emma, you are the best thing that ever happened to us. You are a source of joy and happiness in our lives.

ACKNOWLEDGEMENTS

I would like to take this opportunity to express my sincere gratitude to the people who in one way or another played a role in making this dissertation possible.

First and foremost, I would like to thank my research advisor Prof. M. Graça H. Vicente who took me under her wing and gave me an opportunity to work in her research group. She ignited in me, an interest towards research, and provided an environment whereby I not only grew as a chemist, but also as a person. She helped develop my creativity, where as a synthetic chemist, we are always designing new molecules for various purposes. She has played a pivotal role not only as my research advisor, but also as a confidant, and for that, I will forever be grateful.

I would like to thank Prof. Kevin Smith for his valuable advice and suggestions and for always challenging me during group meetings. I am always amazed at how knowledgeable he is about a wide range of topics. His sense of humor always made group meetings enjoyable. I would like to thank the Chemistry department at LSU for giving me the opportunity to study, and obtain my PhD. I am grateful to the department for providing an environment that was conducive for studies, and also for providing the necessary facilities that I needed to do my research. A special thanks to my committee members, Dr. Carol Taylor, Dr. Bill Crowe, and Dr. Isiah Warner for accepting to participate in my final defense. Dr. Taylor possesses a work ethic, that many aspire to have, but very few achieve. Dr. Crowe is a synthetic chemistry "guru". He was always available to answer my many questions, or just to offer opinions and suggestions. I will forever feel indebted to Dr. Warner for his assistance during a very trying time in the course of my studies.

I would like to thank Dr. Saundra McGuire, who played a very big role in mentoring me during my studies here at LSU. Not only did she mentor me, but she prayed with me and was always there for me when I needed her during difficult times or when I just needed to talk. She will always hold a special place in my heart.

I would like to thank Dr. Dale Treleaven and Dr. Frank Fronczek for their assistance with NMR and x-ray crystallography. I am grateful to my group members, Jamie, Dinesh, Alecia, Krystal, Moses, Benson, Javoris, Haijun, Hillary, Timsy and Waruna, for welcoming me to the group and for always being ready to assist. A special thank you to Dr. Xiaoke Hu, who did an awesome job in obtaining the biological data, without ever complaining, even when I got impatient. I would like to thank my friends, Martha and Mama Lillian for always being there during the good and the bad, and for putting up with me during this roller coaster ride.

I will always be grateful to my parents, Margaret and Solomon Inyama. I can never thank them enough for everything they have done for me since I was a child. Their words of encouragement and advice, their prayers, and their never ending love, helped mould me into the person that I am today. A special thank you to my awesome siblings, Denis, Hannah, Daniel and Peter, who always know the right thing to say to put a smile on my face even when things get tough.

Finally, I would like to thank my wonderful husband, Sam and our daughter Emma, for their support and unconditional love. I am truly blessed to have them in my life.

TABLE OF CONTENTS

LIST OF ABBREVIATIONS

δ- chemical shift

AFM-atomic force microscopy

ALA-5-aminolevulinic acid

BBB- blood brain barrier

BNCT- boron neutron capture therapy

Boc- t-butoxycarbonyl

BPD- benzoporphyrin derivative

br - Broad

^{11}B-NMR- Boron 11 Nuclear Magnetic Resonace

n-BuLi – n- Butyl lithium

t-BuOK-Potassium tert- butoxide

^{13}C-NMR- Carbon 13 Nuclear Magnetic Resonance

d- Doublet

DCM- Dichloromethane

DDQ- 2,3-dichloro-5,6-dicyano-1,4-benzoquinone

DFT- Density Functional Theory

DIEA- N,N'-Diisopropylethylamine

DIPA- N,N’-Diisopropylamine

DME- Dimethyl ether

DMF- N,N’-Dimethylformamide

DMSO- Dimethyl Sulfoxide

DNA- Deoxyribonucleic acid

EDCI- N-(3-Dimethylaminopropyl)-N’-ethylcarbodiimide hydrochloride

EtOAc- Ethyl acetate

EtOH- Ethanol

h- hour(s)

HH-Head-Head

^{1}H-NMR- Proton Nuclear Magnetic resonance

HOBt- 1- hydroxybenzotriazole hydrate

HOMO- Highest Occupied Molecular Orbital

HpD-hematoporphyrin derivative

HPPH- 2-(1-hexyloxyethyl)-2-devinylpyropheophorbide-A

HRMS- High Resolution Mass Spectrum

HT-Head-Tail

Hz- Hertz

IR- Infra red

J- Coupling constant

LDL- Low Density Lipoproteins

LET- Linear Energy Transfer

LUMO- Lowest Unoccupied Molecular Orbital

MALDI- Matrix Assisted Laser Desorption / Ionization

MeOH- Methanol

MS- Mass Spectrometry

m/z- Mass to charge ratio

min- minute(s)

NBS- N-bromosuccinimide

NCT- Neutron Capture Therapy

PAT- Polyamine Transport System

PDT- Photodynamic Therapy

ppm- Parts per million

PT-Polythiophene

q- quartet

RT- Room temperature

s- singlet

t- triplet

TBAF- tetrabutylammonium fluoride

TBP-Tetrabenzoporphyrin

TBTU- O-(Benzotriazol-1-yl)-N,N,N',N'-tetramethyluronium tetrafluoroborate

TFA- Trifluoroacetic acid

TLC- Thin layer chromatography

TMS- trimethylsilane

TMSA- ethynyltrimethylsilane

TPP- 5,10,15,20-tetraphenylporphyrin

UV-Vis – Ultraviolet- visible

ABSTRACT

Cancer remains the second most common cause of death in the United States. It is therefore imperative that a lot of effort be put into finding a cure for this dreadful disease that shows no discrimination, and virtually anybody is at risk of developing the disease.

Chapter 1 introduces basic facts about cancer and the available treatments, including PDT and BNCT. Our focus will be on these two bimodal therapies, which form the basis of my research work, which involves the synthesis of potential sensitizers to be used either in PDT or BNCT or both.

In Chapter 2, I discuss the synthesis of thienyl- appended porphyrins, which have been found to absorb at longer wavelengths. This is favorable for PDT applications. In addition to this I introduce carborane cages to the porphyrin system to obtain compounds that have high ^{10}B concentrations and therefore potential boron delivery agents in BNCT. In this chapter I will also discuss the photophysical and biological studies of the porphyrins that I have synthesized.

Chapter 3 reports the synthesis of various carborane substituted oligothiophenes. Using a base, the closo carboranes are converted to the open nido cages. Insertion of different metals into these cages results in the synthesis of sandwich-type metalla-bis(dicarbollide) compounds, which are further electropolymerized to give the corresponding polymers. Both photophysical and biological studies of the oligothiophenes are carried out to establish their potential as ^{10}B delivery agents in BNCT.

Finally, in chapter 4, I discuss the synthesis of new disubstituted tetrabenzoporphyrins (TBPs). In order to increase selectivity of the compounds towards tumor cells, we conjugate the compounds to the polyamine, spermine, to the macrocycle.

CHAPTER 1: INTRODUCTION

1.1 Cancer Basics

Cancer is characterized by uncontrolled growth and spread of abnormal cells (Figure 1-1). When the spread of these abnormal cells is not prevented, it can lead to death[1]. Cancer is the second most common cause of death after heart diseases. According to the most recent statistics from the American Cancer Society, it was estimated that there would be more than 1.5 million new cancer cases in the year 2010. In addition to this, it was projected that there would be more than 500,000 lives lost as a result of cancer. This translated to about 1,500 deaths a day[2]. Most cancer types are named after the organ or cell they originate from. In the United States, the most common types of cancer include bladder cancer, breast cancer, colon and rectal cancer, endometrial cancer, kidney (renal cell) cancer, leukemia, lung cancer, melanoma, non-hodgkin lymphoma, pancreatic cancer, prostate cancer and thyroid cancer. Cancer can further be classified into four stages, I-IV, depending on the extent of the primary tumor and the extent to which it has spread in the body. Staging is critical in cancer diagnosis since it will determine the mode of treatment that will be used[3]. The most common types of treatment for cancer include surgery, chemotherapy and radiation therapy. Before the development of chemotherapy and radiation therapy, the only treatment that was available was the surgical removal of tumors. Development of the chemotherapies began in the 1940s, with the use of nitrogen mustards the drugs of choice. Nitrogen mustards are strong alkylating agents that have the ability to add alkylating groups onto DNA bases, resulting in the destruction of cancer cells[4]. Since then, there has been the development of many different drugs that have been used in chemotherapeutics. The modes of action of most of these drugs involve the inhibition of DNA replication or interference with its function as a way of destroying cancer cells[5]. A more recent approach has been the use of

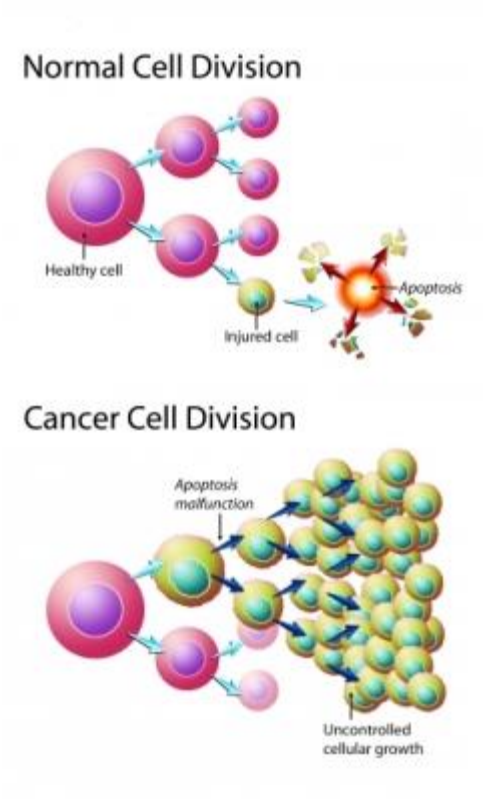

Figure 1-1. Uncontrolled growth of cancer cells[6]

oncolytic viruses which selectively enter neoplastic cells and replicate in the cells leading to their destruction[7]. Despite cancer cells being different from normal cells, they still share the same DNA and major metabolic pathways. As a result, the traditional drugs that attack DNA replication or cell division in cancer cells, can also attack normal cells. This results in serious side effects such as bone marrow and gastrointestinal toxicity which in some cases can prove to be life threatening[4]. As a result, there has been the need for the development of less invasive procedures with fewer side effects. A lot of focus has therefore been put on two relatively new bimodal therapies, photodynamic therapy (PDT) and boron neutron capture therapy (BNCT).

1.2 Photodynamic Therapy (PDT)

The concept of combining light with a chemical agent dates back to approximately 3000 years ago. Ancient Egyptians and Indians used this photochemistry for restoration of pigment in vitiligo patients[8]. In modern science however, PDT was first reported over 100 years ago by Hermann von Tapiener and his student Oscar Raab, when they discovered that illumination of microbial cultures in presence of acridine resulted in cell death. It was not until 1960 that it was reported that neoplastic tissues in patients fluoresced under light after administration of a photosensitizer[9]. In cancer therapy therefore, visible light, a light sensitive drug (photosensitizer) and oxygen are all combined. This leads to production of toxic species which in turn destroy tumor tissue[10]. When the photosensitizer absorbs light, it is excited to a short-lived excited singlet state (S_1) (see Figure 1-2). Through intersystem crossing, this molecule can convert to the excited triplet state (T_1). To explain the cell destruction process, two different mechanisms, type I and type II, are usually invoked. In type I reactions, the photosensitizer in its excited triplet state generates free radicals by electron or proton transfer, while in the type II mechanism, singlet oxygen ($^1O_2$) is produced by energy transfer. In both reactions, oxygen is seen as a major mediator of cell destruction[11].

In the first step in the process of photodynamic therapy, the photosensitizer is administered either orally, topically, or intraveneously (see Figure 1-3). This is followed by a period of incubation, which allows for the photosensitizer to accumulate in the tumor cells. During this time, the ratio of the concentration of the drug in tumor cells to that of normal cells is such that the tumor cells have considerably higher concentrations. Depending on the type of photosensitizer, the incubation period could range from a few hours to a couple of days. The tumor is then irradiated

by a source of light with the desired wavelength. The toxic species that are generated cause the desired cell destruction[10].

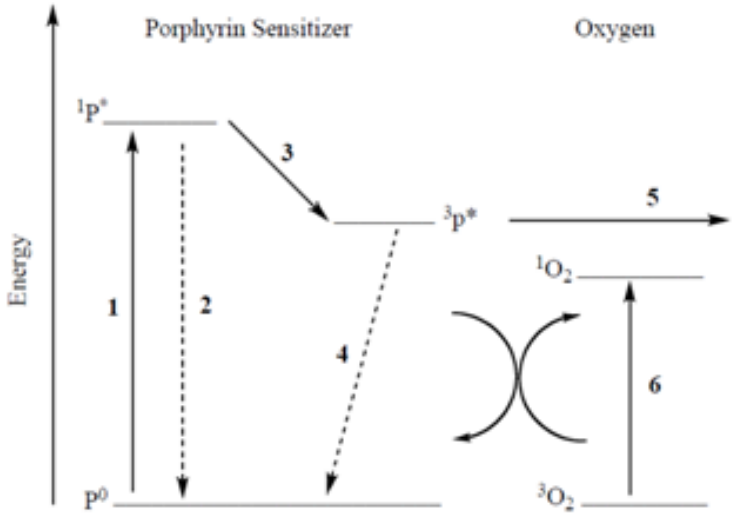

Figure 1-2: Mechanism of PDT[12]: **1**)Absorption of light **2**)Fluorescence **3**) Intersystem Crossing **4**) Phorphorescence **5**) Hydrogen radical or electron transfer **6**) Singlet Oxygen Production

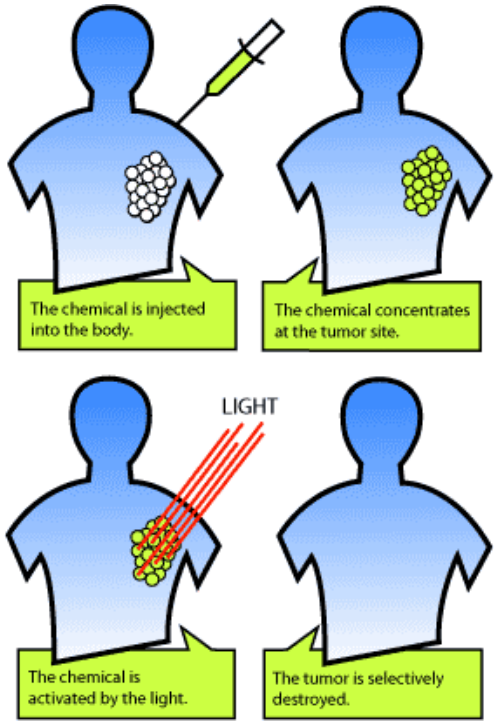

Figure 1-3. The process of photodynamic therapy[13]

As discussed earlier, only subcellular structures that are labeled by the photosensitizers are typically damaged by the photodynamic process. Therefore, the intracellular localization of photosensitizers plays a major role in PDT efficiency. A lot of research has been carried out to determine the mechanism for the preferential retention of photosensitizers by tumors[14]. Although these mechanisms are not fully understood, it has been widely accepted that serum proteins are mainly responsible for transportation of photosensitizers throughout the body. It has been shown that upon administration into the body, photosensitizers associate mainly with low-density lipoproteins (LDL). Several in vitro and in vivo studies have shown that there is an over expression of LDL receptors in tumor cells than in normal cells. LDLs therefore play a major role in the delivery of hydrophobic and/or ampiphilic photosensitizers to cancerous cells[15]. Therefore when designing a photosensitizer for PDT, it is crucial to keep in mind the affinity it has for LDL.

1.3 Classes of Photosensitizers

Photosensitizers can be classified according to their chemical structure. Table 1-1 lists the different families of photosensitizers. The first category consists of compounds that essentially are dyes. Pthalocyanines and naphthalocyanine dyes belong to this group, and they have a lot of potential as PDT photosensitizers. The second category consists of compounds with a chlorophyll and bacterio chlorophyll platform. As expected, these compounds, just like chlorophyll, have excellent photosensing properties. This group is comprised of chlorins, purpurins and bacteriochlorins. The final category has a porphyrin platform. This is perhaps the most promising group of all, and is evidenced by the number of clinical photosensitizers that are based on this platform[16](see Table 1-1). While there are many compounds that can act as

photosensitizers, very few are commercially available. Table 1-2[16] lists various clinical photosensitizers that are currently available.

Table 1-1. The categories of photosensitizers[16]

Porphyrin Platform	Chlorophyll and Bacteriochlorophyll Platform	Dyes
HpD	Chlorins	Phthalocyanines
HpD-based	Purpurins	Napthalocyanines
BPD	Bacteriochlorins	ALA
		Texaphyrins

Table 1-2: Photosensitizers clinically available for PDT[16]

Drug	Substance	Manufacturer	Cancer Treated
Photofrin®	HpD	Axcan Pharma, Inc	Esophageal, Colon and rectal,brain, head, neck
Visudyne®	Vertiprofin BPD	Novartis Pharmaceuticals	Age related macular degeneration
Metvix®	M-ALA	PhotoCure ASA	Skin, neck, head
Levulan®	ALA	DUSA Pharmaceuticals, Inc.	Skin, bladder, actinic keratosis
Antrin®	Lutexaphyrin	Pharmacylics	Arterial vascular disease, breast

Table 1-2 continued

Drug	Substance	Manufacturer	Cancer Treated
Foscan®	Temoporfin	Biolitec Pharma Ltd.	Cutaneous lesions, esophageal, head, neck
LS11	Talaporfin	Light Science	Ongoing clinical studies
Photochlor	HPPH	RPCI	Barrett's esophagus, lung
Photosens®	Phthalocyanine	General Physics Institute	Cutaneous and endobronchial lesions, lip, pharynx, larynx, tongue, head, neck

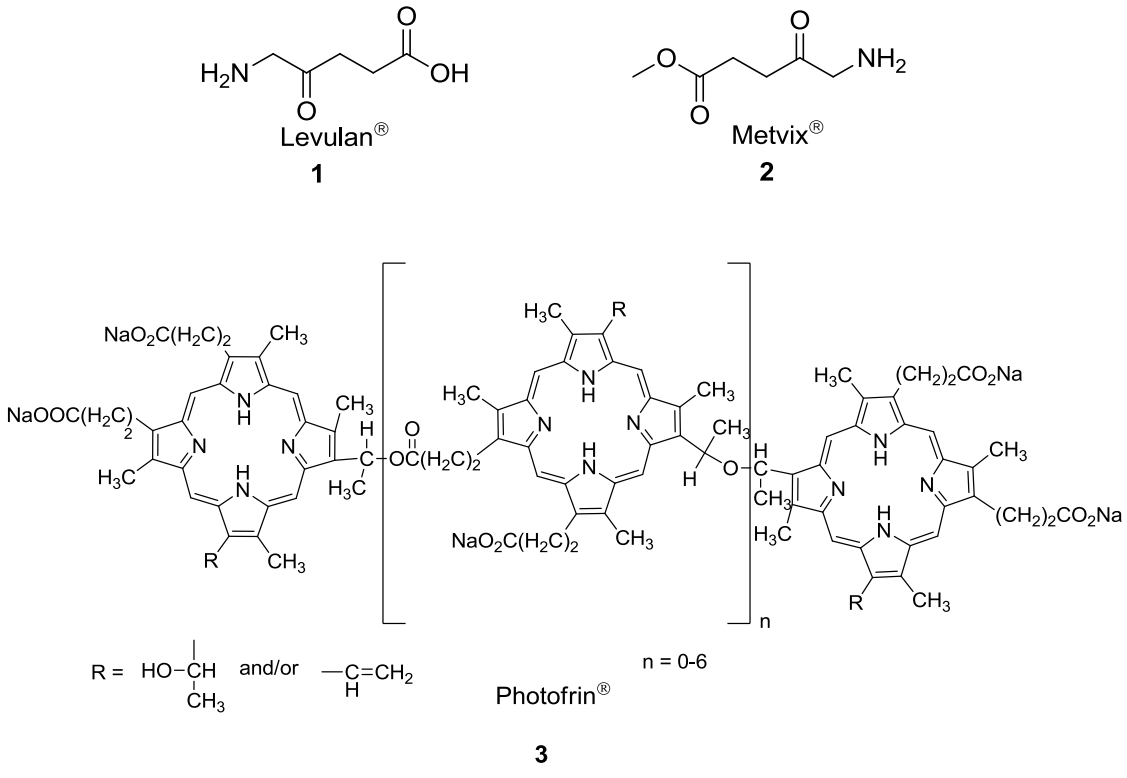

Figure 1-4: Examples of Drugs used in PDT

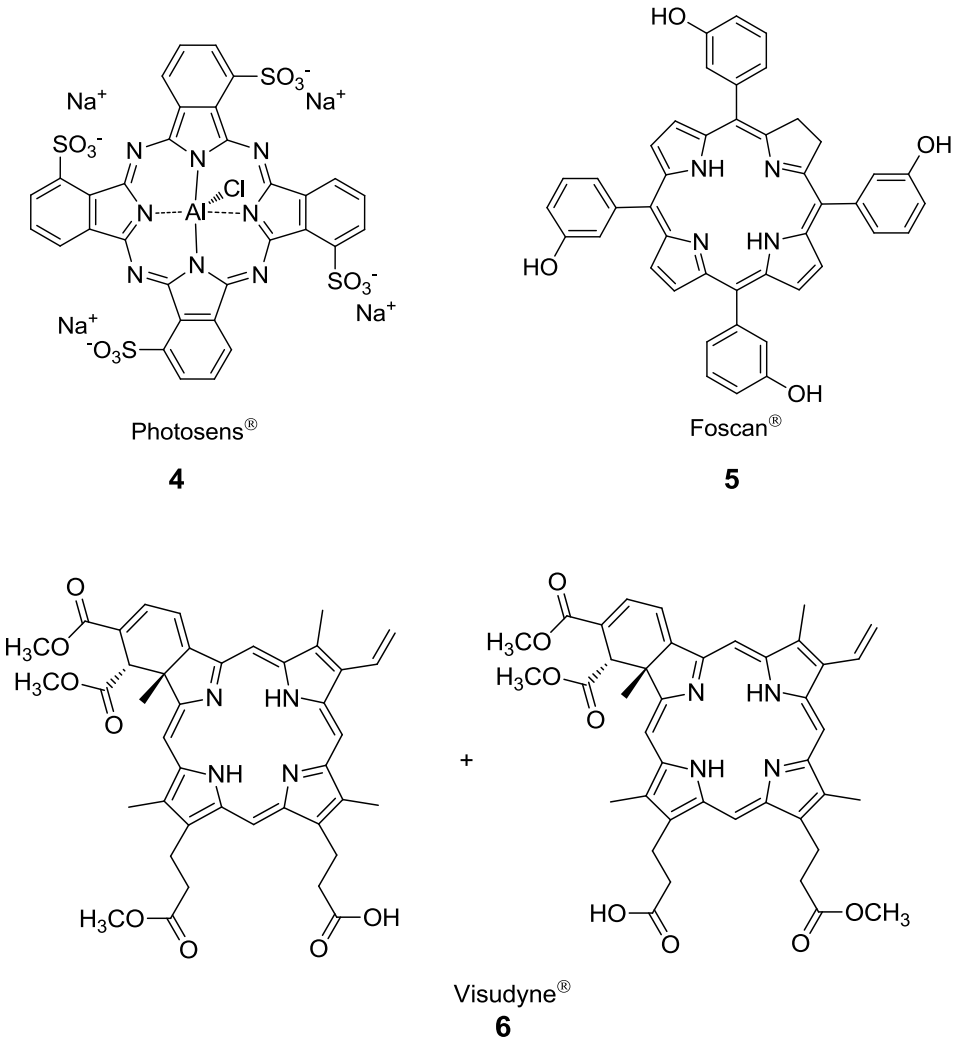

Figure 1-4 cont'd

As seen, most of the photosensitizer drugs currently available are based on a porphyrin platform. This can be attributed to a number of key photophysical, photochemical, and biological properties that they possess. Studies have shown that porphyrins absorb strongly in the visible region of the optical spectrum, they are fluorescent, and generally non- toxic in the dark. In addition to this, they have been found to have a high affinity for serum proteins thereby enhancing their selectivity for tumors. They have been found to exhibit chemical stability, both as free or metal-complexed compounds while retaining their in vivo tumor-localization. Finally,

they have been shown to localize in subcellular structures, lysosomes, endoplasmic reticulum, mitochondria and golgi apparatus[17]. Even though PDT provides a non-invasive procedure in the cure of cancer, there are some drawbacks that are associated with the process. The first major hurdle that needs to be overcome is the fact that normal cells are also destroyed in the process of killing the tumor cells. This can be addressed by finding ways of improving the selectivity of the photosensitizers in the tumor. It has also been reported that after this procedure, some patients experience photosensitive skin, which could last from a few hours to several weeks. This is brought about by the photosensitizer not clearing fast enough from the body[18]. Evidently, a lot of work still needs to be done to improve this promising relatively new cancer therapy.

1.4 Boron Neutron Capture Therapy (BNCT)

As mentioned earlier, surgery, chemotherapy, and radiation therapy are conventional approaches to the treatment of cancer. In case of solid tumors, surgery is the preferred method for removal of the tumor. However there is always a bit of uncertainty as to whether all the cancerous cells were removed or not. As a result, there is always the possibility of recurrence of the tumor. Chemotherapy and radiotherapy offer alternative means of destroying cancer cells. In the case of chemotherapy, the major drawback is that the destructive effects of the drugs used are not limited to the tumor cells only, as normal cells are also destroyed. In radiotherapy, the radiation used to destroy tumors is usually so strong that normal cells are also killed. To make matters worse, in both chemotherapy and radiotherapy, the toxic effects on normal cells are irreversible[19]. Evidently, there has been a need to develop better strategies to combat cancer. This has led to the development of bimodal therapies, which include the use of radiation sensitizers[20], gene therapy[21], photodynamic therapy (PDT)[17] and neutron capture therapies (NCT)[22].

1.5 Fundamental Properties of Nuclides

Neutrons are uncharged nuclear particles which have an atomic mass of 1 and energy of 0.025eV. Their most important property with respect to radiation is that they only react with nuclei and not electrons. This interaction proceeds via scattering and absorption. NCT is therefore based on the ability of some nuclides, both radioactive and non-radioactive to absorb thermal or slow neutrons. These nuclear events liberate lethal particles that possess large amounts of energy. A measure of the probability of neutrons being captured by a nuclide is given by its cross section, which is expressed in barn (1 barn = 10^{-24} cm^2). Table 1-3[19] lists the nuclides with high capture cross sections.

Table 1-3: Cross section values of selected nuclides for thermal neutrons

Nuclide	Cross section (barn)	Nuclide	Cross section (barn)
^{6}Li	942	^{151}Eu	5800
^{10}B	3838	^{155}Gd	61000
^{11}B	0.0055	^{197}Au	98.7
$^{22}Na^{a}$	32000	^{157}Gd	255000
$^{58}Co^{a}$	1900	^{164}Dy	1800
^{113}Cd	19800	^{184}Os	3000
$^{126}I^{a}$	6000	^{199}Hg	2000
$^{135}Xe^{a}$	2600000	$^{230}Pa^{a}$	1500
$^{148}Pm^{a}$	10600	$^{235}U^{a}$	580
^{149}Sm	42000	$^{241}Pu^{a}$	1010
^{1}H	0.332	^{24}Mg	0.052
^{6}Li	940	^{31}P	0.18
^{12}C	0.0034	^{32}S	0.004
^{14}N	1.81	^{35}Cl	43.6

Table 1-3 continued

Nuclide	Cross section (barn)	Nuclide	Cross section (barn)
^{16}O	0.000178	^{39}K	0.0043
^{17}O	0.235	^{40}Ca	0.4
^{23}Na	0.4	^{56}Fe	2.63

[a]Radioactive

The capture cross section and subsequently the reactions arising from them is different for each nuclide. Therefore, even for isotopes of the same elements, the capture cross sections greatly differ. When compared to the capture cross section values of tissue elements, (Table 1-4[19]), it can be seen that these values are at least 2 orders of magnitude greater.

The capture cross-section, however, is just one aspect that is considered when choosing nuclides for use in NCT. Another very important point to take into consideration is whether the toxic radiation produced during the fission process is confined in the cell. If this is not achieved, then it beats the whole purpose of using NCT as a therapeutic procedure. Early development of NCT saw ^{235}U and ^{6}Li as potential nuclides for neutron capture. However, it was soon discovered, that ^{235}U compounds were generally toxic to the body tissues[19, 23], and ^{6}Li being an alkali metal, under biological conditions, its compounds would readily be broken down to lithium cations[19]. In addition to its high capture cross section, studies have shown that when irradiated with low-energy thermal neutrons, ^{10}B yields high linear energy transfer α particles and recoiling ^{7}Li nuclei[24] as shown is Scheme 1-1. These fragments have mean free pathways of travel in tissue (5-9μm) which is approximately equivalent to the diameter of mammalian cells. This means that they can bring about confined biological damage through ionization[19, 25]. In addition to this, ^{10}B can take part in reactions that lead to the synthesis of different compounds which have remarkably stable linkages with other atoms, like carbon, nitrogen, and oxygen[21]. Based on all

these attractive properties, a lot of effort has been put into development of BNCT, with the primary focus being on the treatment of high- grade gliomas and either cutaneous primaries or cerebral metastases of melanoma, and most recently, head, neck and liver cancer[25a].

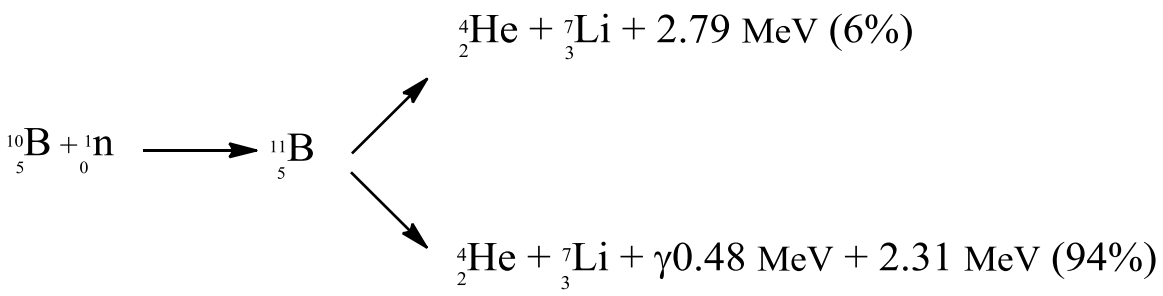

Scheme 1-1: Fission reactions that occur upon boron capture of neutrons

Successful treatment using BNCT depends on the selective delivery of the sensitizers to the tumor and the possibility of achieving sufficiently high endocellular boron concentration[24a, 24c]. Studies have shown that the amount of boron necessary for effective BNCT is between 15 and 30μg of 10B per gram of tumor, depending on its exact location within the tumor[24b]. As expected, the required concentration of ^{10}B for effective BNCT decreases as the position of the ^{10}B nuclei is changed from the external cell wall to the cytoplasm to the nucleus of the cell[22d].

Approximately 2% of all cancer deaths are caused by primary cerebral tumors, with about 13,000 people dying each year in the Unites States[2, 26]. In 1951, Dr. William H. Sweet, a neurosurgeon, suggested the use of BNCT in treatment of brain tumors, in particular, glioblastoma multiforme[19, 27]. The initial clinical trials were not successful mainly due to inadequacies in the neutron beams, and the boron compounds that were used, which offered no selectivity to tumor cells. There was however renewed interest in the therapy after more encouraging results by Dr. Hiroshi Hatanaka for malignant gliomas[28] and those of Dr. Yukata Mishima for malignant

melanoma[19, 29]. The process of treatment using BNCT starts by directing a beam of neutrons towards a patient's head. These neutrons rapidly lose energy as they pass through tissue, by elastic scattering. Consequently, they are captures by ^{10}B atoms, which are in turn excited and converted to ^{11}B atoms for a very short time (~10^{-12} seconds). This is followed by fission of ^{11}B to produce α particles, ^{7}Li recoil nuclei and gamma rays. The α particles produced are responsible for the selective destruction of tumor cells[31] (Figure 1-4).

1.6 Boron Delivery Agents

For BNCT to be successful, not only must there be a sufficient number of ^{10}B atoms that are selectively accumulated in the tumors, but the concentration gradient of ^{10}B atoms between the tumors and surrounding normal cells must be large[30]. The priority for the last ~ 50 years has therefore been the development of boron delivery agents for BNCT. For a boron delivery agent to be considered successful, it must exhibit low toxicities in normal tissue, with high tumor uptake and high tumor/brain and tumor/blood concentration ratios (> 3-4: 1). In addition to this, the agent must be able to supply ^{10}B concentrations between 10 - 30μg ^{10}B per gram of tumor. Finally, during BNCT, there should be rapid clearance of the agent from blood and normal tissues, while maintain the concentrations in tumor cells[31]. To date, only two boron- containing drugs have been used clinically for BNCT of brain tumors, (*L*)-4-dihydroxy-borylphenylalanine (BPA) and sodium mercaptoundecahydro-*closo*-dodecaborate (BSH) (Figure 1-5). These drugs have been established to be safe, although they are not the ideal boron delivery agents[25a, 31].

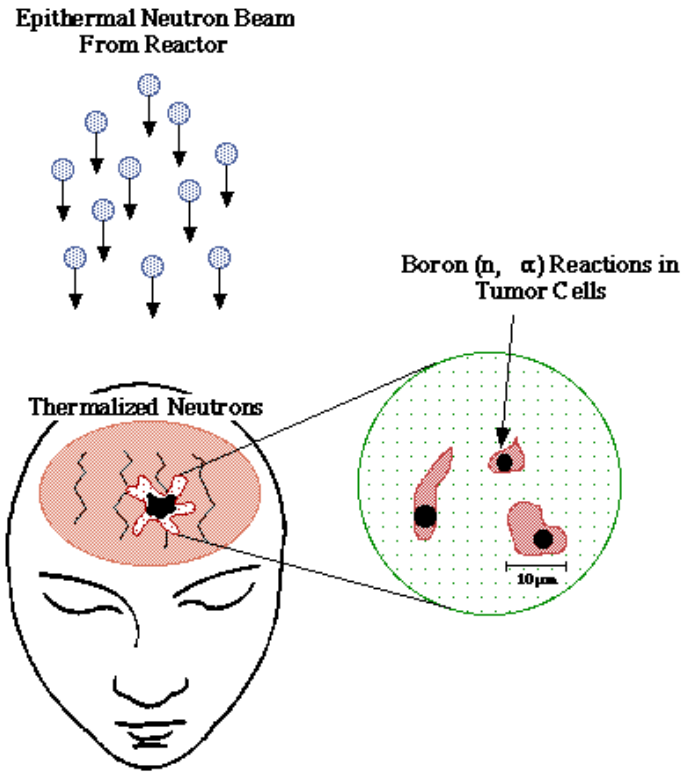

Figure 1-4: The process of boron neutron capture therapy in treatment of brain tumors[32]

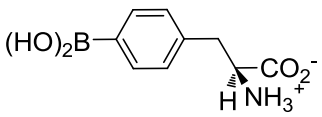

(*L*)-4-dihydroxy-borylphenylalanine
(BPA)
7

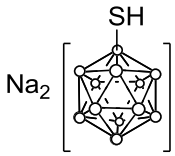

sodium mercaptoundecahydro-*closo*-dodecaborate
(BSH)
8

Figure 1-5: BNCT compounds that have undergone clinical trials

A lot of research work has been put into developing boron rich compounds for BNCT. Figure 1-6 show some BNCT agents that have been synthesized. These include compounds **9** and **10** which have caborane cages linked to nucleosides, and they have both shown promise in animal models. The trimethoxyindole **11** has shown promise in vitro studies, while porphyrin **12** has shown good tumor selectivity[19, 22c, d].

Our research work focuses on the synthesis, characterization, photophysical and biological studies of compounds that are potential PDT and BNCT agents. In one project, our main focus is the introduction of thiophene groups at the *meso* position of the porphyrin macrocylce (Scheme 1-2). The first and obvious reason for this is to extend the conjugation, and therefore shift the wavelength of absorption to longer wavelength. The second reason is based on the fact that thiophene rings are very stable chemically, and many different reactions can be on the free α-carbon of the ring. In fact, one of the modifications that we perform is the introduction of carboranes to the porphyrin system via the free α-carbon of the thiophene. This introduces many attractive properties to the system due to the carborane, and it makes the compounds potential agents for both PDT and BNCT.

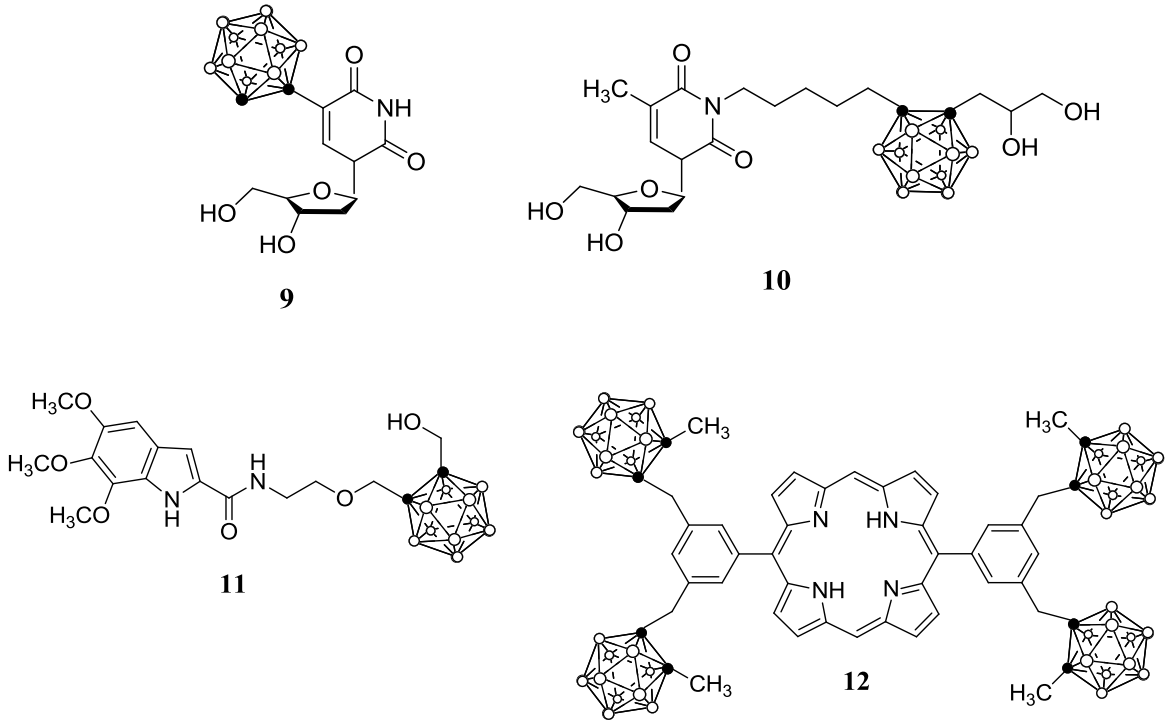

Figure 1-6: Compounds that have been synthesized as potential BNCT agents

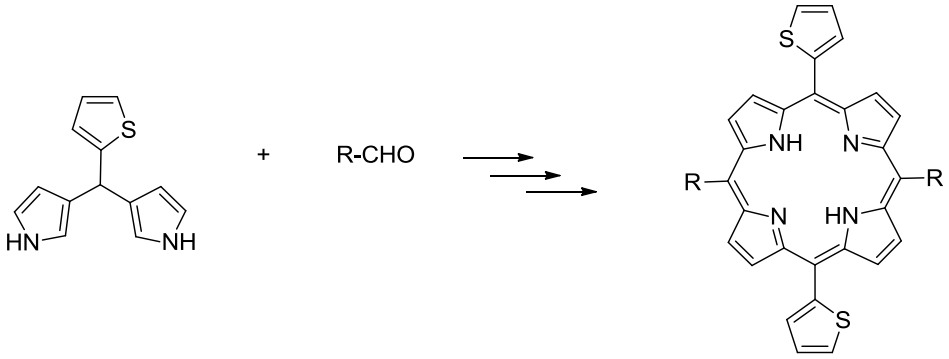

Scheme 1-2: Synthesis of thienyl-appended porphyrins

In the second project, we synthesize carborane appended oligothiophenes (Scheme 1-3). Not only can these compounds be used in BNCT because of the presence of the carborane ring, but also because of their small size we anticipate that they will readily cross the blood brain barrier (BBB) to facilitate treatment of brain tumors. In addition to this, we prepared several metal complexes of the oligothiophenes, which were further electropolymerized to form polythiophenes. These polymers have potential applications in medicine and material science.

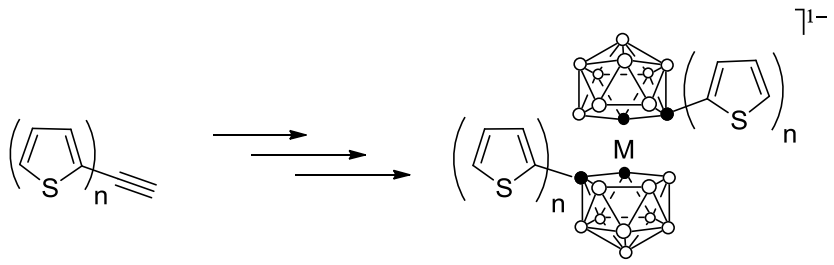

Scheme 1-3: Synthesis of carboranyl functionalized thiophenes

The third project focuses on synthesis of tetrabenzoporphyrins (TBP) (Scheme 1-4), which belong to the family of π-extended porphyrins. This group of porphyrins absorb at longer wavelength due to their extended conjugation. As potential photosensitizers for PDT, these compounds are expected to have good selectivity for tumor cells. To enhance their selectivity,

we introduce polyamine chains to the system. We specifically use spermine, which is found in mammalian cells and has been found to take part in key roles in cellular functions.

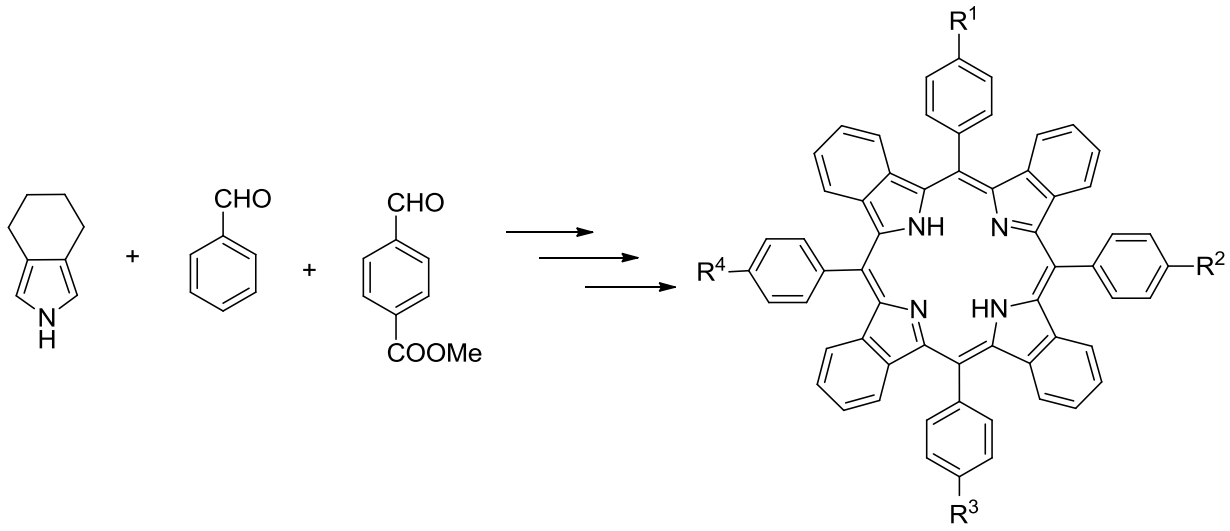

Scheme 1-4: Synthesis of tetrabenzoporphyrins

1.7 References

1. (a) Miller, J., Photodynamic therapy: The sensitization of cancer cells to light. *Journal of Chemical Education* **1999,** *76* (5), 592-593; (b) Miller, J., Second generation drugs and additional applications of PDT. *Journal of Chemical Education* **1999,** *76* (5), 594-594.

2. Jemal, A.; Siegel, R.; Xu, J. Q.; Ward, E., Cancer Statistics, 2010. *Ca-a Cancer Journal for Clinicians* **2010,** *60* (5), 277-300.

3. Edge, S. B.; Compton, C. C., The American Joint Committee on Cancer: the 7th Edition of the AJCC Cancer Staging Manual and the Future of TNM. *Annals of Surgical Oncology* **2010,** *17* (6), 1471-1474.

4. Shewach, D. S.; Kuchta, R. D., Introduction to Cancer Chemotherapeutics. *Chem Rev* **2009,** *109* (7), 2859-2861.

5. (a) Klein, A. V.; Hambley, T. W., Platinum Drug Distribution in Cancer Cells and Tumors. *Chem Rev* **2009,** *109* (10), 4911-4920; (b) Parker, W. B., Enzymology of Purine and Pyrimidine Antimetabolites Used in the Treatment of Cancer. *Chem Rev* **2009,** *109* (7), 2880-2893; (c) Pommier, Y., DNA Topoisomerase I Inhibitors: Chemistry, Biology, and Interfacial Inhibition. *Chem Rev* **2009,** *109* (7), 2894-2902.

6. beliefnet Cell Cancer Growth. http://www.beliefnet.com/healthandhealing/getcontent.aspx?cid=11731 (accessed 3rd March).

7. Alvarez-Breckenridge, C.; Kaur, B.; Chiocca, E. A., Pharmacologic and Chemical Adjuvants in Tumor Virotherapy. *Chem Rev* **2009,** *109* (7), 3125-3140.

8. Celli, J. P.; Spring, B. Q.; Rizvi, I.; Evans, C. L.; Samkoe, K. S.; Verma, S.; Pogue, B. W.; Hasan, T., Imaging and Photodynamic Therapy: Mechanisms, Monitoring, and Optimization. *Chem Rev* **2010,** *110* (5), 2795-2838.

9. Kessel, D., Photodynamic therapy: from the beginning. *Photodiagnosis and Photodynamic Therapy* **2004,** *1* (1), 3-7.

10. DeRosa, M. C.; Crutchley, R. J., Photosensitized singlet oxygen and its applications. *Coordination Chemistry Reviews* **2002,** *233-234*, 351-371.

11. Sol, V.; Lamarche, F.; Enache, M.; Garcia, G.; Granet, R.; Guilloton, M.; Blais, J. C.; Krausz, P., Polyamine conjugates of meso-tritolylporphyrin and protoporphyrin IX: Potential agents for photodynamic therapy of cancers. *Bioorganic & Medicinal Chemistry* **2006,** *14* (5), 1364-1377.

12. Easson, M. W. Syntheses of Ttrimethylamine- and Phosphonatesubstituted Carboranylporphyrins for Application in Boron Neutron Cancer Therapy. LSU, Baton Rouge, 2008.

13. Wildan M>>Open Think Labs Photodynamic Therapy. http://wildan.openthinklabs.com/2010/05/24/photodynamic-therapy-pdt/OpenThinkLabs.indonesia (accessed 10th March).

14. Bonneau, S.; Vever-Bizet, C.; Mojzisova, H.; Brault, D., Tetrapyrrole-photosensitizers vectorization and plasma LDL: A physico-chemical approach. *International Journal of Pharmaceutics* **2007,** *344* (1-2), 78-87.

15. Lajos, G.; Jancura, D.; Miskovsky, P.; García-Ramos, J. V.; Sanchez-Cortes, S., Interaction of the Photosensitizer Hypericin with Low-Density Lipoproteins and Phosphatidylcholine: A Surface-Enhanced Raman Scattering and Surface-Enhanced Fluorescence Study. *The Journal of Physical Chemistry C* **2009,** *113* (17), 7147-7154.

16. Allison, R. R.; Downie, G. H.; Cuenca, R.; Hu, X.-H.; Childs, C. J. H.; Sibata, C. H., Photosensitizers in clinical PDT. *Photodiagnosis and Photodynamic Therapy* **2004,** *1* (1), 27-42.

17. Vicente, M. G., Porphyrin-based sensitizers in the detection and treatment of cancer: recent progress. *Curr Med Chem Anticancer Agents* **2001,** *1* (2), 175-94.

18. (a) Garcia, G.; Sarrazy, V.; Sol, V.; Morvan, C. L.; Granet, R.; Alves, S.; Krausz, P., DNA photocleavage by porphyrin-polyamine conjugates. *Bioorganic & Medicinal Chemistry* **2009,** *17* (2), 767-776; (b) Chaleix, V.; Sol, V.; Guilloton, M.; Granet, R.; Krausz, P., Efficient synthesis of RGD-containing cyclic peptide-porphyrin conjugates by ring-closing metathesis on solid support. *Tetrahedron Letters* **2004,** *45* (27), 5295-5299.

19. Soloway, A. H.; Tjarks, W.; Barnum, B. A.; Rong, F.-G.; Barth, R. F.; Codogni, I. M.; Wilson, J. G., The Chemistry of Neutron Capture Therapy. *Chem Rev* **1998,** *98* (4), 1515-1562.

20. Kennedy, K. A.; Teicher, B. A.; Rockwell, S.; Sartorelli, A. C., The hypoxic tumor cell: A target for selective cancer chemotherapy. *Biochemical Pharmacology* **1980,** *29* (1), 1-8.

21. Caruso, M., Gene therapy against cancer and HIV infection using the gene encoding herpes simplex virus thymidine kinase. *Molecular Medicine Today* **1996,** *2* (5), 212-217.

22. (a) Mehta, S. C.; Lu, D. R., Targeted Drug Delivery for Boron Neutron Capture Therapy. *Pharmaceutical Research* **1996,** *13* (3), 344-351; (b) Gabel, D., Present status and perspectives of boron neutron capture therapy. *Radiotherapy and Oncology* **1994,** *30* (3), 199-205; (c) Morin, C., The chemistry of boron analogues of biomolecules. *Tetrahedron* **1994,** *50* (44), 12521-12569; (d) Hawthorne, M. F., The Role of Chemistry in the Development of Boron Neutron Capture Therapy of Cancer. *Angewandte Chemie International Edition in English* **1993,** *32* (7), 950-984.

23. Liu, H. Y. B.; Brugger, R. M.; Shih, J. L. A., Neutron-Capture Therapy with U-235 Seeds. *Medical Physics* **1992,** *19* (3), 705-708.

24. (a) Fabris, C.; Jori, G.; Giuntini, F.; Roncucci, G., Photosensitizing properties of a boronated phthalocyanine: studies at the molecular and cellular level. *Journal of Photochemistry and Photobiology B: Biology* **2001,** *64* (1), 1-7; (b) Vicente, M. G. H.; Nurco, D. J.; Shetty, S. J.; Osterloh, J.; Ventre, E.; Hegde, V.; Deutsch, W. A., Synthesis, dark toxicity and induction of in vitro DNA photodamage by a tetra(4-nido-carboranylphenyl)porphyrin. *Journal of Photochemistry and Photobiology B: Biology* **2002,** *68* (2-3), 123-132; (c) Giuntini, F.; Raoul, Y.; Dei, D.; Municchi, M.; Chiti, G.; Fabris, C.; Colautti, P.; Jori, G.; Roncucci, G., Synthesis of tetrasubstituted Zn(II)-phthalocyanines carrying four carboranyl-units as potential BNCT and PDT agents. *Tetrahedron Letters* **2005,** *46* (17), 2979-2982.

25. (a) Barth, R. F.; Coderre, J. A.; Vicente, M. G. H.; Blue, T. E., Boron Neutron Capture Therapy of Cancer: Current Status and Future Prospects. *Clinical Cancer Research* **2005,** *11* (11), 3987-4002; (b) Zamenhof, R. G.; Kalend, A. M.; Bloomer, W. D., BNCT: Looking for a Few Good Molecules. *Journal of the National Cancer Institute* **1992,** *84* (16), 1290-1291.

26. (a) Rosenthal, M. A.; Kavar, B.; Hill, J. S.; Morgan, D. J.; Nation, R. L.; Stylli, S. S.; Basser, R. L.; Uren, S.; Geldard, H.; Green, M. D.; Kahl, S. B.; Kaye, A. H., Phase I and Pharmacokinetic Study of Photodynamic Therapy for High-Grade Gliomas Using a Novel Boronated Porphyrin. *Journal of Clinical Oncology* **2001,** *19* (2), 519-524; (b) Surawicz, T. S.; McCarthy, B. J.; Kupelian, V.; Jukich, P. J.; Bruner, J. M.; Davis, F. G.; States, t. c. r. o. t. C. B. T. R. o. t. U., Descriptive epidemiology of primary brain and CNS tumors: Results from the Central Brain Tumor Registry of the United States, 1990-1994. *Neuro-Oncology* **1999,** *1* (1), 14-25.

27. Sweet, W. H., The Uses of Nuclear Disintegration in the Diagnosis and Treatment of Brain Tumor. *New England Journal of Medicine* **1951,** *245* (23), 875-878.

28. Soloway, A. H.; Hatanaka, H.; Davis, M. A., Penetration of Brain and Brain Tumor. VII. Tumor-Binding Sulfhydryl Boron Compounds1,2. *Journal of Medicinal Chemistry* **1967,** *10* (4), 714-717.

29. Soloway, A. H.; Whitman, B.; Messer, J. R., Penetration of Brain and Brain Tumor by Aromatic Compounds as a Function of Molecular Substituents. *Journal of Pharmacology and Experimental Therapeutics* **1960,** *129* (3), 310-314.

30. Suzuki, M.; Sakurai, Y.; Hagiwara, S.; Masunaga, S.; Kinashi, Y.; Nagata, K.; Maruhashi, A.; Kudo, M.; Ono, K., First Attempt of Boron Neutron Capture Therapy (BNCT) for Hepatocellular Carcinoma. *Japanese Journal of Clinical Oncology* **2007,** *37* (5), 376-381.
31. Barth, R. F.; Yang, W.; Al-Madhoun, A. S.; Johnsamuel, J.; Byun, Y.; Chandra, S.; Smith, D. R.; Tjarks, W.; Eriksson, S., Boron-Containing Nucleosides as Potential Delivery Agents for Neutron Capture Therapy of Brain Tumors. *Cancer Research* **2004,** *64* (17), 6287-6295.

32. MIT-Boron Neutron Capture Therapy Research Boron Neutron Capture Therapy. http://web.mit.edu/nrl/www/bnct/info/description/description.html (accessed 10th March).

CHAPTER 2: SYNTHESIS OF THIENYL-APPENDED PORPHYRINS FOR PDT AND BNCT

2.1 Introduction

For centuries, porphyrins have drawn much attention in the science community due to their wide range of applications in the fields of medicine, biochemistry, biology, and chemistry. This can be attributed to their fascinating chemical, physical, and spectroscopic properties[1]. It is therefore not surprising that in the last century, several Nobel prizes were awarded in the field of tetrapyrrole science[2]. Porphyrins are aromatic macrocycles made up of four "pyrrole- type" rings joined by four methine carbons[3]. In the UV-Visible spectrum, they are characterized by the presence of an intense Soret band[1] at ~ 400 nm and several weaker bands, found between 450 nm and 800 nm. Porphyrins contain 22 π-electrons, of which 18 are involved in the delocalization pathway, see Figure 2-1. *Trans*-NHs are the most favored tautomeric forms, while the *cis*-NH tautomers are thought to be intermediates in a NH-migration mechanism[4].

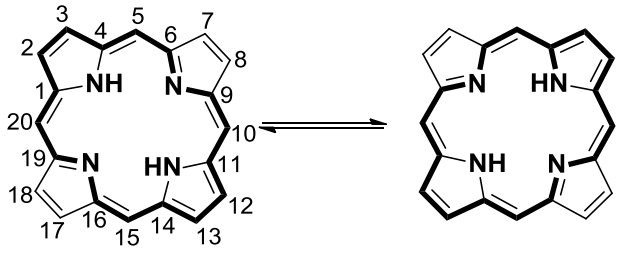

Figure 2-1: Delocalization Pathway of Porphyrins

Because of their many applications, much focus has been directed towards porphyrin synthesis, which involves the arrangement of different substituents about the periphery of the macrocycle. Generally speaking, the electronically most reactive sites at the periphery of the porphyrin macrocycle are the 5, 10, 15 and 20 positions, which are designated as the *meso* positions.

However, in the presence of bulky reactant species, the β-pyrrolic 2, 3, 7, 8, 12, 13, 17 and 18 positions are the preferred reaction sites[4](Figure 2-1). Therefore there are two distinct types of substituents at the porphyrin periphery, the β-substituted porphyrins and *meso*-substituted porphyrins, with the former having a close resemblance to naturally occurring porphyrins (Figure 2-2). *Meso*-substituted porphyrins have gained popularity due to their ease of synthesis, as well as the ability to design elaborate and highly sophisticated groups at the *meso* position. As a result, they have found applications as biomimetic models and also form an integral part in materials science[1]. Several synthetic methods for *meso*-substituted porphyrins have been developed, and these include, the Rothemund, Adler and Lindsey methods.

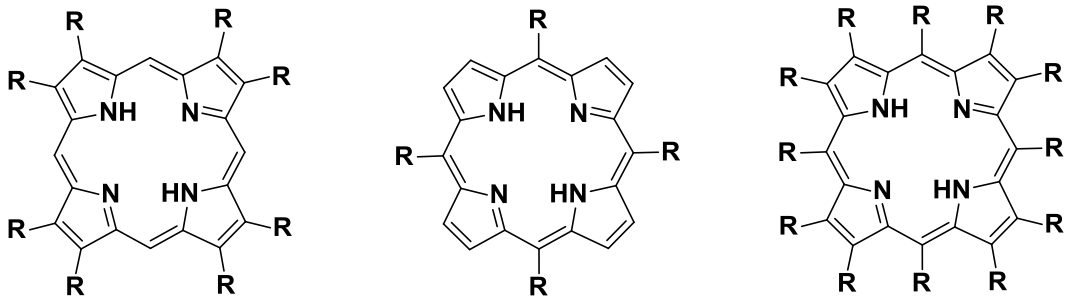

Figure 2-2: Three types of porphyrins

2.2 Methods for Porphyrin Synthesis

Synthesis of meso-porphyrins was initiated by Rothemund in 1935[5]. He carried out the syntheses by reacting different aldehydes with pyrroles at very high temperatures. The most notable porphyrin synthesized using this method was tetramesitylporphyrin (H_2TMP). This was obtained by reaction of mesitaldehyde and pyrrole in presence of pyridine solvent, at 180^{o}C for 48 h. It was found that the methyl groups in Fe^{II}(TMP) prevented dimer formation upon

oxygenation[6] . Despite several variations by different research groups[7], this method has not received much application. This is largely due to the low overall yields obtained.

The Adler method was developed by Adler, Longo, and co-workers in the mid 1960s[8]. This method basically requires the use of acidic solvents at reflux conditions in an open atmosphere. Of the three acids used (propionic acid, acetic acid and acidified benzene) propionic acid is the most preferred leading to overall yields of the porphyrins, ranging between 20 and 40%[1]. This is obviously better than the Rothemund method. In addition to the high yields, another attractive feature of this method is the fact that the porphyrin product can often crystallize out of the cooled acidic solvent. A major drawback however, is the limit in the types of aldehydes that can be used in this synthesis. Many aldehydes with substituents that are sensitive to acids cannot be used to prepare porphyrins using this method, and as a result, extra steps of protection and deprotection of the substituents have to be employed[9]. Both the Rothemund and Adler methods have limitations in their applications, in part due to the harsh reaction conditions that are necessary for porphyrin synthesis. This in turn affects the yields of the final product. Secondly, these two methods do not present a rational method of accessing porphyrins, especially those, with two, three or four distinct *meso*-substituents. There was clearly a need to develop a new method that could not only accommodate a wide range of functional groups, but could also lead to a variety of porphyrins with different number of distinct substituents.

In the early 1980s, Lindsey and co-workers developed the Lindsey protocol which facilitated the synthesis of porphyrins under mild conditions. This method takes advantage of the highly reactive aldehyde and pyrrole starting materials, which do not require harsh conditions to react. The mild conditions include condensation of the aldehyde and pyrrole in the presence of an acid catalyst, normally trifluoroacetic acid (TFA) or $BF_3.OEt_2$, at room temperature to form a

porphyrinogen intermediate. This step is followed by the addition of an oxidant, usually p-chloranil or 2,3-dichloro-5,6-dicyano-1,4-benzoquinone (DDQ), to afford the more stable aromatic porphyrin[10]. The major disadvantage here is that dilute concentrations of aldehyde and pyrrole are required to minimize the competition between oligomerization of pyrromethanes and cyclization to give the porphyrinogen[11](Scheme 2-1). This means that when running large scale synthesis of porphyrins, one has to handle large amounts of solvents. In addition to this, the purification step involves column chromatography, which can be cumbersome[1].

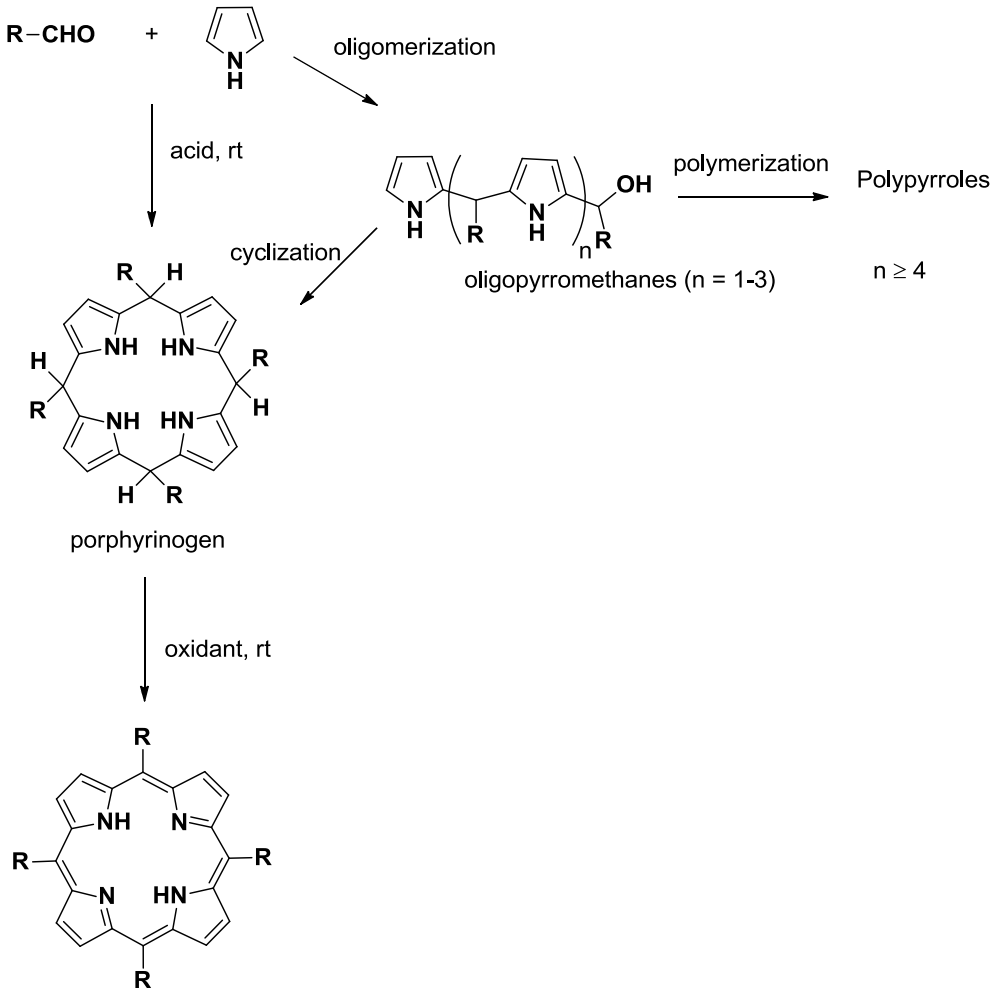

Scheme 2- 1: Mechanism of porphyrin formation

2.3 Thienyl- substituted Porphyrins

Reports on porphyrins with 5-membered heterocycles, such as pyrrole, furan and thiophene, as substituents at the *meso* position are scarce[12]. However, meso-tetrathienyl porphyrins have incited much interest due to their use as models for energy transfer reactions as well as for their conductivity[13]. In 1968, Triebs and co-workers reported the synthesis of the first thienyl substituted porphyrin. This was achieved using the Rothemund method and the porphyrin was obtained in 9% yield[14]. Torréns and co-workers and Bhyrappa and Bhavana later prepared the same porphyrin using the Adler-Longo method, with the latter reporting a yield of 14%[13, 15]. Since then, most studies on this group of porphyrins have adapted the Lindsey protocol, mainly due to the mild reaction conditions involved in the synthesis which the thienyl groups can withstand[16]. Despite the fact that the photophysical and electronic properties of thienyl porphyrins have been studied, there appears to be inconsistencies in describing the effect of the thienyl ring on the electronic properties of the porphyrin molecules[16a]. Compared to the corresponding tetraphenyl-porphyrin, thienyl-porphyrins show red-shifted absorption bands. In addition to this, the shift increases with increased number of thiophene rings. For a long time, it was accepted that this red shift in absorption was due to inductive effects of the thiophene rings. This arose from the expectation that the small ring size of thiophene would be almost co-planar with the porphyrin macrocycle. However, it was found that the dihedral angle formed between the porphyrin plane and the thienyl ring was greater in metal complexed thienyl porphyrins, compared to metal-complexed tetraphenyl- porphyrins. This means that the effective conjugation between the thiophene ring and the porphyrin macrocycle in the thienyl-porphyrin is small[13]. Studies carried out by Gupta and Ravikanth[12, 17] showed that the shift was rather due to a greater π-delocalization of thienyl-porphyrins brought about by a strong resonance interaction between

the porphyrin macrocycle and the thienyl group(s). In general, the introduction of thienyl group(s) on the porphyrin macrocycle allows extension of the π-conjugated system. This in turn imparts fascinating electrochemical properties, making these systems ideal building blocks for not only linear porphyrin arrays, but also supramolecular assemblies. To date, thienyl- polymers have been shown to exhibit higher electrochemical stability than any other porphyrin polymers[16a].

2.4 Synthesis of *trans*- Substituted Porphyrins

Meso-substituted porphyrins possessing substituents in a *trans*-configuration have been used as building blocks in the preparation of a wide range of systems. There are two ways in which these compounds can be prepared. The first is a mixed aldehyde condensation of pyrrole and two different aldehydes. This procedure affords up to six different porphyrins, with *trans*-substituted porphyrins present as ~ 12.5% of the total, and cis-substituted porphyrin present as ~ 25% of the total. The second and preferred method of preparation of *trans*-substituted porphyrins involves the condensation of a dipyrromethane and an aldehyde, also known as the MacDonald [2 + 2] condensation (Scheme 2-2). This method provides a rational approach to the synthesis of *trans*-substituted porphyrins with its success relying on the optimization of reaction conditions in order to minimize scrambling[1, 18]. Scrambling refers to the formation of different products following the initial protonation of dipyrromethane by acid catalyst, whereby a highly reactive species is generated. The mechanism of scrambling is illustrated in Scheme 2-3[19].

In our research, we focus on the synthesis of meso thienyl-porphyrins, with a *trans* configuration. We use the MacDonald [2 + 2] condensation to prepare the trans substituted porphyrins because not only is this method expected to afford better yields than mixed aldehyde

condensations, but it will also make the purification of the porphyrins obtained much easier. We anticipate that these

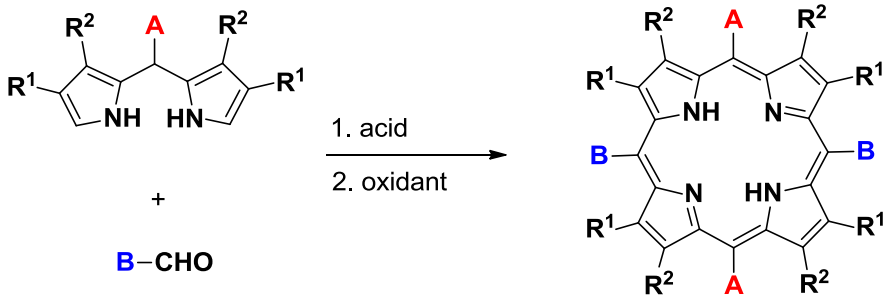

Scheme 2-2: MacDonald 2+2 Condensation

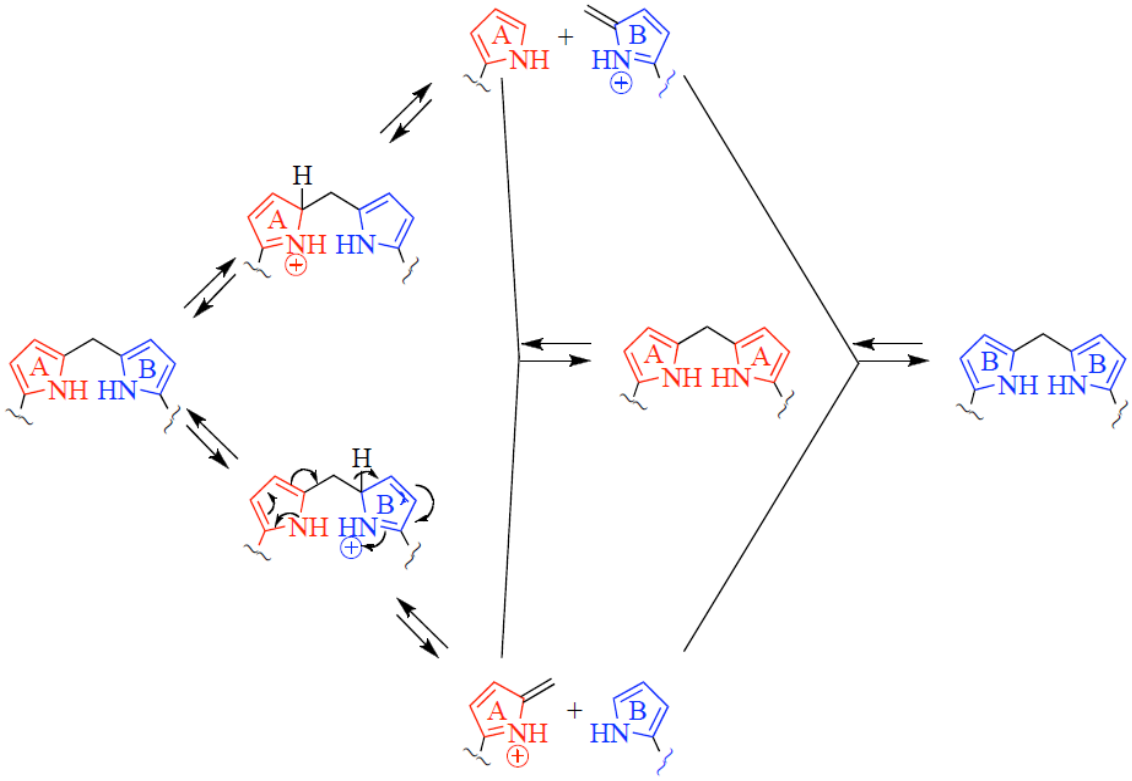

Scheme 2-3: Scrambling of dipyrromethane in the MacDonald[2+2] condensation[19]

systems will exhibit rich electrochemical and possibly biological properties that will make them ideal for both PDT and BNCT. Furthermore, we carry out chemical polymerization on some of

the porphyrins, which we expect to lead to polymers with fascinating properties for different applications.

2.5 Results and Discussion

We began the synthesis with preparation of dipyrromethane, **DP-1**. This was achieved by reacting thiophene-2-carbaldehyde with a large excess of pyrrole in the presence of TFA catalyst to afford **DP-1** in 64% yield[20]as illustrated in Scheme 2-4.

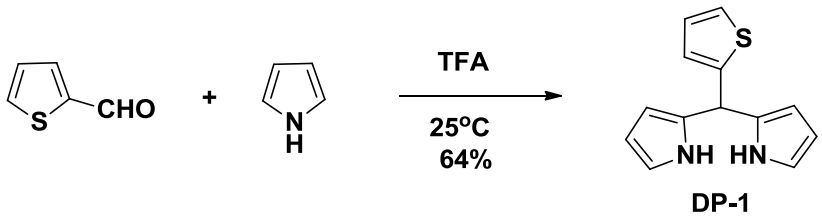

Scheme 2-4: Synthesis of **DP-1**

DP-1 was recrystallized from DCM. The molecular structure of **DP-1** is shown in Figure 1. The structure is seen to be non-planar. The –NH groups are facing away from each other, with the central carbon atom, C10-C5-C6 and C10-C5-C4 having an angle of 111.68^{o} and 112.01^{o} respectively. The thiophene ring is found to be smaller in size compared to the pyrrole ring, as seen from the C13-S1-C10 bond, 91.53^{o}, compared to C1-N1-C4, 109.80^{o}. In addition to this, the S-C bonds (S1-C13, 1.6524Å and S1-C10, 1.7212 Å) are found to be longer than N-C bonds (N1-C1 = 1.3767 Å, N1-C4 = 1.3770 Å and N2-C6 = 1.3681 Å, N2 = 1.3716 Å). This can be attributed to an atom size effect, where S has a larger covalent radius compared to N.

Using Lindsey's protocol, we carried out condensation reactions using different aldehydes, to obtain **PP1, PP2, PP3, PP4, PP6, PP7** and **PP8** in yields between 18% and 56% (see Scheme 2-5). Reaction conditions had to be optimized to minimize "scrambling" which would have resulted in more than one product. As can be seen from Table 2-1, the yields ranged between

18% and 56%. **PP1** recorded the highest yield. This is expected because only one porphyrin can be obtained from this reaction. During the purification of **PP3** and **PP4**, it was observed that in both cases, 2 other products were obtained (see Scheme 2-5).

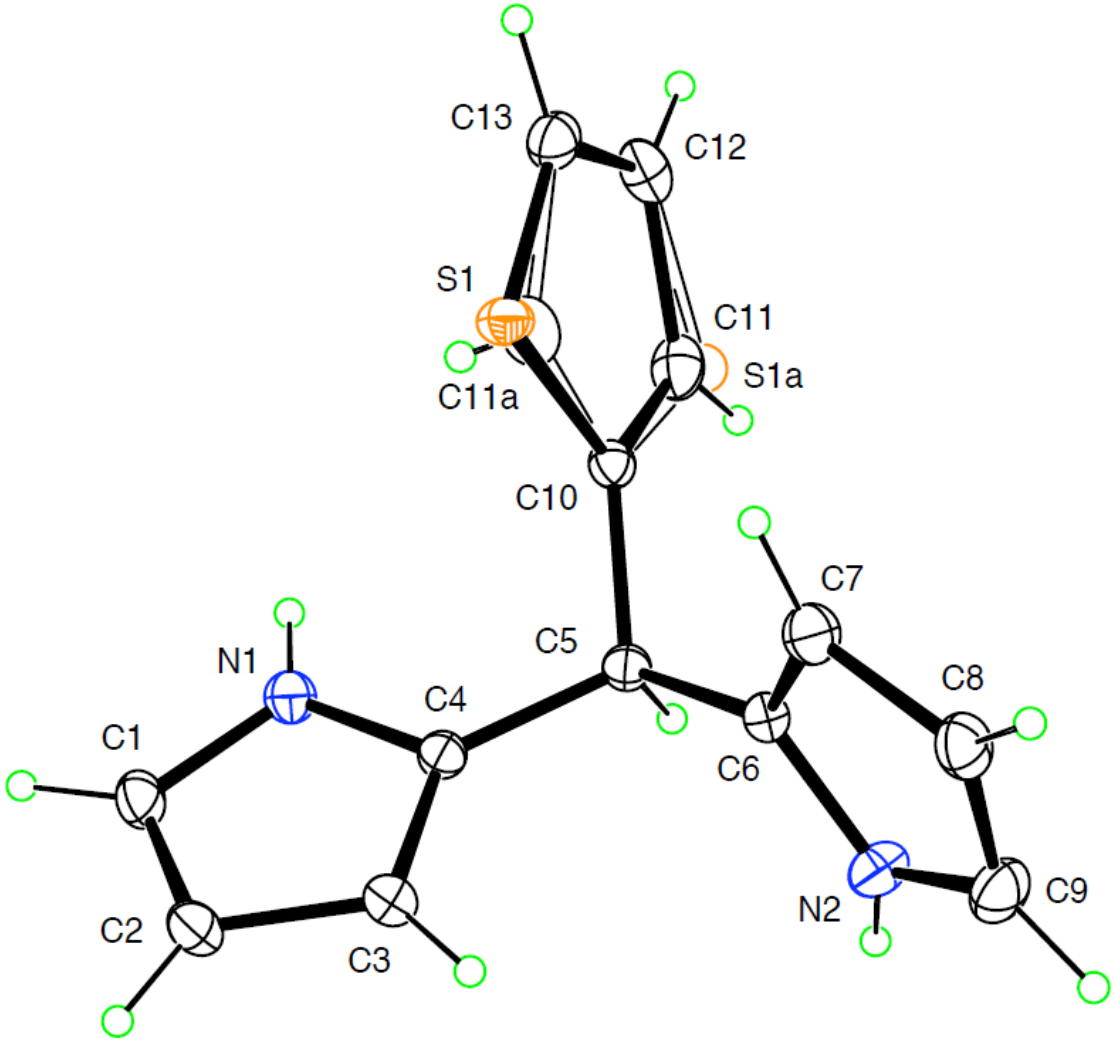

Figure 2-3: X-ray structure of **DP-1**

Scheme 2-4: Synthesis of **PP1-PP7**

Table 2-1: List of Porphyrins synthesized and the yields

Porphyrin	R	% yield
PP1	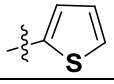	56%
PP2	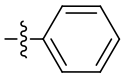	44%
PP3	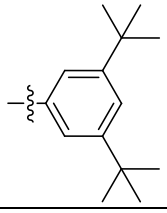	27%
PP4	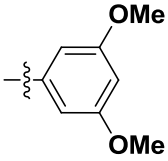	20%
PP5	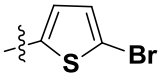	20%
PP6	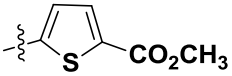	21%
PP7	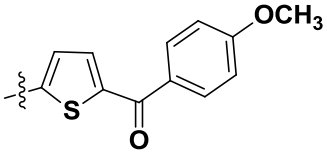	18%

These were confirmed using NMR and MS experiments. Despite efforts to optimize conditions, by changing the ratios of the starting reagents, and purging the reaction solutions with argon for longer periods, these products were still available. The minor products in both cases were easily purified by silica gel chromatography.

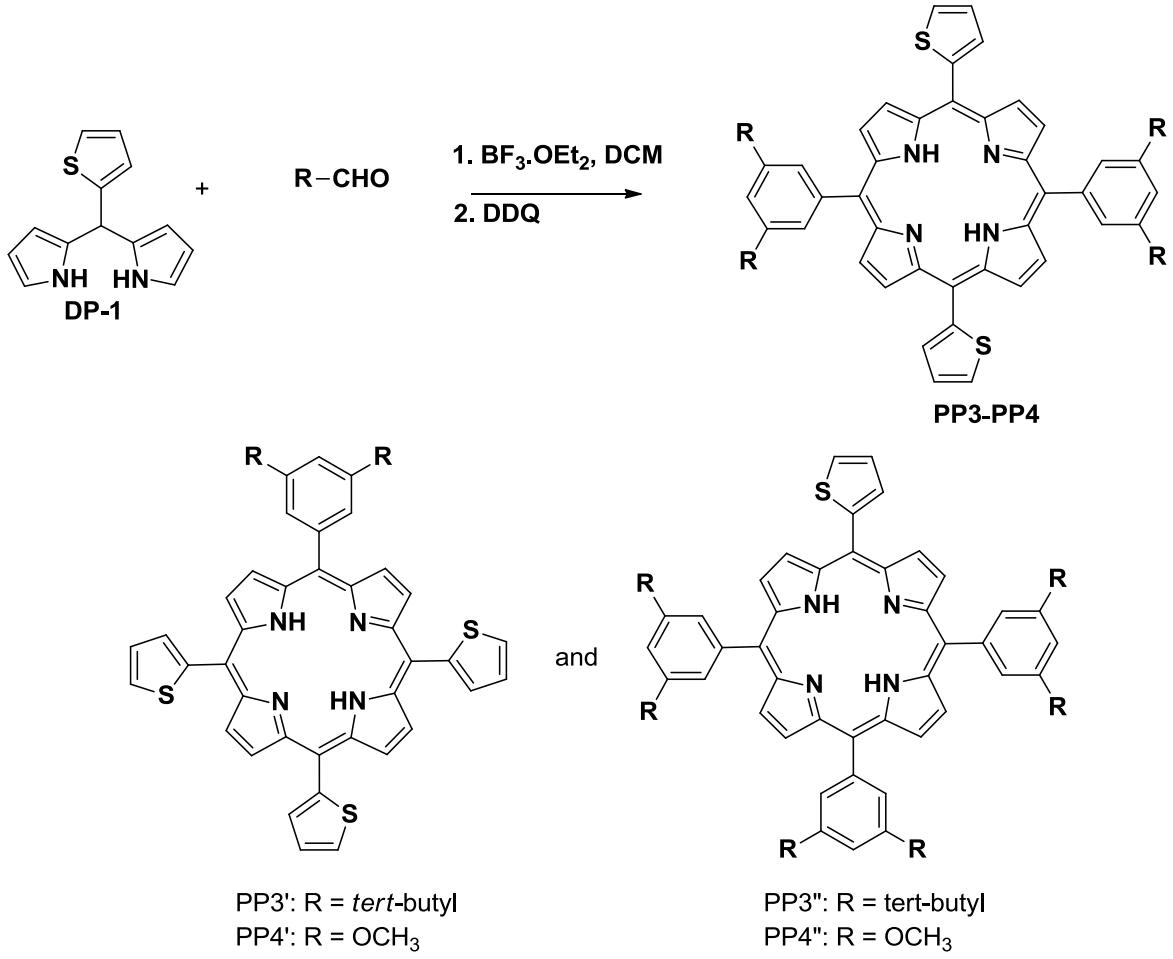

Scheme 2-5: Condensation reaction's minor products, **PP3'**, **PP4'**, **PP3"** and **PP4"**.

Table 2-2: Percentage yields for minor products **PP3', PP4', PP3"** and **PP4"**

Porphyrin	% Yield
PP3'	8%
PP4'	5%
PP3"	6%
PP4"	3%

Starting with thiophene-2-carbaldehyde, we carried out bromination reaction using one equivalent of Br_2 to obtain thiophene **1**. Reaction of **1** with large excess of pyrrole afforded **DP-2** in 67% yield. **DP-2** was condensed with 3,5-ditertbutylbenzaldehyde using Lindsey's method to afford **PP5**. The initial attempt to synthesize **PP5** included the direct bromination of **PP3** using NBS. This however, gave a mixture of products, brominated at both the α and β positions of the thiophene ring. Separation of the brominated products by silica gel chromatography proved to be difficult, and this led to low yields of the product. Better yields were obtained using the strategy outlined in Scheme 2-6.

Unlike the case in **PP3** and **PP4**, no porphyrin minor products in the synthesis of **PP6** and **PP7** were observed. The side products that were obtained could not be assigned structures using the obtained MS data. A possible reason for this could be that there was "scrambling" during the reaction process, and this led to formation of polypyrroles.

We prepared metal-porphyrin complexes by inserting Zn and Cu metals inside the free bases, using $Zn(OAc)_2$ and $Cu(OAc)_2$ respectively. This afforded the corresponding metal complexes in quantitative yields. To obtain the Zn-porphyrin complexes, the free bases and excess amount of $Zn(OAc)_2$ were dissolved in MeOH/DCM (1:3) and allowed to stir at room temperature for 24 h.

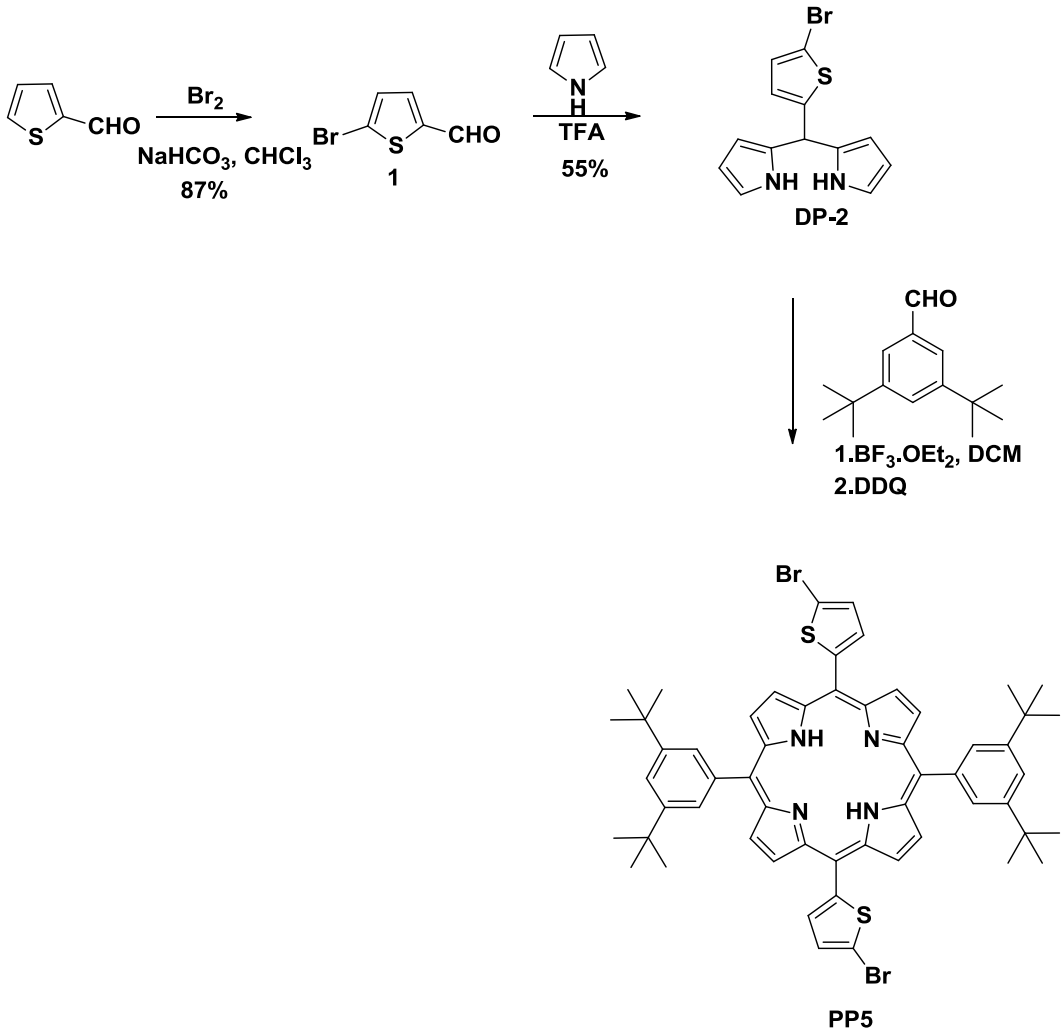

Scheme 2-6: Synthesis of **PP5**

Purification of the products was achieved by use of silica gel chromatography using DCM as eluent. In the case of Cu-porphyrin complexes, the free bases and excess amounts of $Cu(OAc)_2$ were dissolved in MeOH/DCM (1:3) and stirred overnight at room temperature, and then allowed to reflux for 4 hours to push the reaction to completion. Similarly, purification was achieved by silica gel chromatography using DCM for elution (see scheme 2-7).

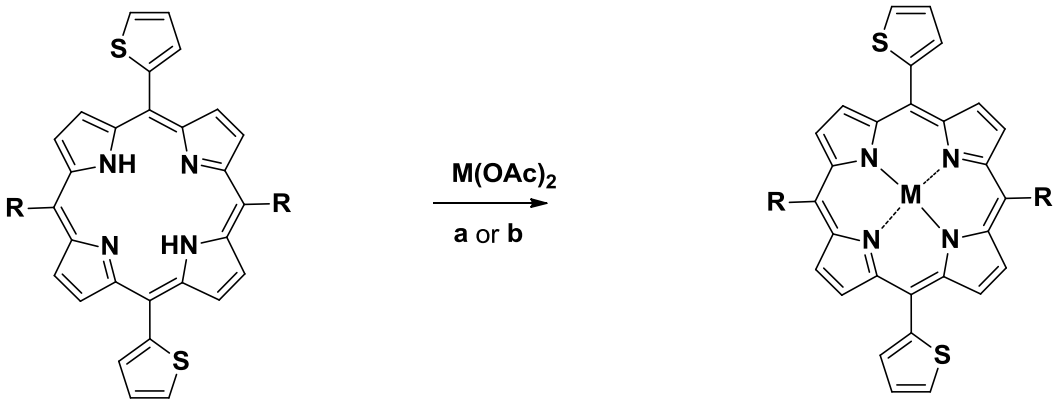

PP1-PP7 **MPP1-MPP7**

M=Zn, Cu

a) for Zn-porphyrin complexes: stir at R.T for 24 h. b) for Cu-porphyrin complexes: stir at R.T for 12 h, followed by reflux for 4 h.

Scheme 2-7: Synthesis of **MPP1-MPP7**

Table 2-3: Percentage yields for metal-porphyrin complexes

Zn-Porphyrin	% Yield	Cu-Porphyrin	% Yield
ZnPP1	54%	**CuPP1**	71%
ZnPP2	98%	**CuPP2**	94%
ZnPP3	53%	**CuPP3**	21%
ZnPP4	41%	**CuPP4**	71%
ZnPP5	62%	**CuPP5**	59%
ZnPP6	98%	**CuPP6**	21%
ZnPP7	72%	**CuPP7**	56%

As stated earlier, we were interested in synthesizing porphyrins for application in BNCT. Boron-containing porphyrins were therefore synthesized as shown in schemes 2-9, 2-10, 2-14 and 2-17. The deprotection of methoxy groups on **PP4** was performed using excess BBr_3 to give **PP8** in

87% yield[21]. Through a nucleophilic opening of the dioxane ring by the phenolate groups, **PP8** was conjugated with compound **2**[22], which was synthesized from commercially available COSAN[23]. Purification of the final product was achieved by column chromatography using 1:1 EtOAc/Hexane to afford **PP9** in 60% yield.

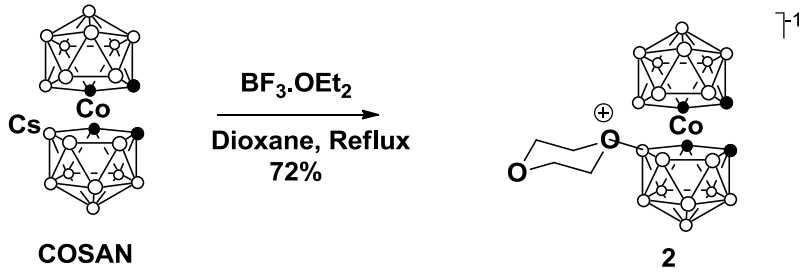

Scheme 2-7: Synthesis of Compound **2**

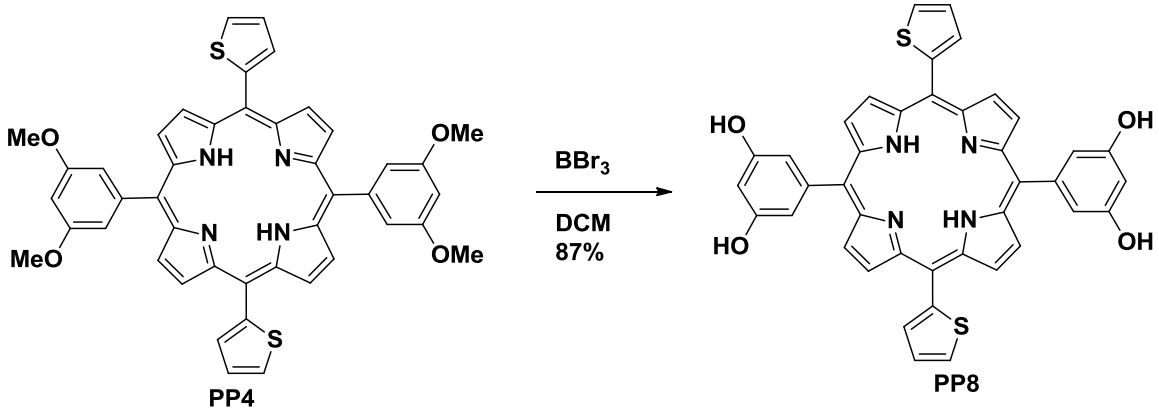

Scheme 2-8: Deprotection of **PP4** to give **PP8**

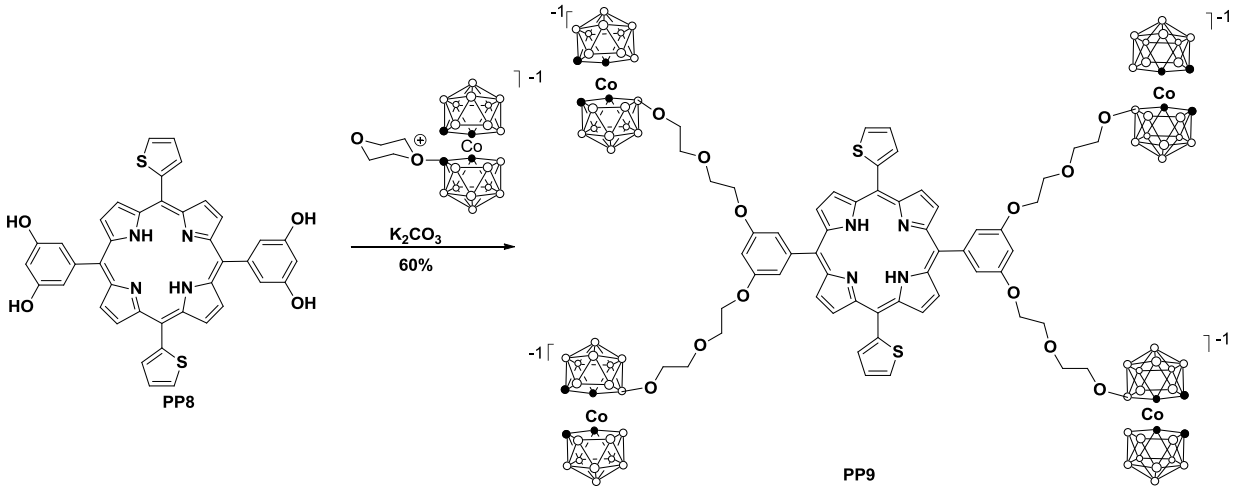

Scheme 2-9: Synthesis of **PP9**

PP10 was synthesized from commercially available 3,5-dimethylbromobenzene. Bromination of 3,5-dimethylbromobenzene with NBS in presence of BPO, a radical initiator, gave **3**[24]. Compound **3** reacted with 1-lithium-2-methyl-o-carborane, which was prepared *in situ*, to give dicarboranylbromobenzene, **4**, in 60% yield[24]. Reaction of **4** with n-BuLi followed by dry DMF and acid hydrolysis afforded dicarboranylbenzaldehyde **5**, in 55% yield[24]. Finally, aldehyde **6** was condensed with **DP-1** to afford **PP10** in 6% yield (see Scheme 2-10).

In an attempt to synthesize **PP11**, we started with commercially available 2-ethynylthiophene, as shown in Scheme 2-11. This compound was reacted with decarborane in presence of ethyl sulfide under reflux to afford **6** in 53% yield[25]. Attempts to introduce a formyl group at position 5 of the thiophene ring using n-BuLi and dry DMF and also using the Vilsmeier-Haack reaction[26] conditions were unsuccessful. This could be as a result of the strong electron-withdrawing character of the *o*-carborane unit which facilitates the metalation of the carborane C-H group as shown by Equation 2-1[27]. In addition to this, it has been shown that closo-carboranes undergo degradation in the presence of DMF[27b, 28].

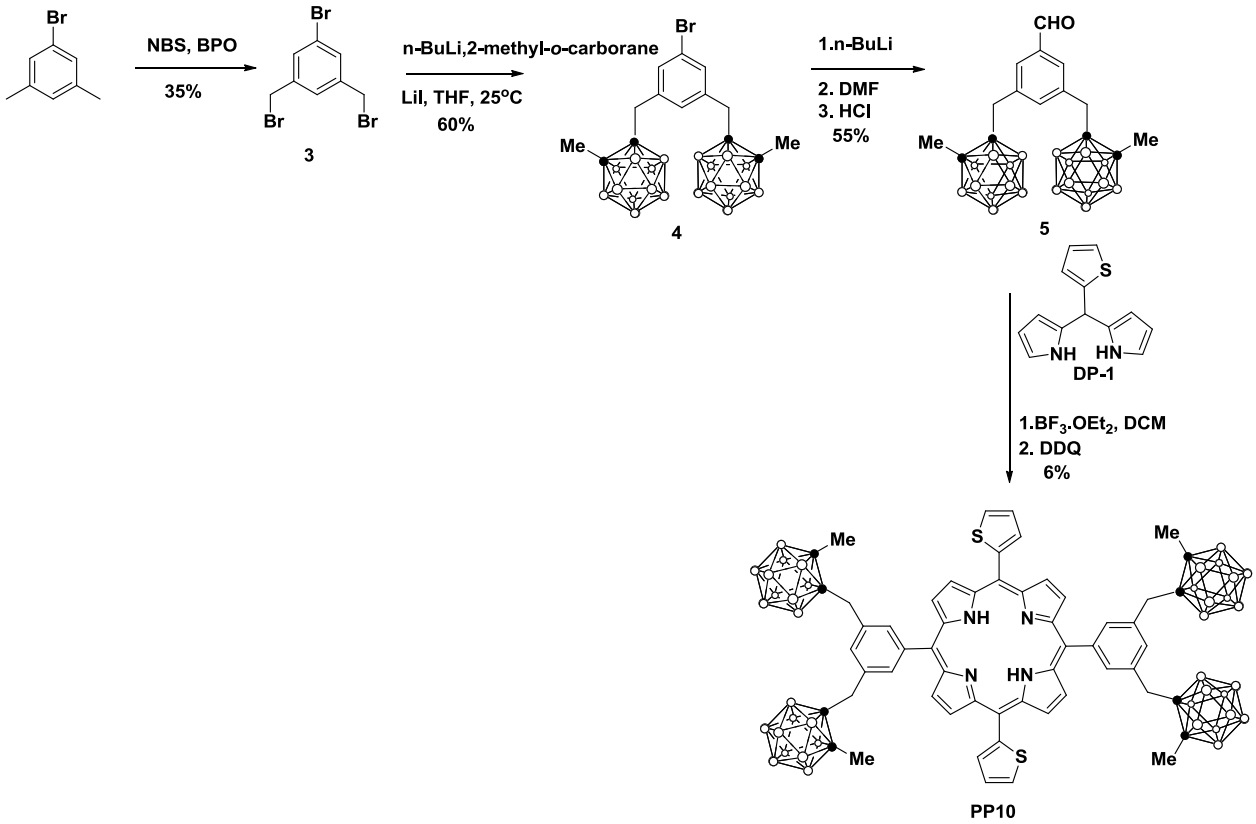

Scheme 2-10: Synthesis of **PP10**

$$RCB_{10}H_{10}CH + RLi \longrightarrow HCB_{10}H_{10}CLi + RH$$

Equation 2-1: Metalation of the *o*-carborane C-H group

The synthesis strategy was changed so that we started with thiophene-2-carbaldehyde. This compound was brominated with Br_2 to afford 87% of compound **1**[29]. Compound **1** was reacted with TMSA in a Sonogashira coupling reaction, in the presence of $PdCl_2(PPh_3)_2$ and CuI catalysts to afford 43% of compound **7**[30]. Deprotection of **7** using K_2CO_3 afforded **8** in 87% yield[31]. An attempt to add the carborane ring to compound **8** using a similar procedure described

in Scheme 2-11 was unsuccessful. Attempts to protect the aldehyde using 1,2-ethanedithiol, as described in literature, also proved to be difficult, as a result of formation of products that were difficult to purify.

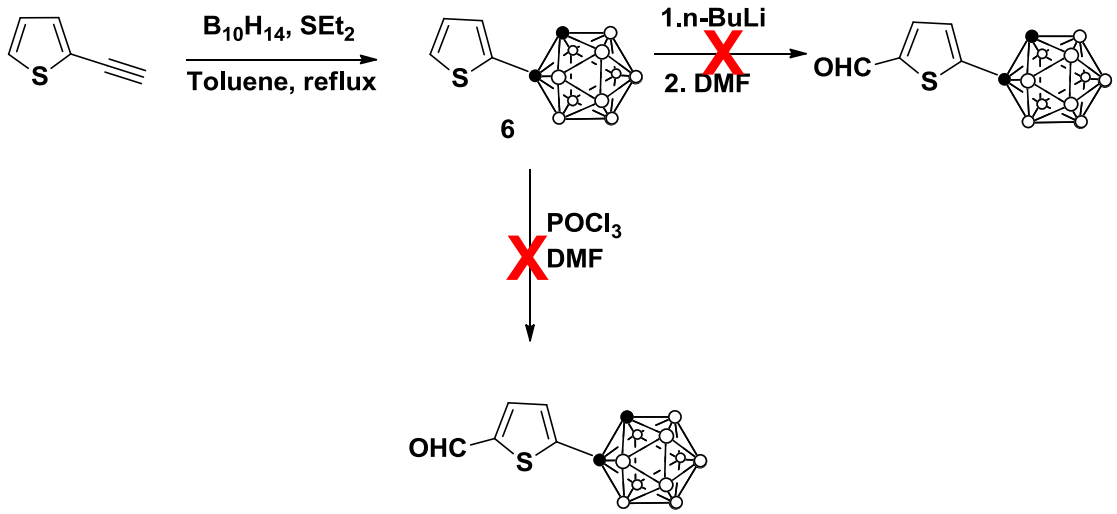

Scheme 2-11: Attempted introduction of formyl group on thiophene ring

Compound **8** was then condensed with excess pyrrole in presence of TFA catalyst to afford **DP-3** in 23% yield. Because of the low yield obtained for **DP-3** we decided to synthesize the dipyrromethane directly from compound **7**. This was achieved by reacting **7** with excess pyrrole in presence of TFA catalyst to afford **DP-4** in 63% yield. Deprotection of the trimethylsilane group using K_2CO_3 afforded **DP-3** in 78% yield[31]. Finally reaction of **DP-3** with decaborane afforded **DP-5** in 51% yield. Condensation of **DP-5** with 3,5-ditertbutylbenzaldehyde afforded **PP11** in 34% yield. From the MS data obtained on the other fractions obtained during purification, no other porphyrins were obtained. However, we detected presence of unreacted starting aldehyde and dipyrromethane.

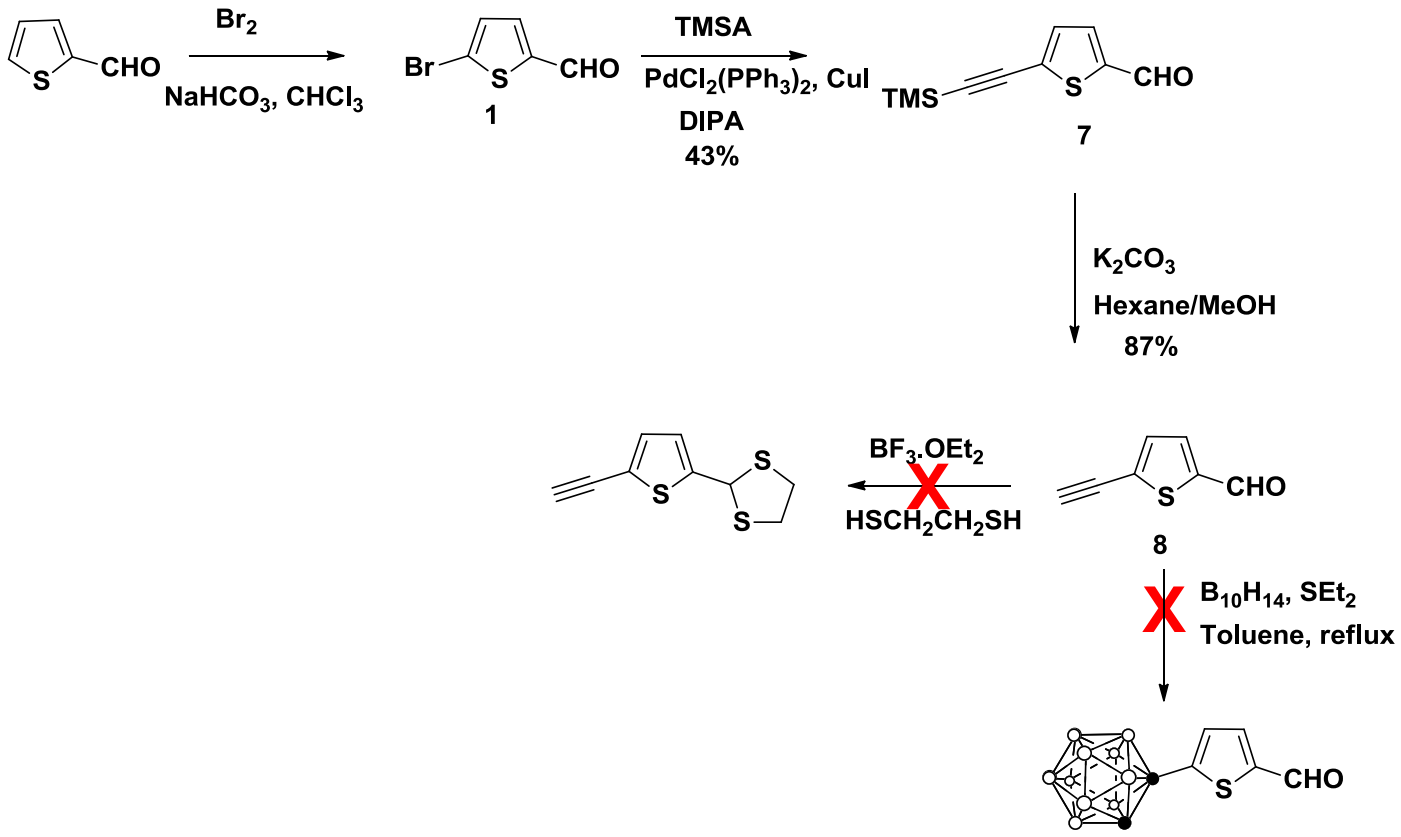

Scheme 2-12: Attempted incorporation of carborane on Compound **8**

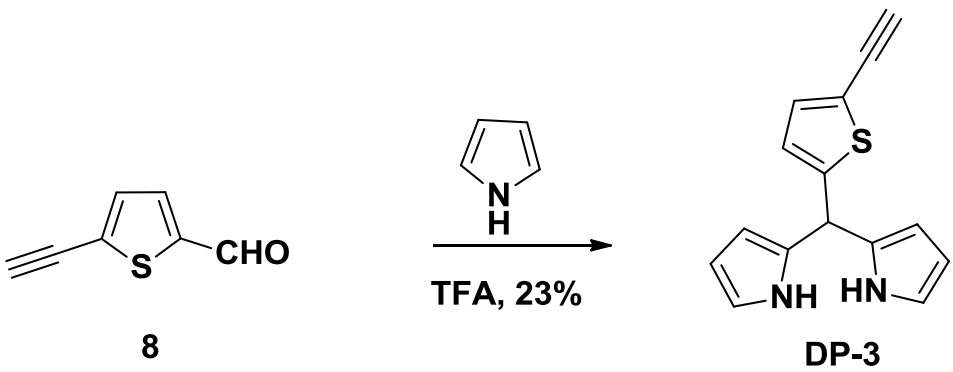

Scheme 2-13: Synthesis of **DP-3**

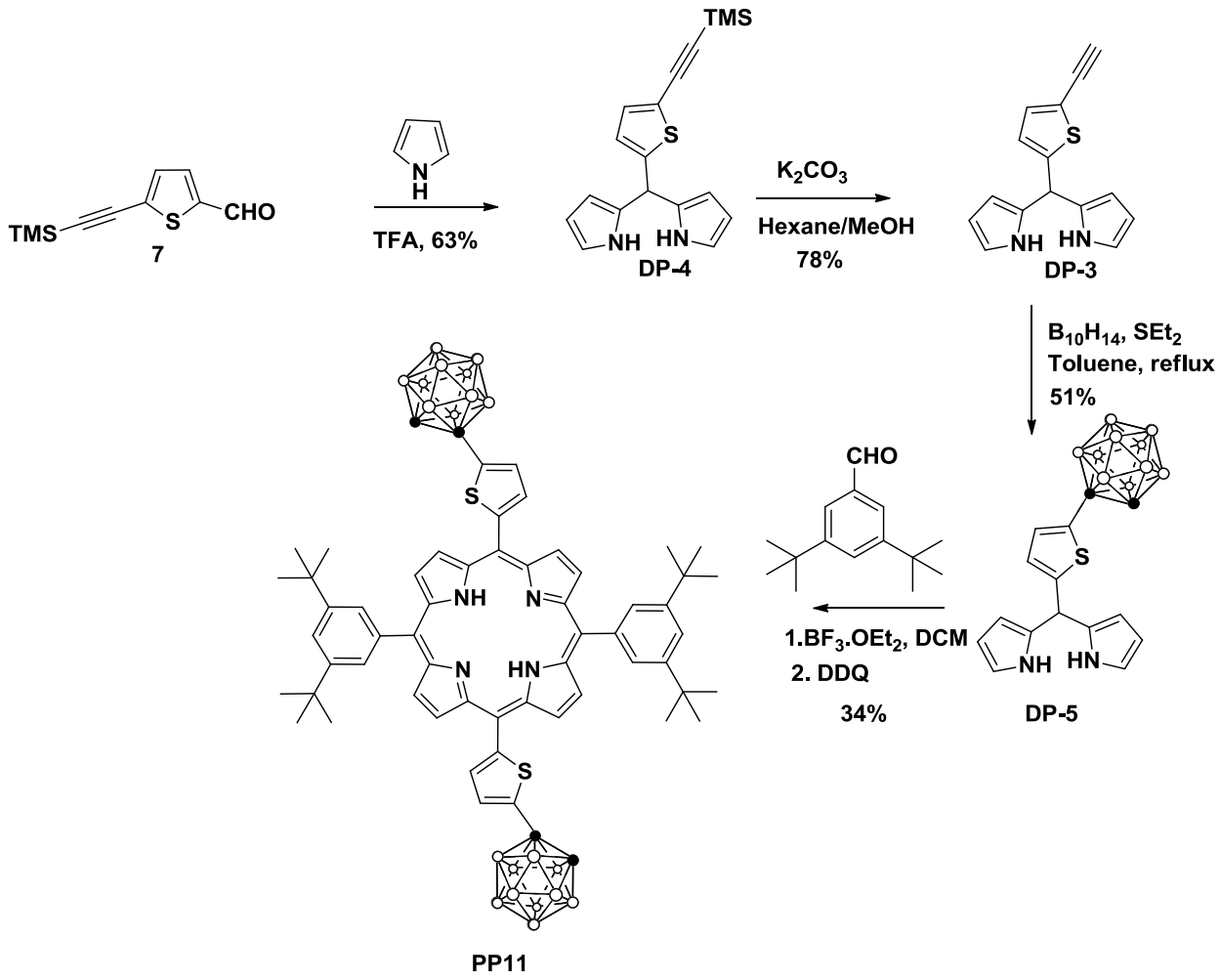

Scheme 2-14: Synthesis of **PP11**

The first attempt in the synthesis of **PP12** similarly started with commercially available 5-bromo-2,2'-bithiophene (see Scheme 2-15). This compound was reacted with TMSA under Sonogashira coupling reaction conditions, with $PdCl_2(PPh_3)_2$ and CuI as the catalysts, to afford **9** in 47% yield[30]. Deprotection of the trimethylsilane group was achieved by reacting **9** with K_2CO_3 to afford **10** in 80% yield[31]. Using similar conditions described earlier for introduction of carborane, **11** was obtained in 73% yield[25]. Attempts to introduce an aldehyde functional group at this point were unsuccessful.

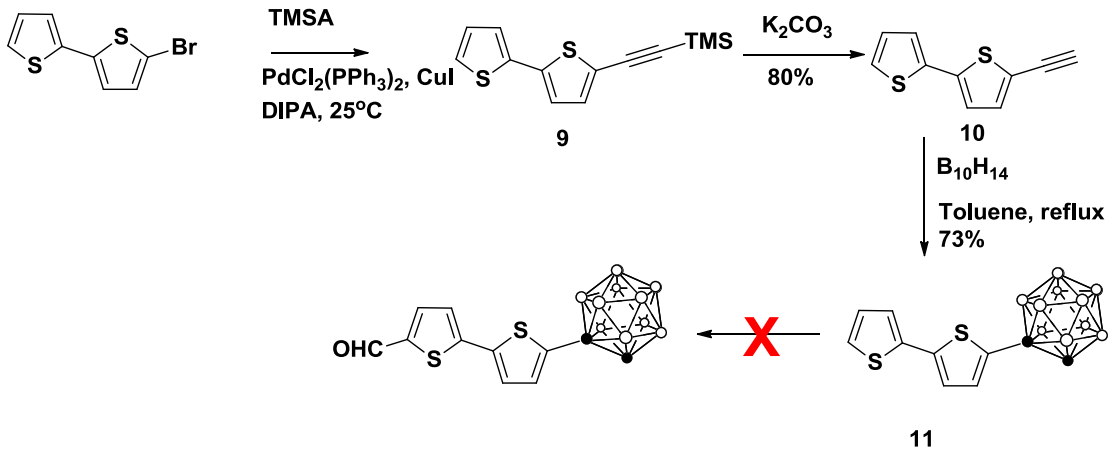

Scheme 2-15: Attempted introduction of formyl functional group on Compound **11**.

Bromination of [2,2'-bithiophene]-5-carbaldehyde using Br_2 afforded 89% of compound **12**[32] (Scheme 2-16). Reaction of **12** with TMSA under Sonogashira conditions afforded 37% of **13**[30]. Condensation of **13** with excess pyrrole afforded 65% of **DP-6**. This was followed by deprotection of the trimethylsilane group to obtain **DP-7** in 73% yield[31]. Reaction of **DP-7** with decaborane under reflux afforded 55% of **DP-8**[25]. **DP-8** was condensed with 3,5-ditertbutylbenzaldehyde to afford 8% of **PP12**.

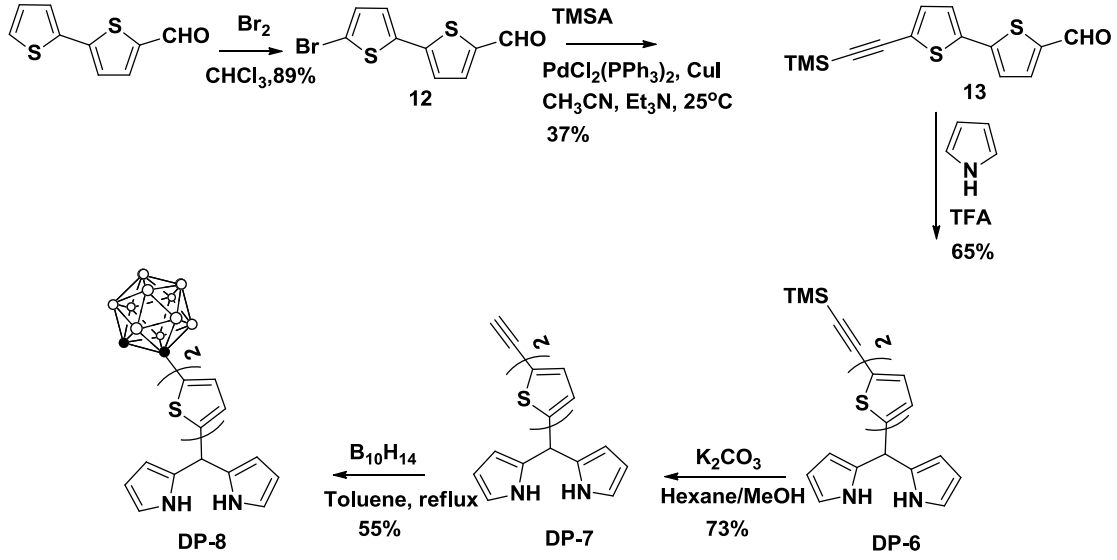

Scheme 2-16: Synthesis of **DP-8**

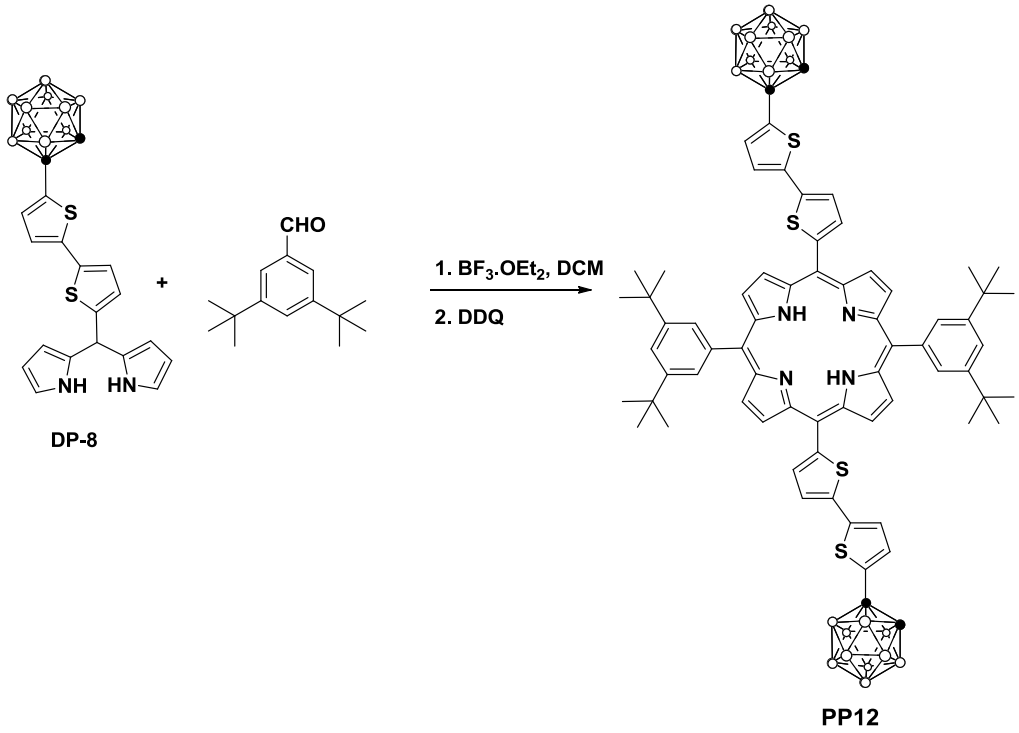

Scheme 2-17: Synthesis of **PP12**

Synthesis of **DP-9** was achieved by reaction of [2,2'-bithiophene]-5-carbaldehyde with excess pyrrole in presence of TFA. This afforded the target product in 64% yield, see Scheme 2-18. **DP-9** was then condensed with 3,5-ditertbutylbenzaldehyde and 3,5-dimethoxybenzaldehyde using the Lindsey method to afford **PP12** and **PP13** in 21% and 18% yields, respectively (see Scheme 2-19).

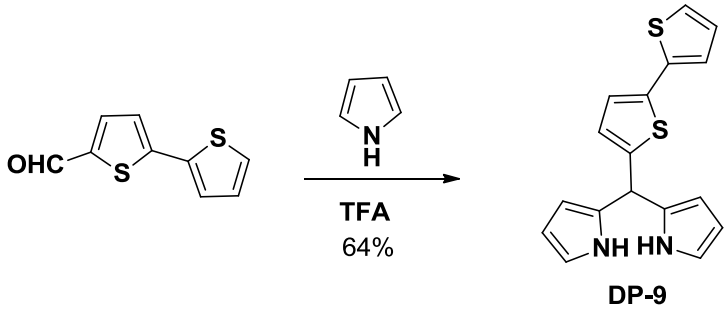

Scheme 2-18. Synthesis of **DP-9**

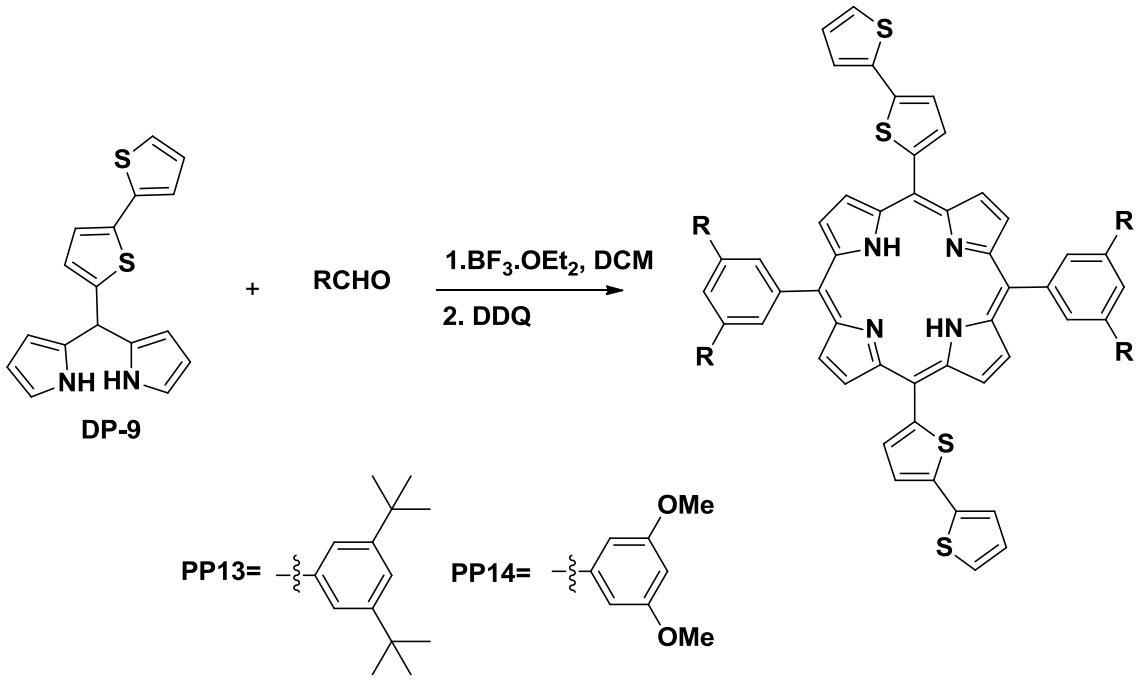

Scheme 2-19: Synthesis of **PP13** and **PP14**

Table 2-4: Percentage Yields for **PP13** and **PP14**

Porphyrin	% Yield
PP13	21%
PP14	18%

We attempted to polymerize **PP5** using Sonogashira coupling reaction conditions as shown in Scheme 2-20. We reacted **PP5** with commercially available 1,4-diethynylbenzene. Unfortunately no polymer was obtained. MS showed that the starting reagents were recovered. It is clear that the reaction conditions should be optimized. This can be achieved by either reacting for a longer time or by heating at higher temperatures, or by changing the catalyst used in the reaction.

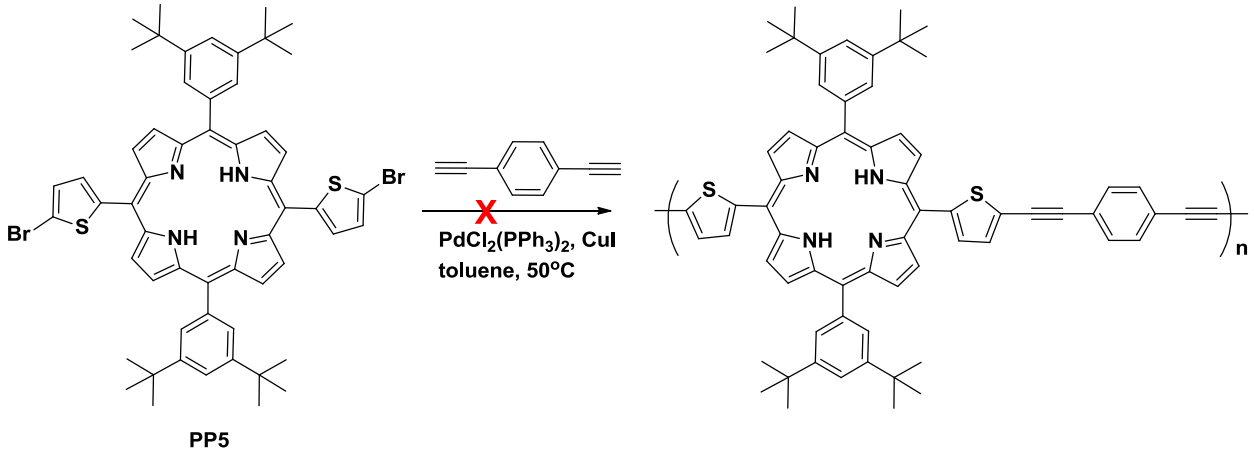

PP5

Scheme 2-20: Attempted polymerization of **PP5**

2.6 Photophysical Studies

The maximum wavelengths of absorptions and molar extinction coeffecients for **PP1-PP9** in toluene and DMF are listed in Tables 2-5 and 2-6. Compared to **TPP**, the absorption bands of thienyl-porphyrins are slightly bathochromically shifted by 3-14 nm, with the biggest shift being observed in the cobaltabarborane containing, **PP9**. These shifts indicate that replacing the six-membered phenyl ring with a five membered thienyl ring, significantly alters the electronic properties of the porphyrin, which leads to a greater π-delocalization of the porphyrin into the thienyl group by resonance interaction[33]. A study of the Zn- complexes of the thienyl-porphyrins, further indicated that the metal complexes in general showed red-shift Soret bands relative to the free bases. This observation is consistent with what has been observed in literature[13]. This can be as a result of change in geometry when the Zn metal is inserted inside the porphyrin core, a process that leads to the loss of $2H^+$. Thienyl-porphyrins typically exhibit Q-bands in the 550-800 nm region[34].The emission data for the thienyl-porphyrin free bases, **PP1-PP9**, as well as the Zn complexes in both toluene and DMF are listed in Tables 2-5, 2-6, 2-7 and 2-8. Both the free

bases and the **ZnPPs** show a considerable red shift in emission bands relative to **TPP** and **ZnTPP** respectively. When determining quantum yields of unknowns, the common practice is to do this by comparing with a standard of known fluorescence yield. In our case, the standard used is **TPP** (Φ_F = 0.11)[35] for the free bases, and **ZnTPP** (Φ_F = 0.033)[35] for ZnPPs. Compared to **TPP**, thienyl-porphyrins have been shown to have lower quantum yields[34]. This can be attributed to the presence of the heavy atom, sulfur, which quenches fluorescence. In our study, the same trend was observed, not only for the free bases, but also for the Zn complexes. One observation worth mentioning was the strikingly different quantum yields of **PP9** in toluene and DMF. **PP9** showed a quantum yield value of 0.164 in toluene, but a significantly lower value of 0.029 in DMF. This correlates with literature findings which showed that in polar solvents, compounds containing nido-carboranes exhibited low quantum yields. This has been attributed to presence of hydrogen bonding, which enhances non-radioactive decay, and in turn reduced quantum yield[36]. **CuPPs** showed a slightly blue shift in their absorption bands compared to both the **ZnPPs** and the free bases. This could be attributed to the geometry of the Cu-porphyrin complexes. Cu^{II} has a d^9 electronic configuration. The unpaired electron in the $d_{x^2-y^2}$ orbital pairs with the porphyrin (π,π^*) excited states. As a result, these complexes do not exhibit the typical fluorescence as in the case of Zn-porphyrin complexes, which has a closed shell. Rather, it undergoes strong phosphorescence[37].

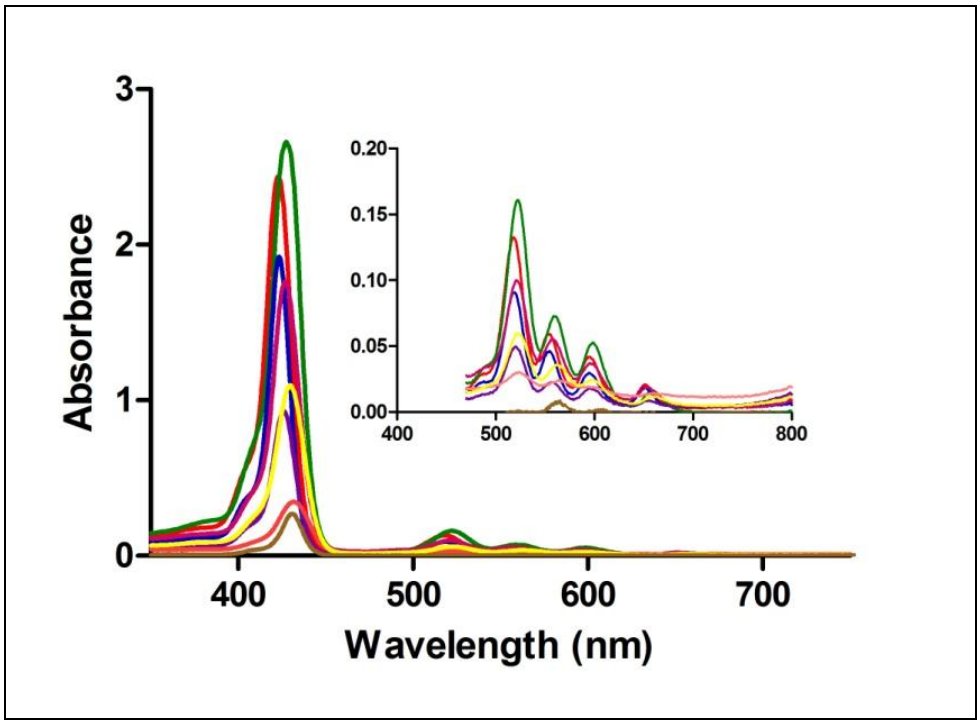

Figure 2-4: UV-Vis Absorption Spectra for **PP1** (red), **PP2** (green), **PP3** (blue), **PP4** (purple), **PP5** (maroon), **PP6** (pink), **PP7** (yellow), and **PP9** (brown) at 6μM concentration in Toluene

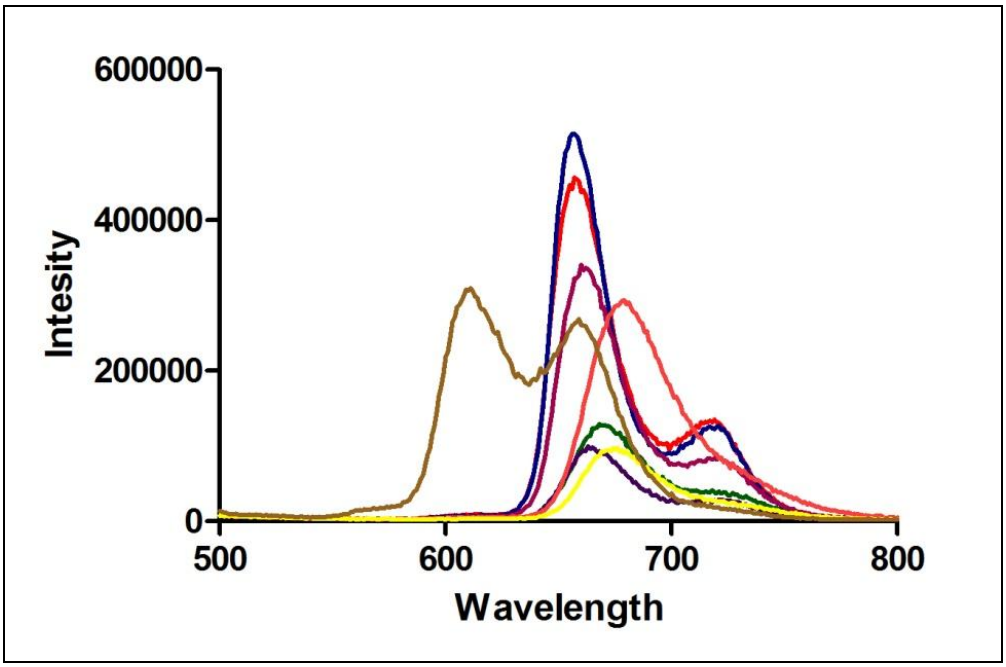

Figure 2-5: Emission Spectra for **PP1** (red), **PP2** (green), **PP3** (blue), **PP4** (purple), **PP5** (maroon), **PP6** (pink), **PP7** (yellow), and **PP9** (brown) at 1μM concentration in Toluene

Table 2-5: Photophysical Data for **PP1-PP9** and in Toluene

Compound	Absorbance λ_{max}(nm)	Q-bands λ_{max} (nm)	Emission λ_{max} (nm)	Stoke's Shift (nm)	Quantum Yield (Φ)	Log Ɛ ($M^{-1}cm^{-1}$)
TPP	418	505,539,580,640	644,702(sh)	225, 284	0.11	-
PP1	421	510,547,588,646	656, 709(sh)	235, 288	0.030	5.62
PP2	423	516,554,593,649	667, 711(sh)	244, 288	0.009	5.64
PP3	423	511,547,588,644	654, 711(sh)	231, 288	0.043	5.65
PP4	425	514,559,589,647	664, 712(sh)	239, 287	0.015	5.06
PP5	425	514,553,590,646	659, 711(sh)	234, 286	0.027	5.58
PP6[a]	428	516,558,595,654	674	246	0.015	5.64
PP7	427	516,556,594,653	673, 724(sh)	246, 297	0.014	5.63
PP9	429	558, 598,652	608, 655(sh)	179, 226	0.164	5.45

a -2 drops of TFA added to solution

Table 2-6: Photophysical Data for **PP1-PP9** in DMF

Compound	Absorbance λ_{max} (nm)	Q-bands λ_{max} (nm)	Emission λ_{max} (nm)	Stoke's Shift (nm)	Quantum Yield (Φ)	Log Ɛ (M^{-1} cm^{-1})
TPP	416	505,547	646,708(sh)	230, 292	0.11	-
PP1	420	511,547,588,643	652,707(sh)	232, 287	0.030	5.64
PP2	425	515,553,590,649	670, 716(sh)	245, 291	0.010	5.59
PP3	421	512,547,586,643	653, 712(sh)	232, 291	0.044	5.47
PP4	424	514,552,588,648	663, 710(sh)	239, 286	0.015	5.36
PP5	424	513,551,589,644	657, 709(sh)	233, 285	0.026	5.48
PP6[a]	426	516,558,593,650	672	246	0.025	5.53
PP7	426	515,555,591,650	671, 723(sh)	245, 297	0.015	5.50
PP9	430	560, 598,645	616, 661(sh)	186, 231	0.029	5.35

a 2 drops of TFA added to solution

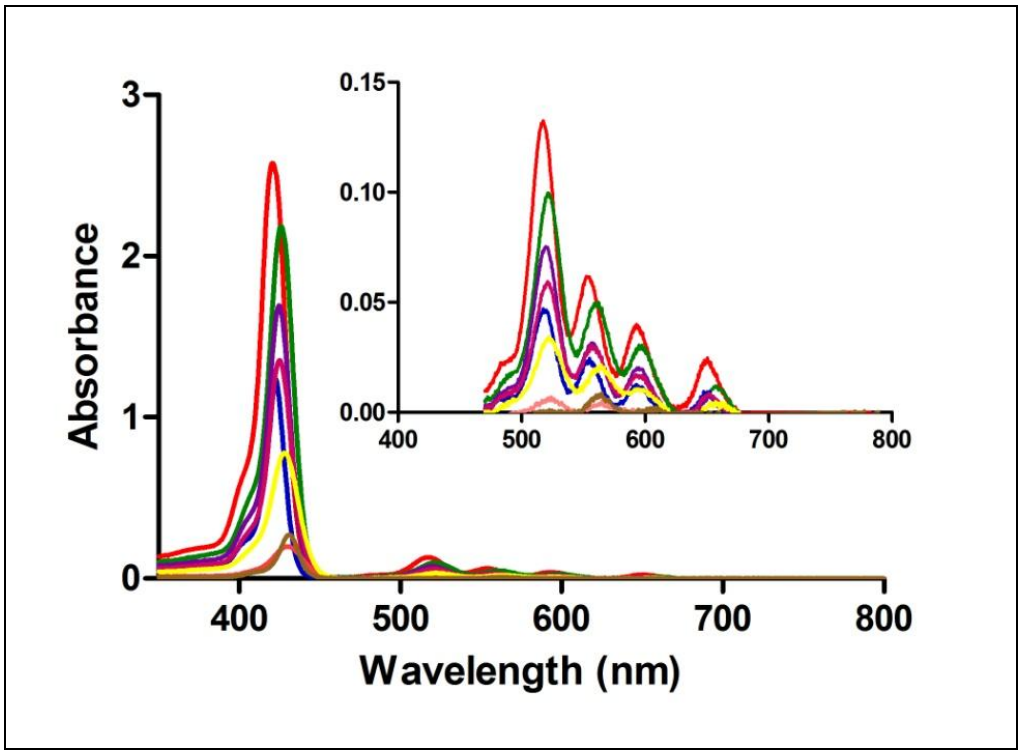

Figure 2-6: UV-Vis Absorption Spectra for **PP1** (red), **PP2** (green), **PP3** (blue), **PP4** (purple), **PP5** (maroon), **PP6** (pink), **PP7** (yellow), and **PP9** (brown) at 6μM concentration in DMF

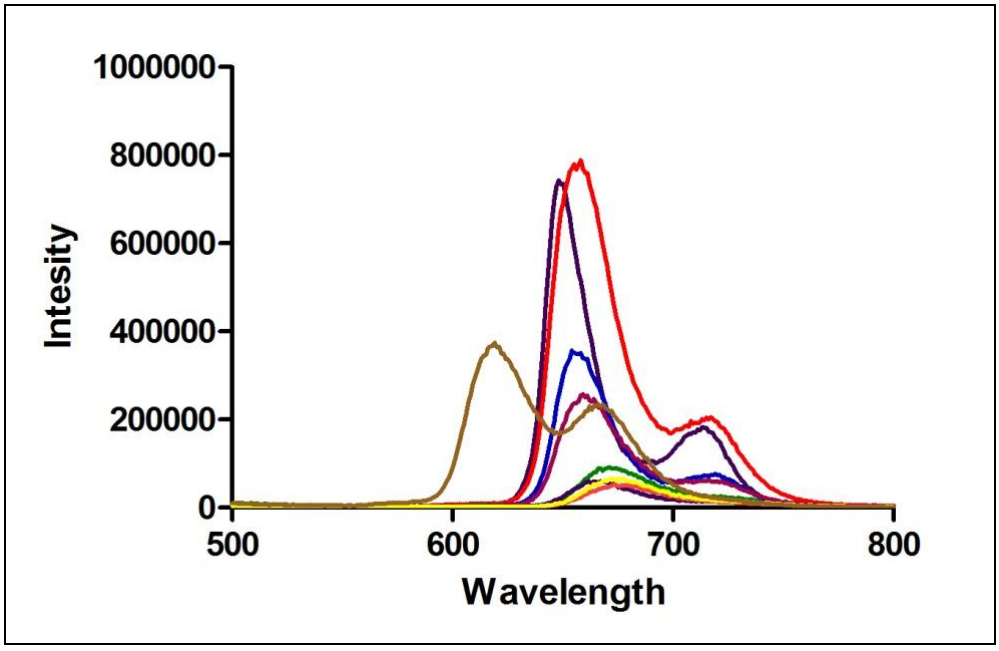

Figure 2-7: Emission Spectra for **PP1** (red), **PP2** (green), **PP3** (blue), **PP4** (purple), **PP5** (maroon), **PP6** (pink), **PP7** (yellow), and **PP9** (brown) at 1μM concentration in DMF

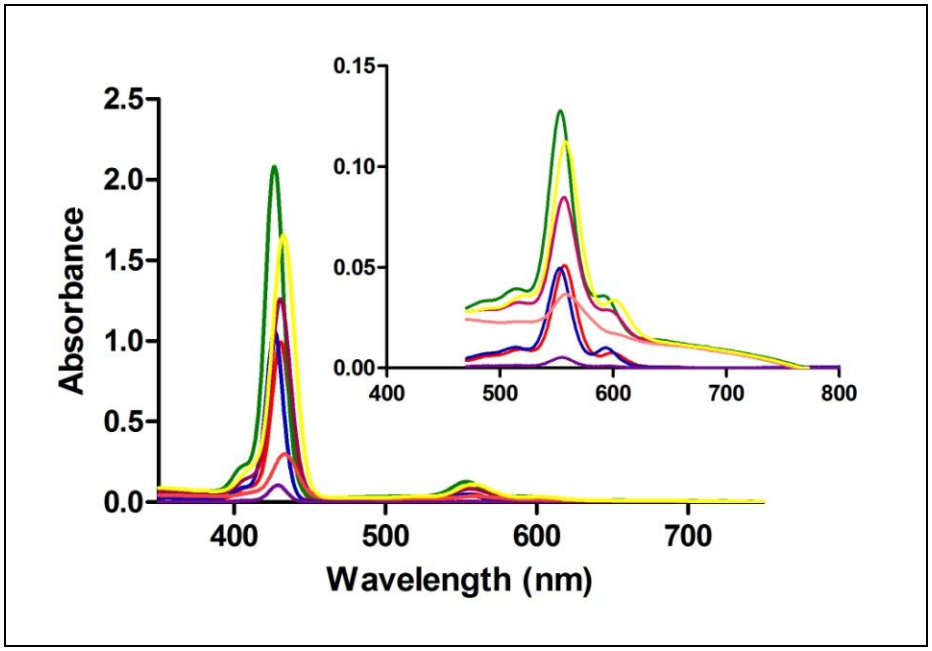

Figure 2-8: UV-Vis Absorption Spectra for **ZnPP1** (red), **ZnPP2** (green), **ZnPP3** (blue), **ZnPP4** (purple), **ZnPP5** (maroon), **ZnPP6** (pink), and **ZnPP7** (yellow) at 4μM concentration in Toluene

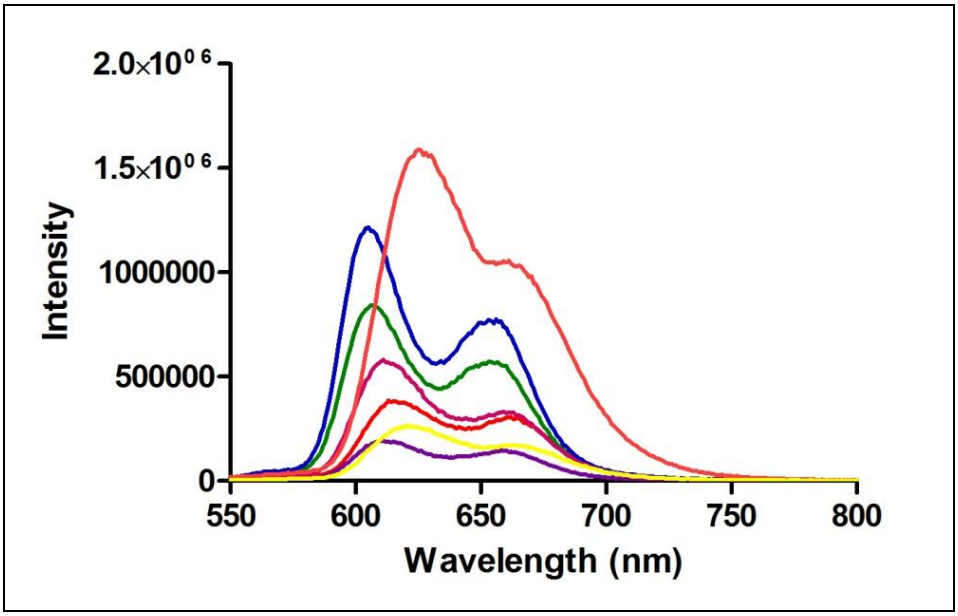

Figure 2-9: Emission Spectra for **ZnPP1** (red), **ZnPP2** (green), **ZnPP3** (blue), **ZnPP4** (purple), **ZnPP5** (maroon), **ZnPP6** (pink), and **ZnPP7** (yellow) at at 1μM concentration in Toluene

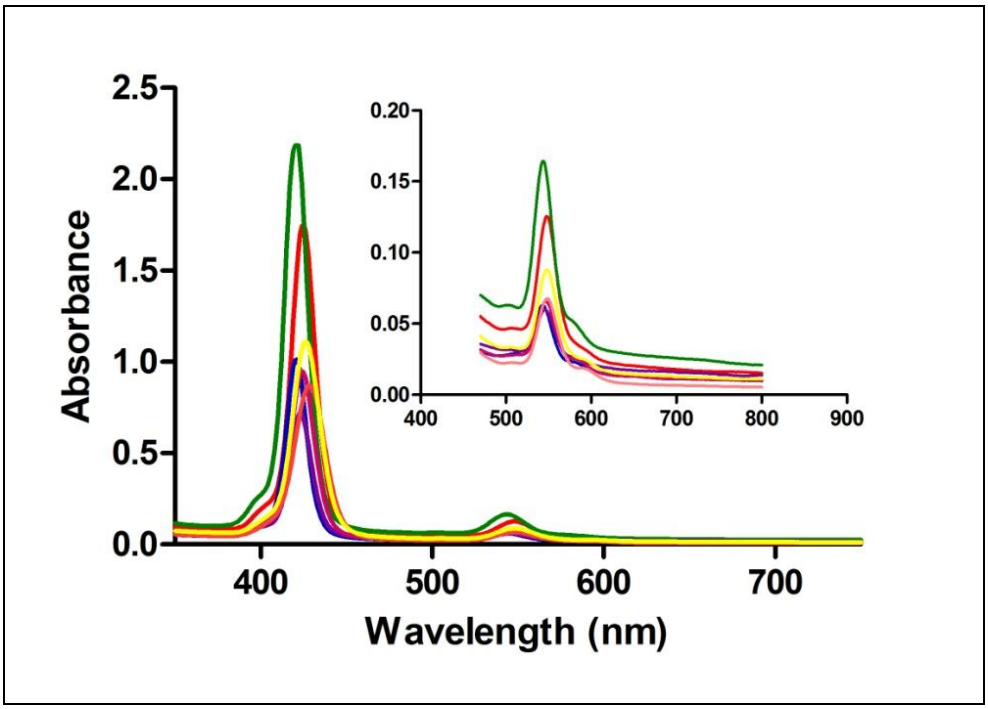

Figure 2-10: UV-Vis Absorption Spectra for **ZnPP1** (red), **ZnPP2** (green), **ZnPP3** (blue), **ZnPP4** (purple), **ZnPP5** (maroon), **ZnPP6** (pink), and **ZnPP7** (yellow) at 4μM concentration in DMF.

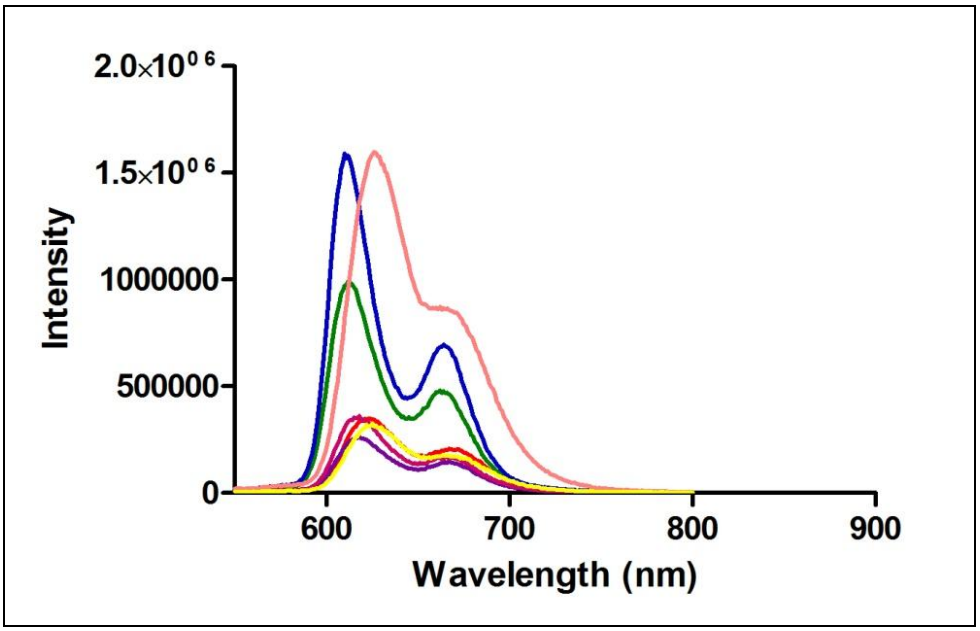

Figure 2-11: Emission Spectra for **ZnPP1** (red), **ZnPP2** (green), **ZnPP3** (blue), **ZnPP4** (purple), **ZnPP5** (maroon), **ZnPP6** (pink), and **ZnPP7** (yellow) at 6μM concentration in at 1μM DMF

Table 2-7: Photophysical Data for **ZnPPs** in Toluene

Compound	Absorbance λ_{max} (nm)	Q-bands (nm)	Emission λ_{max} (nm)	Stoke's shift (nm)	Quantum Yield (Φ)	Log Ɛ (M^{-1} cm^{-1})
ZnPP1	428	551,596	613,657	185, 229	0.02	5.3
ZnPP2	426	548	604,648	178, 222	0.04	5.5
ZnPP3	426	547	602,649	176, 223	0.03	5.5
ZnPP4	428	551	608,656	180, 228	0.02	4.6
ZnPP5	430	552	609,653	179, 223	0.001	5.7
ZnPP6	432	554	621,657	189, 225	0.01	4.6
ZnPP7	431	557	618,658	187, 227	0.02	5.6

Table 2-8: Photophysical Data for **ZnPPs** in DMF

Compound	Absorbance λ_{max} (nm)	Q-bands (nm)	Emission λ_{max} (nm)	Stoke's shift (nm)	Quantum Yield (Φ)	Log Ɛ (M^{-1} cm^{-1})
ZnPP1	428	560, 603	618,664	190, 236	0.01	5.5
ZnPP2	428	558, 599	609,658	181, 230	0.02	5.2
ZnPP3	429	557, 598	609,659	180, 230	0.02	5.6
ZnPP4	430	559	616,664	186, 234	0.01	4.8
ZnPP5	431	559, 603	615,661	184, 230	0.01	5.7
ZnPP6	433	560, 604	624,662	191, 229	0.05	4.7
ZnPP7	433	560, 604	622,664	189, 231	0.01	5.6

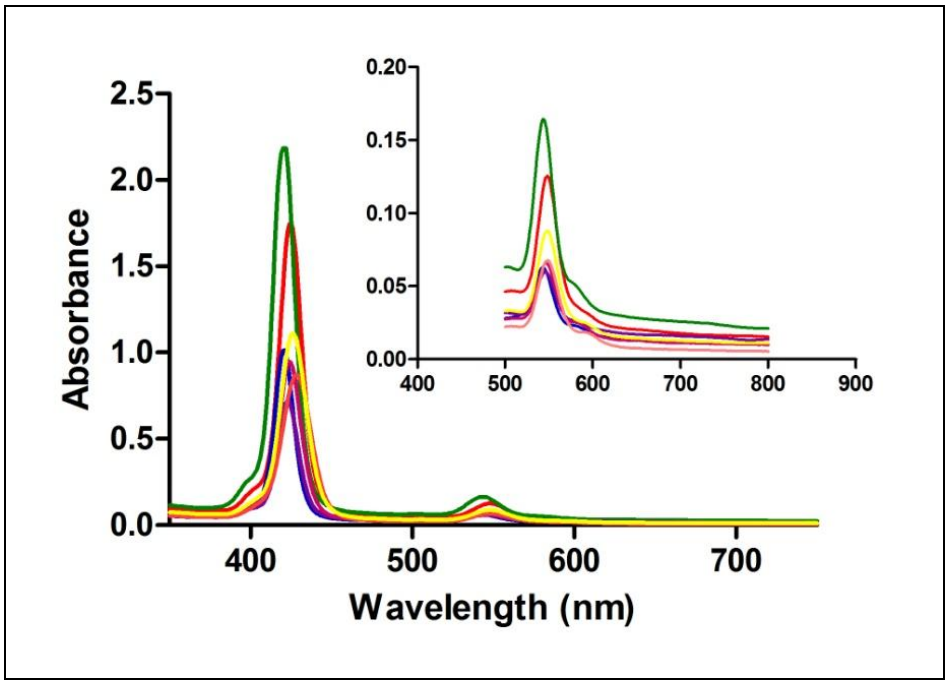

Figure 2-12: UV-Vis Absorption Spectra for **CuPP1** (red), **CuPP2** (green), **CuPP3** (blue), **CuPP4** (purple), **CuPP5** (maroon), **CuPP6** (pink), and **CuPP7** (yellow) at 4μM concentration in Toluene.

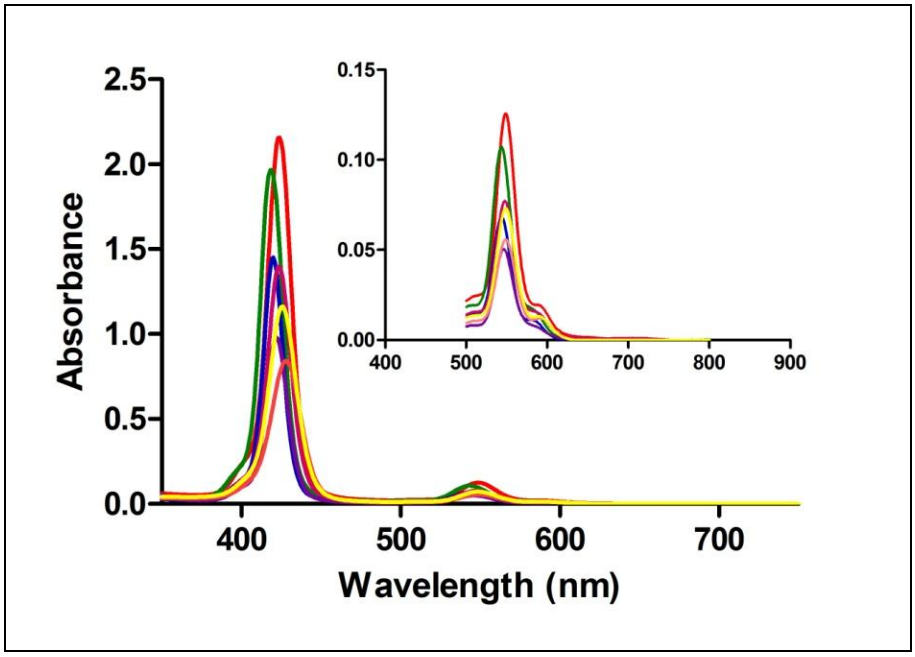

Figure 2-13: UV-Vis Absorption for **CuPP1** (red), **CuPP2** (green), **CuPP3** (blue), **CuPP4** (purple), **CuPP5** (maroon), **CuPP6** (pink), and **CuPP7** (yellow) at 4μM concentration in DMF.

Table 2-9: Photophysical Data for **CuPPs** in Toluene

Compound	Absorbance λ_{max} (nm)	Q-bands (nm)	Log Ɛ (M^{-1} cm^{-1})
CuPP1	423	537	5.2
CuPP2	418	533	5.5
CuPP3	419	532	5.5
CuPP4	421	534	4.5
CuPP5	422	537	5.0
CuPP6	426	538	4.6
CuPP7	424	537	5.0

Table 2-10: Photophysical Data for **CuPPs** in DMF

Compound	Absorbance λ_{max} (nm)	Q-bands (nm)	Log Ɛ (M^{-1} cm^{-1})
CuPP1	422	537	5.5
CuPP2	416	533	5.6
CuPP3	418	533	5.9
CuPP4	420	535	4.7
CuPP5	422	538	4.9
CuPP6	425	539	4.8
CuPP7	424	540	5.2

The UV-Vis data of **PP12** and **PP13** unfortunately showed aggregation of the porphyrins. Addition of 2 drops of TFA to the solution containing the free bases did not change the outcome. Different solvents, including Toluene, DMF, DCM, $CHCl_3$ were used, but unfortunately there still was aggregation as seen in figure 2-12 and 2-13.

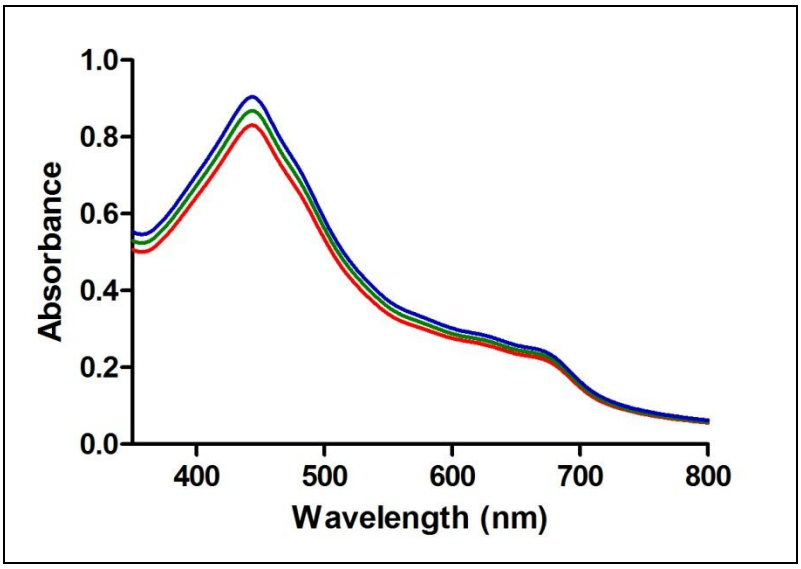

Figure 2-14: UV-Vis Spectra of **PP14** at 0.24M (red), 0.25M(green), and 0.26M (blue)M in Toluene

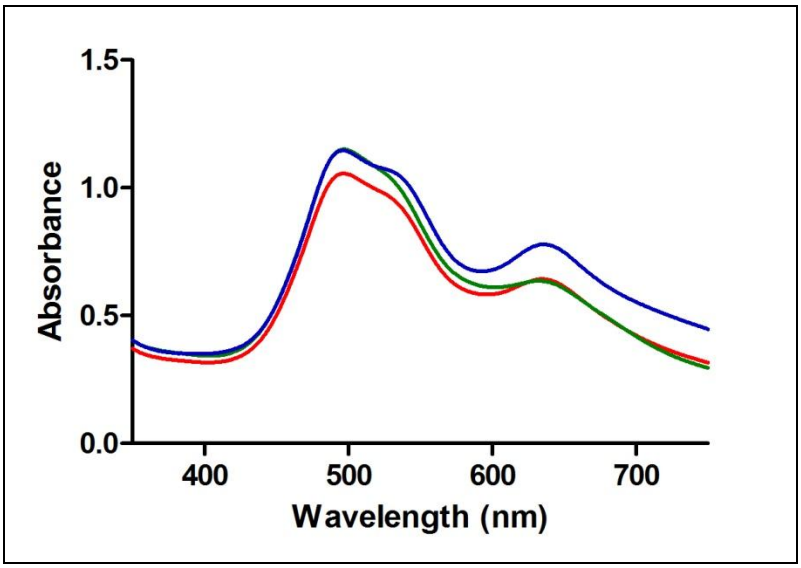

Figure 2-15: UV-Vis spectrum of **PP14** 0.24M (red), 0.25M (green), and 0.26 (blue)M in Toluene with 2 drops of TFA added to solution.

2.7 Biological Studies

Porphyrins **PP1-9** and **ZnPP3** were all submitted for biological studies, which were performed by Dr. Xiaoke Hu. The in vitro studies were carried out on the porphyrins using human carcinoma HEp2 cells for the assays. With the exception of **PP8,** which recorded an IC_{50} value of~380 μM, all the porphyrins showed no dark toxicities (see Figure 2-12). When exposed to low light dose (1 J/ cm), they all showed no phototoxicity(see Figure 2-13). At a concentration of 10μM, all porphyrins accumulated within the cells over time, with **PP4** being taken up slightly more than the other porphyrins (see Figure 2-14).

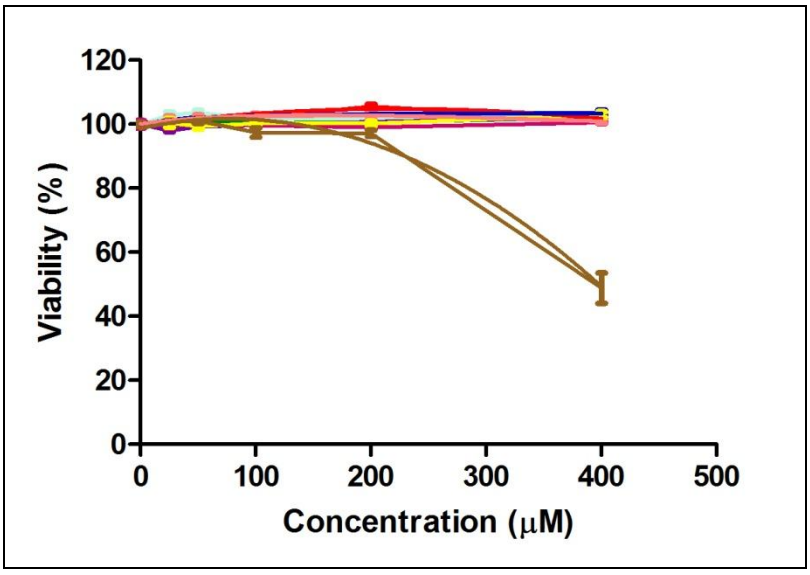

Figure 2-16: Dark Toxicities of porphyrins **PP1**(red)**, PP2**(green), **PP3**(blue), **PP4** (purple), **PP5** (maroon), **PP6** (pink), **PP7** (yellow), **PP9** (brown) and **ZnPP3** (light blue) toward HEp2 cells using Cell Titer Blue assay.

To determine the efficiency of tumor destruction, the subcellular localizations of porphyrins **PP1-9** and **ZnPP3** in HEp2 cells were studied. The compounds were allowed to incubate overnight at concentrations of 10μM, after which they were evaluated by fluorescence

microscopy. The tracers used were BODIPY Ceramide (golgi), LysoSensor Green (lysosomes), Mitotracker Green (mitochondria), and ER-tracker Green (ER).

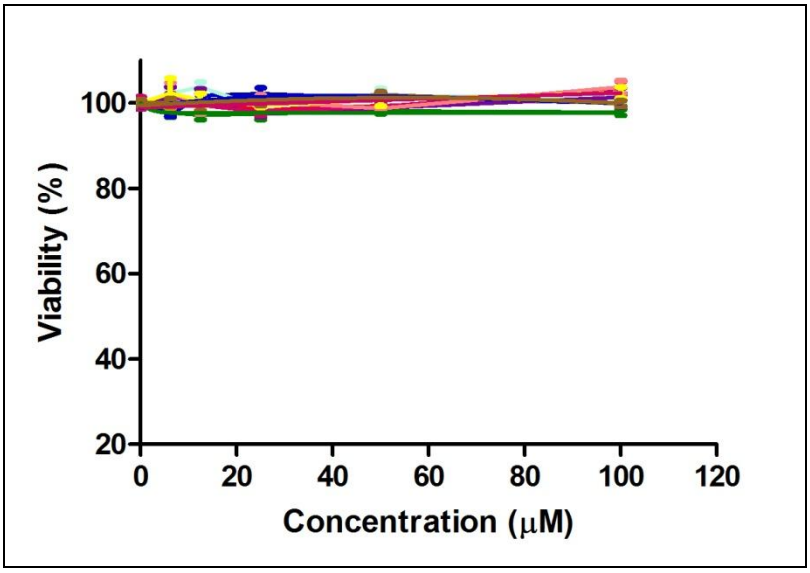

Figure 2-17: Phototoxicities of porphyrins **PP1** (red), **PP2** (green), **PP3** (blue), **PP4** (purple), **PP5** (maroon), **PP6** (pink), **PP7** (yellow) and **PP9** (brown) and **ZnPP3** (light blue) toward HEp2 cells at 1 J/cm light dose using the Cell Titer Blue assay.

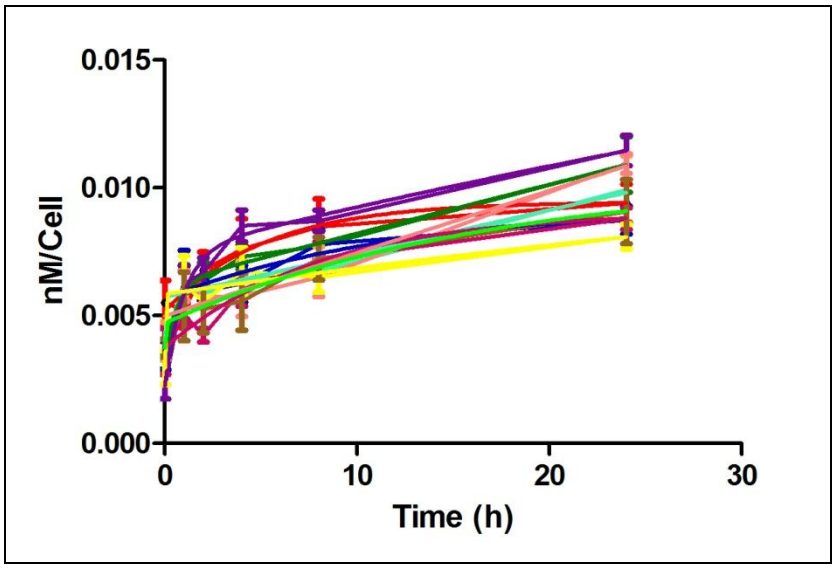

Figure 2-18: Time-dependent uptake of porphyrins **PP1** (red), **PP2** (green), **PP3** (blue), **PP4** (purple), **PP5** (maroon), **PP6** (pink), **PP7** (yellow), **PP9** (brown) and **ZnPP3** (light blue) at 10μM by HEp2 cells.

In all the micrographs, (a) shows the phase contrast (b) shows the overlay of phase contrast with fluorescence of the compound, (c) shows fluorescence of ER-Tracker green, (d) shows the fluorescence of ER-tracker green and the compound (e) shows the fluorescence of MitoTracker Green (f) shows the overlay of the fluorescence of MitoTracker Green and the compound (g) shows the fluorescence of LysoSensor Green (h) shows the overlay of the fluorescence of LysoSensor Green and the compound (i) shows the fluorescence of BODIPY Ceramide, (j) shows the overlay of the fluorescence of BODIPY Ceramide and the compound. To our pleasant surprise, all compounds showed localization in mitochondria. This is a remarkable discovery, because mitochondria is considered the "powerhouse" of the human cell. Therefore, destroying of the cells will be more effective if the photosensitizer is located within the mitochondria.

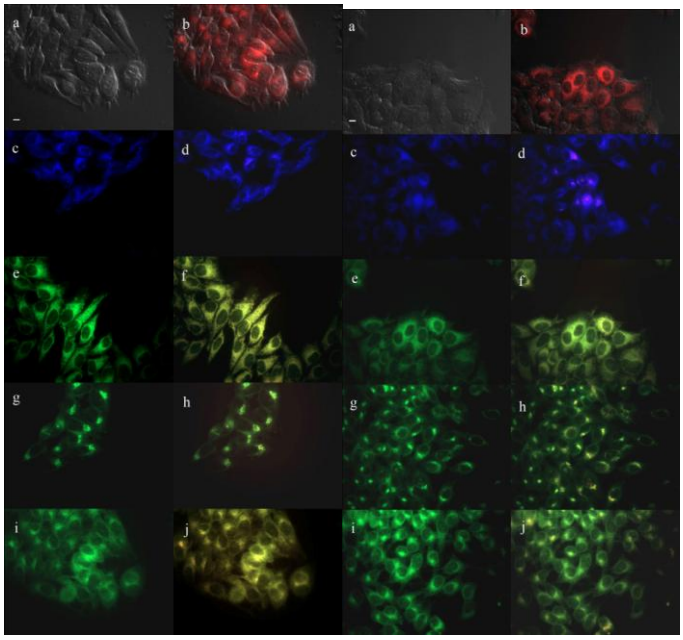

PP1 **PP2**

Figure 2-19 Subcellular localization of **PP1** and **PP2** in HEp2 cells at 10μM for 24 h. (a) Phase contrast, (b) overlay of **PP1** and **PP2** and phase contrast, (c) ER-tracker green fluorescence (e) MitoTracker Green Fluorescence (g) LysoSensor Green fluorescence, (i) BODIPY Ceramide fluorescence, (d), (f), (j) overlays of organelle tracers with **PP1** and **PP2**. Scale bar: 10 μM.

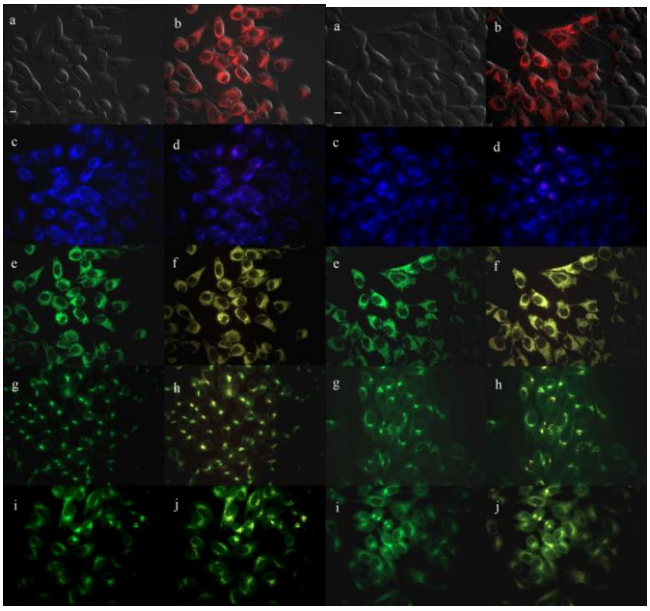

PP3 **PP4**

Figure 2-20: Subcellular localization of **PP3** and PP4 in HEp2 cells at 10μM for 24 h. (a) Phase contrast, (b) overlay of **PP3** and **PP4** and phase contrast, (c) ER-tracker green fluorescence (e) MitoTracker Green Fluorescence (g) LysoSensor Green fluorescence, (i) BODIPY Ceramide fluorescence, (d), (f), (j) overlays of organelle tracers with **PP3** and **PP4**. Scale bar: 10 μM.

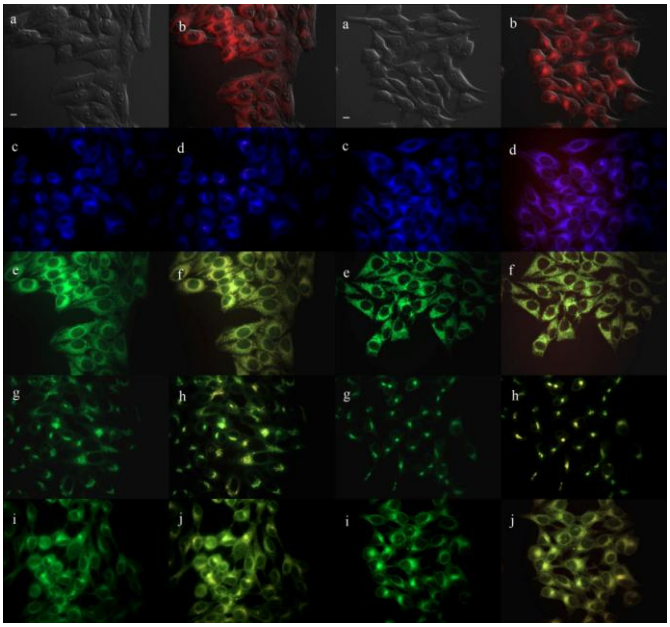

PP5 **PP6**

Figure 2-21: Subcellular localization of **PP5** and **PP6** in HEp2 cells at 10μM for 24 h. (a) Phase contrast, (b) overlay of **PP5** and **PP6** and phase contrast, (c) ER-tracker green fluorescence (e) MitoTracker Green Fluorescence (g) LysoSensor Green fluorescence, (i) BODIPY Ceramide fluorescence, (d), (f), (j) overlays of organelle tracers with **PP5** and **PP6**. Scale bar: 10 μM.

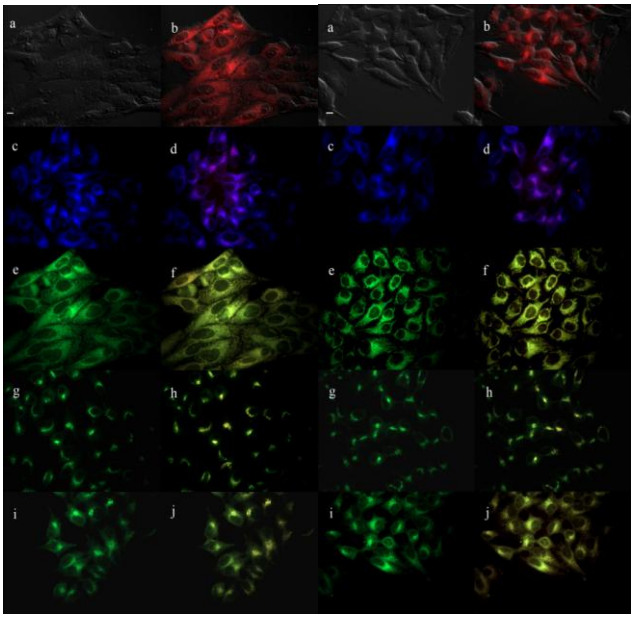

PP7 **PP9**

Figure 2-22: Subcellular localization of **PP7** and **PP9** in HEp2 cells at 10μM for 24 h. (a) Phase contrast, (b) overlay of **PP7** and **PP9** and phase contrast, (c) ER-tracker green fluorescence (e) MitoTracker Green Fluorescence (g) LysoSensor Green fluorescence, (i) BODIPY Ceramide fluorescence, (d), (f), (j) overlays of organelle tracers with **PP7** and **PP9**. Scale bar: 10 μM.

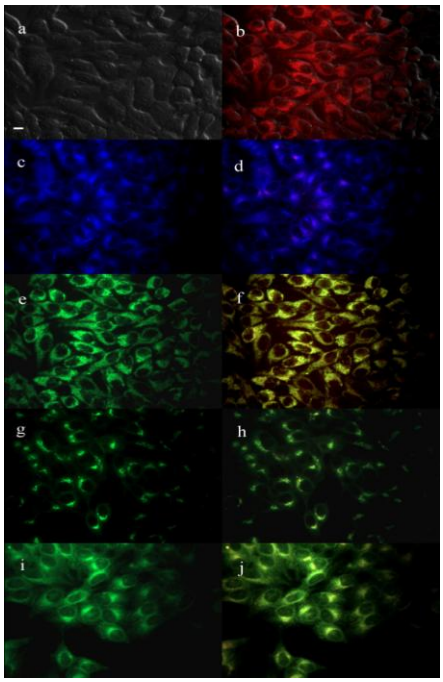

Figure 2-23: Figure 3-18: Subcellular localization of **ZnPP3** in HEp2 cells at 10μM for 24 h. (a) Phase contrast, (b) overlay of **ZnPP3** and phase contrast, (c) ER-tracker green fluorescence (e) MitoTracker Green Fluorescence (g) LysoSensor Green fluorescence, (i) BODIPY Ceramide fluorescence, (d), (f), (j) overlays of organelle tracers with **ZnPP3**. Scale bar: 10 μM.

Table 2-11: A summary of the porphyrins **PP1-9** and **ZnPP3** localizations.

Compound	Localization	Partial Localization
PP1	Mitochondria, Golgi	Lysosome
PP2	Mitochondria	Golgi, Lysosome, ER
PP3	Mitochondria	Lysosome
PP4	Mitochondria	Golgi, Lysosome
PP5	Mitochondria, Golgi	Lysosome
PP6	Mitochondria, Golgi	Lysosome, ER
PP7	Mitochondria, Golgi	Lysosome, ER
PP9	Mitochondria, Golgi	Lysosome, ER
ZnPP3	Mitochondria	Lysosome, Golgi

2.8 Conclusions

The MacDonald [2+2] condensation was successfully used to synthesize a total of thirteen thienyl-substituted porphyrins. In all cases, silica gel chromatography was used to purify the products using mixtures of EtOAc/Hexane for elution. The photophysical data obtained showed that the porphyrins were indeed potential candidates for PDT and BNCT. This was further supported by the biological studies, which showed that all of them localized in various cell organelles, including mitochondria, lysosome, golgi and the ER. Further work which entails attempts to polymerize the porphyrins is currently underway.

2.9 Experimental

General Procedure

All reactions were monitored by thin layer chromatography (TLC) using 0.25mm silica gel plates purchased from Sorbent technologies, with or without UV indicator (60F-254). All column

chromatographies were run using silica gel, 32-63μm from Sorbent Technologies. ^{1}H and ^{13}C NMR spectra were obtained either on a DPX-250 or AV-400 Bruker spectrometer. Chemical shifts (δ) are given in ppm relative to $CDCl_3$ (7.26ppm, ^{1}H; 77.2ppm, ^{13}C), or acetone-d_6 (2.05ppm, ^{1}H; 54.0ppm ^{13}C). MALDI-TOF mass spectra were obtained on a Bruker OmniFLEX MALDI-TOF mass spectrometer. ESI-TOF was obtained on Agilent 6210. Decarborane and 1-methyl-o-carborane were obtained from Katchem, Inc. (Czech Republic), while the other reagents and solvents were obtained from either Sigma-Aldrich or Fischer Scientific, and were used without further purification.

Cell Culture

All tissue culture media and reagents were obtained from Invitrogen. HEp2 cells were plated on LabTek II two chamber coverslips. They were allowed to grow for a duration of 24-48h. Compounds being investigated were then added at 10μM and incubated overnight. This was then followed by the addition of the tracers, which were added concurrently with the compound for the remainder of the incubation period. The tracers used were: BODIPY Ceramide, ERTracker Green, LysoSensor Green and MitoTracker Green. Distribution of the compound was determined using a Zeiss AxioVert 200M inverted fluorescent microscope fitted with standard texas Red, FITC, DAPI and Cy5LP filter sets.

Phototoxicity

The HEp2 cells were placed at 7500 per well in costar 96-well plate and allowed to grow overnight. Compounds were diluted to 100μM in medium, and then diluted to the final working concentrations of 6.25μM. (If DMSO was required to dissolve the compound, a 1% DMSO concentration was maintained throughout the experiment and dilutions by replacing the growth

medium with medium plus 1% DMSO before making dilutions) The cells were then incubated overnight (20-24h). The loading medium was then removed and the cells were fed medium containing 50mM HEPES pH 7.4. The plate was placed on ice. It was then exposed to a 610nm LP filtered light from a halogen lamp for 20 minutes (~1 Jcm^{-2}). IR radiation was filtered using a 10nm water layer contained in a petri dish placed on top of the 96 well plate. The medium was removed and cells fed medium containing 20µL CellTiter Blue per 100µL medium and then incubated for 4 hours. This was followed by conversion of the substrate by viable cells which was measured by fluorescence.

Dark Toxicity

HEp2 cells were plated at 7500 cells per well in Costar 96-well plates and allowed to grow for 48h. Compounds were diluted to 100µM in medium, and then diluted to 6.5µM.(If DMSO was required to dissolve the compound, a 1% DMSO concentration was maintained throughout the experiment and dilutions by replacing the growth medium with medium plus 1% DMSO before making dilutions) The cells were incubated overnight (20-24h). Loading medium was then removed and cells were fed medium containing 20µL CellTiter Blue per 100µL medium and then incubated for 4h. This was followed by conversion of the substrate by viable cells which was measured by fluorescence at 570/615nm.

Time Dependent Cellular Uptake

HEp2 cells were plated at 7500 per well on Costar 96-well dish and allowed to grow for 48h. Compounds were diluted to a 20µM stock in medium. Equal volume of the stock was added in triplicate wells containing cells (100µL) to give a final concentration of 10µM. The cells were exposed to the compounds for 1h, 2h, 4h, 8h and 24h. At the end of the incubation time, the

medium was removed and the cells washed with 200μL of PBS. After removal of PBS, the cells and compounds were then solubilized using 100μL of 0.25% Triton X-100 in PNS. To determine the compound concentration, fluorescence emission was read using FLUOstar plate reader using excitation/emission wavelengths appropriate for the compound under study. The cell numbers were quantified using the CyQuant cell proliferation assay reagent.

Fluorescence Measurements

All experiments were performed at room temperature, in toluene and DMF. In some cases, a drop of TFA was added to the dilute solutions to prevent aggregation. UV-Vis absorbance was measured using a Perkin Elmer Lambda 35 UV-Vis Spectrometer. Fluorescence measurements were taken on a Fluorolog®-HORIBA JOBINVYON, Model LFI-3751 Spectrofluorimeter. Fluorescence quantum yields (Φ_f) were calculated by using the following equation:

$$\phi_F = \left(\frac{[F(\text{sample})][A(\text{standard})]}{[F(\text{standard})][A(\text{sample})]}\right) \phi_f(\text{standard})$$

Where [F(sample)] and [F(standard)] are the integrated emission areas of the porphyrins and the standard respectively. [A(standard)] and [A(sample)] are the optical densities of the standard and the porphyrins, respectively, at the excitation wavelengths. Free base, **TPP** ($\Phi_f = 0.11$) was used as the standard for free base porphyrins, and the Zn-complexed derivative, **ZnTPP** ($\Phi_f = 0.033$) was used as the standard for **ZnPPs**.

General Procedure for Metal Insertion

Starting material was dissolved in DCM/MeOH (3:1) and excess amount of $Zn(OAc)_2$/$Cu(OAc)_2$ added. For Zn-porphyrin complexes, the reaction mixture was stirred at

room temperature for 24 hours. For Cu-porphyrin complexes, the reaction mixtures were stirred at room temperature for 12 hours and then refluxed for 4 h. The resulting mixtures were dried under vacuum and purified using column chromatography using DCM as eluent to afford the final products.

Synthesis of DP-1

2-Thiophene carboxaldehyde (1.0g, 8.9 mmol) was added to freshly distilled pyrrole (25.7g, 382.7mmol) in a round bottom flask, under nitrogen. To this mixture was added TFA (0.1g, 0.89 mmol) and the mixture allowed to stir for 30 minutes at room temperature. The mixture was poured in water (50 mL) and extracted with DCM (3 x 50mL). The organic layer was washed with saturated $NaHCO_3$ (3 x 50 mL), followed by water (3 x 50 mL). The organic layers were dried over Na_2SO_4 and dried under vacuum. Crude product was purified by column chromatography using 1:5 EtOAc:Hexane to obtain 1.3g of the title compound as 64% yield. ^{1}H NMR ($CDCl_3$, 400MHz) δ 7.83 (2H, bs s), 7.11 (1H, dd, *J* = 4 Hz, *J*= 1.2Hz), 6.86 (1H, m), 6.78 (1H, m), 6.58 (2H, d, *J*= 4Hz), 6.07 (2H, d, *J*= 4Hz), 5.94 (2H, br s), 5.62 (1H, S). ^{13}C NMR ($CDCl_3$, 100MHz) 145.8, 132.1, 126.9, 125.7, 124.7, 117.5, 108.6, 107.2, 39.2. ESI-TOF *m/z* calcd for $C_{13}H_{10}N_2S$ 228.07, found 228.06 m.p. 117-118^{o}C.

Synthesis of PP1

A solution of **DP-1** (0.04g, 0.177mmol) and 2-thiophene-carboxaldehyde (0.0198g, 0.177mmol) in 18 mL DCM was purged with argon for 15 minutes. $BF_3.OEt_2$ (0.0022g, 0.018mmol) in 18 mL DCM was also purged with argon for 15 minutes. The $BF_3.OEt_2$ solution was then added to the solution containing the dipyrromethane and the aldehyde, and the mixture stirred at room temperature for 2h. The reaction was monitored by TLC. After TLC confirmed no starting

material present, DDQ(0.06g, 0.266mmol) was added to the reaction flask and the reaction mixture stirred for 30 minutes. The reaction mixture was then filtered through a pad of silica gel, and the filtrate dried under vacuum. The product was purified using column chromatography, using 1:5 EtOAc:Hexane to afford 0.043g of the title compound as 56% yield.^{1}H NMR ($CDCl_3$, 250MHz) δ 9.04 (8H, s), 7.91 (4H, d, *J*= 3.4Hz), 7.85 (4H, d, *J*=3.4Hz), 7.50 (4H, m). **ZnPP1** obtained in 54% yield MALDI-TOF m/z calcd for $C_{36}N_{20}N_4S_4Zn$, 699.99, found 699.99. **CuPP1** obtained in 71% yield MALDI-TOF m/z calcd for $C_{36}N_{20}N_4CuS_4$, 698.99, found 698.99.

Synthesis of PP2

A solution of **DP-1** (0.04g, 0.177mmol) and benzaldehyde (0.019g, 0.177mmol) in 18 mL DCM was purged with argon for 15 minutes. $BF_3.OEt_2$ (0.0022g, 0.018mmol) in 18 mL DCM was also purged with argon for 15 minutes. The $BF_3.OEt_2$ solution was then added to the solution containing the dipyrromethane and the aldehyde, and the mixture stirred at room temperature for 2h. The reaction was monitored by TLC. After TLC confirmed no starting material present, DDQ(0.06g, 0.266mmol) was added to the reaction flask and the reaction mixture stirred for 30 minutes. The reaction mixture was then filtered through a pad of silica gel, and the filtrate dried under vacuum. The product was purified using column chromatography, using 1:5 EtOAc:Hexane to afford 0.048 g of the title compound as 44% yield. ^{1}H NMR ($CDCl_3$, 250MHz) δ 9.06 (4H, d, *J*= 4Hz), 8.85 (4H, m), 8.23 (4H, m), 7.94 (2H, m), 7.87 (2H, m), 7.79 (6H, m), 7.52 (2H, m). ^{13}C NMR (acetone-d6, 100MHz) 137.6, 134.3, 133.2, 131.5, 128.9, 128.1, 127.5, 126.5, 126.0, 125.2. **ZnPP2** obtained in 98% yield. MALDI-TOF m/z calcd for.$C_{40}H_{24}N_4S_2Zn$, 688.07, found 688.06. CuPP2 obtained in 94% MALDI-TOF m/z calcd for $C_{40}H_{24}CuN_4S_2$, 687.07, found 687.089.

Synthesis of PP3

A solution of **DP-1** (0.02g, 0.088mmol) and 3,5-ditertbutyl benzaldehyde (0.019g, 0.088mmol) in 9 mL DCM was purged with argon for 15 minutes. $BF_3.OEt_2$ (0.0012g, 0.0088mmol) in 9 mL DCM was also purged with argon for 15 minutes. The $BF_3.OEt_2$ solution was then added to the solution containing the dipyrromethane and the aldehyde, and the mixture stirred at room temperature for 2h. The reaction was monitored by TLC. After TLC confirmed no starting material present, DDQ(0.03g, 0.131mmol) was added to the reaction flask and the reaction mixture stirred for 30 minutes. The reaction mixture was then filtered through a pad of silica gel, and the filtrate dried under vacuum. The product was purified using column chromatography, using 1:5 EtOAc:Hexane to afford 0.02 g of the title compound as 27% yield. ^{1}H NMR ($CDCl_3$, 400MHz) δ 9.06 (4H, m), 8.90 (4H, m), 8.14 (4H, m), 8.03 (2H, s), 8.00 (2H, d, *J*= 3Hz), 7.96 (2H, s), 7.56 (2H, m), 1.53 (36H, s). ^{13}C NMR (acetone-d_6, 100MHz) 149.0, 140.9, 133.9, 129.4, 128.1, 126.2, 121.5, 34.8, 31.1. HRMS(ESI) *m/z* calcd for $C_{56}H_{58}N_4S_2$, 851.4175, found 851.4193. **ZnPP3** obtained in 53% yield. MALDI-TOF *m/z* calcd for $C_{56}H_{56}N_4S_2Zn$, 914.58, found 914.33. **CuPP3** obtained in 21% yield. MALDI-TOF m/z calcd for $C_{56}H_{56}CuN_4S_2$, 911.32, found 911.21.

Synthesis of PP4

Procedure used was the same as that for **PP1**. Reagents used were, **DP-1** (0.02g, 0.088mmol) and 3,5-methoxy benzaldehyde (0.015g, 0.088mmol), $BF_3.OEt_2$ (0.0012g, 0.0088mmol), and DDQ(0.03g, 0.131mmol). The product was purified using column chromatography, using 1:5 EtOAc:Hexane to afford 0.013 g of the title compound as 20% yield.^{1}H NMR ($CDCl_3$, 400MHz) δ 9.04 (4H, m), 8.93 (4H, m), 7.93 (2H. d, *J*= 4Hz), 7.86 (2H, d, *J*= 4Hz), 7.51 (2H, m), 7.40

(4H, s), 6.91 (2H, s), 3.97 (12H, s). HRMS(ESI) calcd for $C_{44}H_{34}N_4O_4S_2$, 747.2094, found 747.2121. **ZnPP4** obtained in 41% yield. MALDI-TOF m/z Calcd for $C_{44}H_{32}N_4O_4S_2Zn$, 808.12, found 808.17.

Synthesis of 5-bromothiophene-2-carbaldehyde (1)

Thiophene-2-carbaldehyde (1.0g, 8.92 mmol) and $NaHCO_3$ (0.82g, 9.81 mmol) were dissolved in dry $CHCl_3$ (40 mL). The temperature was lowered to 0^oC. The mixture was allowed to stir for 30 minutes. Bromine (1.43g, 8.92 mmol) was then added dropwise while stirring, and the reaction allowed to warm to room temperature. The reaction mixture was stirred at this temperature for 3 h. It was then poured into water. The organic layer was washed with saturated NaHCO3 (2 x 20 mL), then water (3 x 20 mL) and the organic layers combined and dried over Na_2SO_4. The product was then dried under vacuum, and purified by column chromatography using 1:5 EtOAc:Hexane.^{1}H NMR ($CDCl_3$, 400MHz) 9.78 (1H, s), 7.53 (1H, d, *J*= 4Hz), 7.20 (1H, d, *J*= 4Hz).

Synthesis of DP-2

5-Bromothiophene-2-carbaldehyde (**1**) (1.0g, 5.23 mmol) was added to freshly distilled pyrrole (15.1g, 224.89 mmol) in a round bottom flask, under nitrogen. To this mixture was added TFA (0.06g, 0.523 mmol) and the mixture allowed to stir for 30 minutes at room temperature. The mixture was poured in water (50 mL) and extracted with DCM (3 x 50mL). The organic layer was washed with saturated $NaHCO_3$ (3 x 50 mL), followed by water (3 x 50 mL). The organic layers were dried over Na_2SO_4 and dried under vacuum. Crude product was purified by column chromatography using 1:5 EtOAc:Hexane to obtain the title compound in 55 % yield. ^{1}H NMR ($CDCl_3$, 400MHz) δ 9.81 (2H, br s), 6.94 (1H, d, *J*= 4Hz), 6.70 (2H, d, J= 1.6Hz), 6.59 (1H, dd,

J=2, *J*= 2 Hz), 6.00 (2H, m), 5.90 (2H, m), 5.67 (1H, s). ^{13}C NMR ($CDCl_3$, 100MHz) 147.4, 129.5, 126.7, 125.8, 117.7, 108.6, 107.3, 39.5.

Synthesis of PP5

Procedure used was the same as that for **PP1**. Reagents used were, **DP-2** (0.02g, 0.065mmol) and 3,5-ditertbutyl benzaldehyde (0.014g, 0.065mmol), $BF_3.OEt_2$ (0.0001g, 0.0065mmol), and DDQ(0.022g, 0.0975 mmol). The product was purified using column chromatography, using 1:5 EtOAc:Hexane to afford 0.013 g of the title compound as 20% yield. ^{1}H NMR ($CDCl_3$, 400MHz) δ 9.10 (6H, m), 8.89 (4H, m), 8.07 (4H, m), 7.72 (3H, m), 7.67 (3H, m), 7.49 (4H, m), 1.53 (36H, s). ^{13}C NMR ($CDCl_3$, 100MHz). 161.2, 161.4, 143.2, 137.6, 129.1, 128.3, 127.2, 125.4,105.3, 117.7, 31.1, 20.5. ESI-TOF calcd for $C_{56}H_{56}Br_2N_4S_2$, 1009.01, found 1009.2329. **ZnPP5** obtained in 62% yield. MALDI-TOF m/z calcd for $C_{56}H_{54}Br_2N_4S_2Zn$ 1072.37, found 1072.138. **CuPP5** obtained in 59% yield. MALDI-TOF m/z calcd for $C_{56}H_{54}Br_2CuN_4S_2$ 1069.14, found 1069.12.

Synthesis of PP6

Procedure used was the same as that for **PP1**. Reagents used were, DP-1 (0.1g, 0.44mmol) and methyl 5-formyl-1H-pyrrole-2-carboxylate (0.067g, 0.44mmol), $BF_3.OEt_2$ (0.0062g, 0.044mmol), and DDQ(0.15g, 0.655 mmol). The product was purified using column chromatography, using 1:3 EtOAc:Hexane to afford 0.067 g of the title compound as 21% yield. ^{1}H NMR ($CDCl_3$, 400MHz) δ 9.07 (6H, m), 7.94 (2H, m), 7.88 (2H, m), 7.53 (4H, m), 7.29 (4H, s), 1.55 (6H, s). MALDI-TOF calcd for $C_{40}H_{28}N_6O_4S_2$, 720.82, found 720.137**. ZnPP6** obtained in 98% yield. MALDI-TOF m/z calcd for $C_{40}H_{26}N_6O_4S_2Zn$ 784.18, found 784.077.

Synthesis of PP7

Procedure used was the same as that for **PP1**. Reagents used were, DP-1 (0.1g, 0.44mmol) and 5-(4-methoxybenzoyl)-1H-pyrrole-2-carbaldehyde (0.089g, 0.44mmol), $BF_3.OEt_2$ (0.0062g, 0.044mmol), and DDQ(0.15g, 0.655 mmol). The product was purified using column chromatography, using 1:3 EtOAc:Hexane to afford the title compound in 18% yield. ^{1}H NMR (acetone-d_6, 400MHz) δ 9.17 (4H, br s), 9.10 (4H, m), 8.11(4H, d, *J*= 5Hz), 8.04 (4H, m), 7.26 (4H, m), 7.43 (1H, m), 7.36 (1H, m), 7.05 (4H, m), 3.91 (6H, s). **ZnPP7** obtained in 72% yield. ^{13}C NMR (acetone-d6, 100MHz) 151.1, 143.6, 133.4, 131.8, 131.7, 128.9, 128.1, 127.6, 126.0, 125.2, 114.9, 50.6, 20.5. MALDI-TOF m/z calcd for $C_{52}H_{34}N_6O_4S_2Zn$ 936.37, found 936.15.

Synthesis of Compound 2

To a solution of Cs[3,3'-Co(1,2-$C_2B_9H_{11})_2$] (1.0g, 2.2 mmol) in anhydrous 1,4-dioxane (100 mL) was added $BF_3.OEt_2$ (2.49g, 17.52 mmol) and the reaction mixture heated at reflux under N_2 atmosphere for 5h. The reaction mixture was allowed to cool temperature. It was then filtered, and the filtrate dried under vacuum. The product was purified by column chromatography using 30% DCM/Hexane, followed by 100% DCM to obtain the title compound. Yield 72%. ^{1}H NMR data correlates to literature data.

Synthesis of PP8

BBr_3 (0.2g, 0.81 mmol) was dissolved in DCM (0.5 mL) and the solution temperature lowered to -20^{o}C. Under N_2 atmosphere, a solution of **PP4** (0.02g, 0.027 mmol) in DCM (1 mL) was added to the BBr_3 solution slowly with stirring, over 15 minutes. The reaction mixture was then allowed to warm up to room temperature, and allowed to stir for 24h. It was then poured into water, followed by extraction with EtOAc. The organic layer was washed with brine, then

saturated $NaHCO_3$ solution. The organic layers were then dried over Na_2SO_4, filtered and dried under vacuum to give the title product. Yield, 0.0162g, 87% ^{1}H NMR (acetone-d_6, 400MHz) δ 9.01 (8H, br s), 8.67 (4H, m), 8.02 (4H, m), 7.54 (2H, m), 7.20 (4H, s), 6.80 (2H, t).

Synthesis of PP9

In a round bottom flask, **PP8** (0.0162g, 0.023 mmol) and K_2CO_3 (0.025g, 0.184 mmol) were dissolved in 15 mL acetone. The reaction mixture was allowed to stir at room temperature and compound **2** (0.037g, 0.092 mmol) added in one portion. The reaction mixture was allowed to stir at room temperature for 2h. This was followed by reflux for 24h, after which it was allowed to cool to room temperature and a second portion of compound **2** (0.018g, 0.046 mmol) was added. The reaction mixture was then refluxed for 24 h. After this period, it was cooled to room temperature and a third portion of compound **2** (0.018, 0.046 mmol) added, followed by reflux for 24 h. After cooling it to room temperature, the reaction mixture was dried under vacuum. The product was purified by column chromatography using 1:1 EtOAc: Hexane to afford 60% yield. ^{1}H NMR (acetone-d_6, 250MHz) δ 8.98 (6H, m), 7.94 (2H, d, *J*= 4Hz), 7.86 (2H, d, *J*= 4Hz), 7.51 (4H, m), 7.13 (4H, m), 6.73 (2H, s), 5.13 (8H, m), 2.73 (8H, m), 2.21 (8H, m), 2.18 (8H, m), 1.8-0.5 (72H, br, BH).

Synthesis of Compound 3

3,5-Dimethylbromobenzene (0.1g, 0.54 mmol) was dissolved in dry CCl_4 (7 mL). Under argon, NBS (0.21g, 1.19 mmol) was added and benzoyl peroxide (0.02g, 0.07 mmol) added to the reaction mixture in portions over 1 hr period. The final reaction mixture was refluxed with stirring for 16 h. It was then allowed to cool to room temperature, after which it was filtered and the filtrate washed with saturated $NaHCO_3$ and once with water. The organic layer was dried

over Na_2SO_4 and dried under vacuum. The resulting residue was purified by column chromatography using DCM/PET ether 1/9 as eluant. ^{1}H NMR ($CDCl_3$, 400MHz) 7.62 (2H, d, *J*= 4Hz), 7.49 (1H, s), 4.55 (4H, s).

Synthesis of Compound 4

1-Methyl-o-carborane (0.202g, 1.276 mmol) was dissolved in dry THF (13 mL) and temperature kept between -5 and 0^{o}C. n-BuLi (2.5M/Hexane) (0.49ml, 1.22 mmol) was added dropwise to the solution under argon. The mixture was stirred at this temperature range for 1.5h, and temperature lowered between between -15^{o}C and - 20^{o}C. A solution of LiI (0.02g, 0.18 mmol) in dry THF (1.7 mL) and 1-bromo-3,5-bis(bromomethyl)benzene (0.2g, 0.58 mmol) in THF (3 mL) were added to the reaction mixture, and the final mixture allowed to warm to room temperature and stirred for 16h at this temperature. The reaction was quenched with water, and the resulting mixture extracted with diethyl ether (3 x 10 mL). The organic layers were combined and washed with water, and brine. The organic layer was then dried over Na_2SO_4, and dried under vacuum. Product was purified using column chromatography using DCM/PET ether 1/4. ^{1}H NMR ($CDCl_3$, 400MHz) δ 7.48 (2H, s), 7.32 (1H, s), 4.41 (4H, s), 3.42 (6H, s), 2.9-1.5(20H, br, BH).

Synthesis of Compound 5

Dicarboranylbromobenzene (0.286g, 0.57 mmol) was dissolved in THF (6 mL) and the solution put under argon. It was then cooled to -78^{o}C and nBuLi (2.5M/Hexane) (0.26 ml, 0.64 mmol) was added dropwise via syringe. After stirring the reaction mixture for 30 minutes at this temperature, dry DMF (0.21g, 2.85 mmol) was slowly added. The resulting mixture was stirred at -78^{o}C for 30 minutes and then warmed up to 0^{o}C and stirred for 1h at this temperature. A 5%

aqueous HCl solution was added until the pH of the reaction mixture was between 2 and 3. The final mixture was stirred at room temperature for 15 minutes. The aqueous layer was extracted with diethyl ether, and the organic fraction dried over anhydrous $MgSO_4$ and the solvent evaporated under vacuum. The product was purified by column chromatography using DCM/PET ether 2/3 to obtain 50% of title compound. ^{1}H NMR ($CDCl_3$, 400MHz) δ 9.98 (1H, s), 7.62 (2H, d, *J* = 1.5Hz), 7.28 (1H, d, *J* = 1.5Hz), 3.52 (4H, s), 2.18 (6H, s), 1.3-3.2 (20H, br)

Synthesis of PP10

Procedure used was the same as that for **PP1**. Reagents used were, **DP-1** (0.02g, 0.088mmol), compound **6** (0.04g, 0.088mmol), $BF_3.OEt_2$ (0.0012g, 0.0088mmol), and DDQ (0.003g, 0.0132mmol). Product was purified using silica gel chromatography using 1:3 EtOAc/Hexane to give 0.007g, 6% of the title compound. ^{1}H NMR ($CDCl_3$, 400MHz) δ 9.00 (4H, m), 8.93 (4H, m), 8.07 (4H, m), 8.02 (2H, s), 7.98 (2H, m), 7.96 (2H, s), 7.54 (2H, m), 3.92 (s, 8H), 2.33 (s, 12H), 1.2-3.3 (br, 40H).

Synthesis of Compound 7

5-Bromothiophene-2-carbaldehyde (1.674g, 8.765 mmol), $PdCl_2(PPh_3)_2$ (0.154g, 0.219 mmol), and CuI(0.0834g, 0.438 mmol) were dissolved in THF (30 mL). TMSA (0.947g, 9.64 mmol) was added to the reaction mixture under argon and Et_3N (36 mL) added to the reaction mixture. The reaction was allowed to stir at room temperature for 24 h. The reaction mixture was then poured into water, and extracted with EtOAc. Product was purified using 1:5 EtOAc/Hexane ^{1}HNMR ($CDCl_3$, 400MHz) δ 9.85 (1H, s), 7.62 (1H, d, *J*= 4), 7.28 (1H, d, *J*=4), 0.27 (9H, s).

Synthesis of DP-4

5-((trimethylsilyl)ethynyl)thiophene-2-carbaldehyde (0.3g, 1.44mmol) was added to freshly distilled pyrrole (1.93g 28.80 mmol) in a round bottom flask, under nitrogen. To this mixture was added TFA (0.033g, 0.288 mmol) and the mixture allowed to stir for 30 minutes at room temperature. The mixture was poured in water (5 mL) and extracted with DCM (3 x 5mL). The organic layer was washed with saturated $NaHCO_3$ (3 x 5 mL), followed by water (3 x 5 mL). The organic layers were dried over Na_2SO_4 and dried under vacuum. Crude product was purified by column chromatography using 1:3 EtOAc:Hexane to obtain the title compound in 54 % yield. ^1H NMR ($CDCl_3$) δ 7.97 (2H, br s), 7.09 (1H, d, *J*=4Hz), 6.73 (3H, m), 6.17 (2H, d, *J*= 2.5Hz), 6.05 (2H, s), 5.68 (1H, s), 0.23 (9H, s).

Synthesis of DP-3

Trimethylsilane protecting group was removed by reacting **DP-4** (0.03g, 0.092 mmol) with K_2CO_3 (0.038g, 0.276mmol) dissolved in a Hexane/MeOH mixture (8:2) (5 mL) at room temperature for 2h. The reaction was quenched by adding water. This was extracted with Et2O, and the organic layer dried over Na_2SO_4 and dried under vacuum. The title compound was obtained in 73% yield. ^1H NMR ($CDCl_3$, 400MHz) δ 8.01 (2H, br s), 7.13 (1H, d, J= 4), 6.76 (1H. d, J= 4), 6.72 (2H, d, J= 1.5 Hz), 6.18 (2H, dd, J= 4Hz), 6.06 (2H, s), 5.70 (1H, s), 3.3 (1H, s). ESI-TOF calcd for $C_{15}H_{12}N_2S$, 252.33 found, 253.08.

Synthesis of DP-5

Decarborane (0.15g, 0.60 mmol), **DP-3** (0.15g, 1.20 mmol), dry CH_3CN (1.5 mL) and dry toluene (4.5 mL) was mixed in a round bottom flask. The reaction was stirred under N_2 at 80^oC for 24h. After it was cooled to room temperature, MeOH (3.0 mL) was added to the reaction

flask and stirred for 30 minutes. The reaction mixture was dried under vacuum, and the product purified by column chromatography using 20% DCM/Hexane as eluent, to yield 34% of the title product. 1H NMR 7.93 (2H, br s), 7.63 (1H, s), 7.47 (1H, s), 6.93 (2H, m), 6.65 (3H, m), 6.07 (1H, d, *J*= 4), 5.94 (1H, s), 1.8-0.5 (10H, br, BH).

Synthesis of PP11

Procedure used was the same as that for **PP1**. Reagents used were, **DP-5** (0.006g, 0.016mmol) and 3,5-ditertbutyl benzaldehyde (0.004g, 0.0.016mmol), $BF_3.OEt_2$ (0.00023g, 0.0016 mmol), and DDQ(0.005g, 0.024 mmol). The product was purified using column chromatography, using 1:5 EtOAc:Hexane to afford the title compound in 6% yield. 1H NMR ($CDCl_3$, 400MHz) δ 9.23 (4H, m), 8.97 (4H, m), 7.91 (2H, d, J= 4Hz), 7.47 (2H, m), 7.87 (2H, d, J= 4Hz), 7.34 (4H, m), 1.89 (s, 36H), 1.3-3-2 (br, 20H). MALDI-TOF m/z calcd for $C_{60}H_{78}B_{20}N_4S_2$, 1134.76, found 1134.97.

Synthesis of Compound 9

[2,2'-Bithiophene]-5-carbaldehyde (2.0g, 10.29 mmol) was dissolved in $CHCl_3$ (20 mL). The temperature was lowered to 0^oC. Bromine (1.65g, 10.29 mmol) was added dropwise to the reaction flask, and the reaction mixture allowed to warm to room temperature. It was allowed to stir at this temperature for 2h. The reaction mixture was poured into 20 mL water. The organic layer was then washed with saturated $NaHCO_3$ and dried over Na_2SO_4. The product was purified by column chromatography using 1:3 EtOAc/Hexane to obtain 2.5g of the target compound. ^1H NMR ($CDCl_3$, 250MHz) 9.86 (1H, s), 7.66 (1H, d, *J*= 4), 7.19 (1H, d, *J*= 4), 7.11 (1H, d, *J*= 4), 7.03 (1H, d, *J*= 4).

Synthesis of Compound 13

5'-Bromo-[2,2'-bithiophene]-5-carbaldehyde (1.0g, 3.65 mmol), $PdCl_2(PPh_3)_2$ (0.064g, 0.091 mmol), and CuI(0.035g, 0.183 mmol) were dissolved in THF (40 mL). TMSA (0.39g, 4.0 mmol) was added to the reaction mixture under argon and Et3N (40 mL) added to the reaction mixture. The reaction was allowed to stir at room temperature for 24 h. The reaction mixture was then poured into water, and extracted with EtOAc. Product was purified with column chraomatography using 1:3 EtOAc/Hexane. ^{1}H NMR ($CDCl_3$, 400MHz) ^{1}H NMR ($CDCl_3$, 400MHz) δ 9.87 (1H, s), 7.67 (1H, d, *J*= 4Hz), 7.24 (1H, d, *J*= 4), 7.20 (1H, d, *J*=4), 7.17 (1H, d, *J*= 4), 0.26 (9H, s).

Synthesis of DP-6

5'-((Trimethylsilyl)ethynyl)-[2,2'-bithiophene]-5-carbaldehyde (0.124g, 0.43mmol) was added to freshly distilled pyrrole (0.57g, 8.55 mmol) in a round bottom flask, under nitrogen. To this mixture was added TFA (0.0097g, 0.086 mmol) and the mixture allowed to stir for 30 minutes at room temperature. The mixture was poured in water (2 mL) and extracted with DCM (3 x 2mL). The organic layer was washed with saturated $NaHCO_3$ (3 x 2 mL), followed by water (3 x 2 mL). The organic layers were dried over Na_2SO_4 and dried under vacuum. Crude product was purified by column chromatography using 1:3 EtOAc:Hexane to obtain the title compound. ^{1}H NMR ($CDCl_3$, 400MHz) 8.04 (2H, br s), 7.18 (1H, m), 7.08 (1H, m), 6.94 (1H, m), 6.84 (1H, d, *J*= 4), 6.80 (1H, d, *J*= 4), 6.73 (2H, s), 6.27 (1H, d, *J*= 1.8Hz), 6.19 (2H, d, *J*= 3Hz), 5.71(1H, s), 0.25 (9H, s). ESI-TOF calcd for $C_{22}H_{22}N_2S_2Si$, 406.10, found 406.09.

Synthesis of DP-7

Trimethylsilane protecting group was removed by reacting **DP-6** (0.12g, 0.30 mmol) with K_2CO_3 (0.12g, 0.89mmol) dissolved in a Hexane/MeOH mixture (8:2) (20 mL) at room temperature for 2h. The reaction was quenched by adding water. This was extracted with Et_2O, and the organic layer dried over Na_2SO_4 and dried under vacuum. ^{1}H NMR ($CDCl_3$, 400MHz) δ 8.06 (2H, br s), 7.19 (1H, d, *J*= 4), 7.09 (1H, m), 6.99 (2H, m), 6.73 (3H, m), 6.19 (2H, d, *J*= 2.8Hz), 6.09 (1H, s), 5.72 (1H, s), 3.34 (1H, s). ESI-TOF calcd for $C_{19}H_{14}N_2S_2$, 334.06, found 334.05.

Synthesis of DP-8

Decarborane (0.10g, 0.30 mmol), **DP-7** (0.07g, 0.60 mmol), dry CH_3CN (1.0 mL) and dry toluene (3.0 mL) was mixed in a round bottom flask. The reaction was stirred under N_2 at 80^{o}C for 24h. After it was cooled to room temperature, MeOH (2.0 mL) was added to the reaction flask and stirred for 30 minutes. The reaction mixture was dried under vacuum, and the product purified by column chromatography using 20% DCM/Hexane as eluent

Synthesis of PP12

Procedure used was the same as that for **PP1**. Reagents used were, **DP-8** (0.010g, 0.022mmol) and 3,5-ditertbutyl benzaldehyde (0.005g, 0.022mmol), $BF_3.OEt_2$ (0.0003g, 0.0022mmol), and DDQ(0.008g, 0.033mmol). The product was purified using column chromatography, using 1:3 EtOAc:Hexane to afford 0.002g of the title compound as 8% yield. 7.91 (4H, br s), 7.57 (2H, d, *J*=4Hz), 7.52 (4H, m), 7.29 (4H, m), 7.17 (4H, m), 6.60 (4H, m), 1.94 (36H, s), 1.4-3-5 (br, 20H).

Synthesis of DP-9

(2,2'-Bithiophene)-5-carboxaldehyde (1.0g, 5.15 mmol) dissolved in minimal DCM was added to freshly distilled pyrrole (6.91g, 102.95 mmol) in a round bottom flask, under nitrogen. To this mixture was added TFA (0.04g, 0.515 mmol) and the mixture allowed to stir for 30 minutes at room temperature. The mixture was poured in water and washed with saturated $NaHCO_3$. The organic layers were dried over Na_2SO_4 and dried under vacuum. Crude product was purified by column chromatography using 1:4 EtOAc:Hexane. ^{1}H NMR ($CDCl_3$, 250MHz) δ 7.95 (2H, br s), 7.26 (1H, d, *J*= 4), 7.24 (1H, d, *J*= 4), 7.20 (2H, m), 6.73 (2H, m), 6.26 (2H, m), 6.04 (2H, s), 5.70 (1H, s).

Synthesis of PP13

Procedure used was the same as that for **PP1**. Reagents used were, **DP-9** (0.15g, 0.48mmol) and 3,5-ditertbutyl benzaldehyde (0.105g, 0.48 mmol), $BF_3.OEt_2$ (0.0069g, 0.048 mmol), and DDQ(0.165g, 0.727 mmol). The product was purified using column chromatography, using 1:5 EtOAc:Hexane to afford the title compound in 18% yield. ^{1}H NMR ($CDCl_3$, 400MHz) δ 7.99 (4H, br s), 7.69 (2H, d, *J*= 4Hz), 7.62 (2H, d, *J*=4Hz), 7.54 (4H, m), 7.33 (4H, m), 7.22 (4H, m), 6.73 (4H, m), 1.96 (36H, s). ESI-TOF calcd for $C_{64}H_{62}N_4S_4$, 1015.46, found 1015.84. **ZnPP13** MALDI-TOF m/z calcd for $C_{64}H_{60}N_4S_4Zn$ 1078.83, found 1078.085.

Synthesis of PP14

Procedure used was the same as that for **PP1**. Reagents used were, **DP-9** (0.097g, 0.315mmol) and 3,5-dimethoxy benzaldehyde (0.052g, 0.315 mmol), $BF_3.OEt_2$ (0.0045g, 0.0315 mmol), and DDQ(0.143g, 0.629 mmol). The product was purified using column chromatography, using 1:5 EtOAc:Hexane to afford the title compound in 21% yield. ^{1}H NMR ($CDCl_3$, 400MHz) δ 7.89

(4H, br s), 7.52 (8H, m), 7.25 (8H, m), 6.09 (4H, m), 2.01 (12H, s). ESI-TOF calc for $C_{52}H_{38}N_4O_4S_4$, 911.14, found 911.48. **ZnPP14** MALDI-TOF m/z calcd for $C_{52}H_{36}N_4O_4S_4Zn$ 972.09, found 972.069. **CuPP14** MALDI-TOF m/z calcd for $C_{52}H_{36}CuN_4O_4S_4$, 972.67, found 973.22.

2.10 References

1. Kadish, K. M.; Smith, K. M.; Guilard, R., *The porphyrin handbook*. Academic Press: San Diego, 2000.

2. Vicente, M. G., Porphyrin-based sensitizers in the detection and treatment of cancer: recent progress. *Curr Med Chem Anticancer Agents* **2001,** *1* (2), 175-94.

3. Becker, E. D.; Bradley, R. B.; Watson, C. J., Proton Magnetic Resonance Studies of Porphyrins. *Journal of the American Chemical Society* **1961,** *83* (18), 3743-&.

4. Graca, M.; Vicente, M. G. H., Porphyrins and derivatives: Synthetic strategies and reactivity profiles. *Current Organic Chemistry* **2000,** *4* (2), 139-174.

5. (a) Rothemund, P., Formation of porphyrins from pyrrole and aldehydes. *Journal of the American Chemical Society* **1935,** *57*, 2010-2011; (b) Rothemund, P., A new porphyrin synthesis. The synthesis of porphin. *Journal of the American Chemical Society* **1936,** *58*, 625-627.

6. Cheng, R. J.; Latosgrazynski, L.; Balch, A. L., Preparation and Characterization of Some Hydroxy Complexes of Iron(III) Porphyrins. *Inorg Chem* **1982,** *21* (6), 2412-2418.

7. Traylor, P. S.; Dolphin, D.; Traylor, T. G., Sterically Protected Hemins With Electronegative Substituents - Effecient Catalysts for Hydroxylation and Epoxidation. *Journal of the Chemical Society-Chemical Communications* **1984,** (5), 279-280.

8. (a) Adler, A. D.; Shergali.W; Longo, F. R., Mechanistic Investigations of Porphyrin Syntheses .I. Preliminary Studies on MS-Tetraphenylporphin. *Journal of the American Chemical Society* **1964,** *86* (15), 3145-&; (b) Adler, A. D.; Longo, F. R.; Finarell.Jd; Goldmach.J; Assour, J.; Korsakof.L, A Simplified Synthesis for Meso-Tetraphenylporphin. *Journal of Organic Chemistry* **1967,** *32* (2), 476-&.

9. (a) Cavaleiro, J. A. S.; Defatima, M.; Condesso, P. N.; Olmstead, M. M.; Oram, D. E.; Snow, K. M.; Smith, K. M., an Anomalous Dipyrrole Product From Attempted Synthesis of a Tetrarylporphyrin. *Journal of Organic Chemistry* **1988,** *53* (25), 5847-5849; (b) Berenbaum, M. C.; Akande, S. L.; Bonnett, R.; Kaur, H.; Ioannou, S.; White, R. D.; Winfield, U. J., Meso-Tetra(hydroxyphenyl)porphyrins, a New Class of Potent Tumor Photosensitizers with Favorable Selectivity. *British Journal of Cancer* **1986,** *54* (5), 717-725.

10. Lindsey, J. S., Synthetic Routes to meso-Patterned Porphyrins. *Accounts Chem Res* **2010,** *43* (2), 300-311.

11. Geier, G. R.; Lindsey, J. S., Investigation of porphyrin-forming reactions. Part 1. Pyrrole plus aldehyde oligomerization in two-step, one-flask syntheses of meso-substituted porphyrins. *Journal of the Chemical Society-Perkin Transactions 2* **2001,** (5), 677-686.

12. Gupta, I.; Ravikanth, M., Spectroscopic properties of meso-thienylporphyrins with different porphyrin cores. *Journal of Photochemistry and Photobiology a-Chemistry* **2006,** *177* (2-3), 156-163.

13. Bhyrappa, P.; Bhavana, P., Meso-tetrathienylporphyrins: electrochemical and axial ligation properties. *Chem Phys Lett* **2001,** *349* (5-6), 399-404.

14. Treibs, A.; Haberle, N., Synthesis and Electron Spectra of MS-Substituted Porphines. *Annalen Der Chemie-Justus Liebig* **1968,** *718* (DEC), 183-&.

15. Torrens, M. A.; Straub, D. K.; Epstein, L. M., Mossbauer Studies on oxo-bridged Iron(III) porphines. *Journal of the American Chemical Society* **1972,** *94* (12), 4160-&.

16. (a) Boyle, N. M.; Rochford, J.; Pryce, M. T., Thienyl-Appended porphyrins: Synthesis, photophysical and electrochemical properties, and their applications. *Coordination Chemistry Reviews* **2010,** *254* (1-2), 77-102; (b) Eu, S.; Hayashi, S.; Umeyama, T.; Oguro, A.; Kawasaki, M.; Kadota, N.; Matano, Y.; Imahori, H., Effects of 5-membered heteroaromatic spacers on structures of porphyrin films and photovoltaic properties of porphyrin-sensitized TiO2 cells. *J Phys Chem C* **2007,** *111* (8), 3528-3537; (c) Medforth, C. J.; Haddad, R. E.; Muzzi, C. M.; Dooley, N. R.; Jaquinod, L.; Shyr, D. C.; Nurco, D. J.; Olmstead, M. M.; Smith, K. M.; Ma, J. G.; Shelnutt, J. A., Unusual aryl-porphyrin rotational barriers in peripherally crowded porphyrins. *Inorg Chem* **2003,** *42* (7), 2227-2241.

17. Bruckner, C.; Foss, P. C. D.; Sullivan, J. O.; Pelto, R.; Zeller, M.; Birge, R. R.; Crundwell, G., Origin of the bathochromically shifted optical spectra of meso-tetrathien-2 '- and 3 '-ylporphyrins as compared to meso-tetraphenylporphyrin. *Phys Chem Chem Phys* **2006,** *8* (20), 2402-2412.

18. Geier, G. R.; Littler, B. J.; Lindsey, J. S., Investigation of porphyrin-forming reactions. Part 3. The origin of scrambling in dipyrromethane plus aldehyde condensations yielding trans-A(2)B(2)-tetraarylporphyrins. *Journal of the Chemical Society-Perkin Transactions 2* **2001,** (5), 701-711.

19. Easson, M. W. Syntheses of Trimethylamine- and Phosphonatesubstituted Carboranylporphyrins for Application in Boron Neutron Cancer Therapy. LSU, Baton Rouge, 2008.

20. Littler, B. J.; Miller, M. A.; Hung, C. H.; Wagner, R. W.; O'Shea, D. F.; Boyle, P. D.; Lindsey, J. S., Refined synthesis of 5-substituted dipyrromethanes. *Journal of Organic Chemistry* **1999,** *64* (4), 1391-1396.

21. Jiao, L.; Hao, E.; Fronczek, F. R.; Smith, K. M.; Vicente, M. G. H., Syntheses and properties of functionalized oxacalix[4]arene porphyrins. *Tetrahedron* **2007,** *63* (19), 4011-4017.

22. Hao, E. Syntheses and Evaluation of Porphyrin Derivatives for Applications in Medicine and in Material Science. LSU, Baton Rouge, 2007.

23. Teixidor, F.; Pedrajas, J.; Rojo, I.; Vinas, C.; Kivekas, R.; Sillanpaa, R.; Sivaev, I.; Bregadze, V.; Sjoberg, S., Chameleonic capacity of 3,3 '-Co(1,2-C2B9H11)(2) (-) in coordination. Generation of the highly uncommon s(thioether)-Na bond. *Organometallics* **2003,** *22* (17), 3414-3423.

24. Vicente, M. G. H.; Wickramasinghe, A.; Nurco, D. J.; Wang, H. J. H.; Nawrocky, M. M.; Makar, M. S.; Miura, M., Synthesis, toxicity and biodistribution of two 5,15-di[3,5-(nido-carboranylmethyl)phenyl]porphyrins in EMT-6 tumor bearing mice. *Bioorganic & Medicinal Chemistry* **2003,** *11* (14), 3101-3108.

25. Fabre, B.; Hao, E. H.; LeJeune, Z. M.; Amuhaya, E. K.; Barriere, F.; Garno, J. C.; Vicente, M. G. H., Polythiophenes Containing In-Chain Cobaltabisdicarbollide Centers. *Acs Applied Materials & Interfaces* **2010,** *2* (3), 691-702.

26. Jiao, L. Synthesis and Functionalizations of Tetrapyrrole Derivatives. LSU, Baton Rouge, 2007.

27. (a) Grimes, R. N., *Carboranes*. Academic Press: New York,, 1970; p xiv, 272 p; (b) Bregadze, V. I., Dicarba-closo-dodecaboranes C2B10H12 and their derivatives. *Chem Rev* **1992,** *92* (2), 209-223.

28. Zakharkin, L. I.; Zhigareva, G. G.; Polyakov, A. V.; Yanovskii, A. I.; Struchkov, Y. T., Molecular-Structure of the 7-phenyl-12-(1'-phenyl-1',2'-dicarba-closo-dodecaboran-2'-yl)-7,8-dicarb a-nido-dodecaborate anion - a representative of a new type of dicarba-nido-dodecaborate anion formed as a Result of the Opening of the closo Structure of 1-phenyl-2-lithia-1,2-dicarba-closo-dodecaborane in the presence of HCONMe2 or Me2SOB. *Bulletin of the Academy of Sciences of the Ussr Division of Chemical Science* **1987,** *36* (4), 798-803.

29. Yang, F.; Xu, X.-L.; Gong, Y.-H.; Qiu, W.-W.; Sun, Z.-R.; Zhou, J.-W.; Audebert, P.; Tang, J., Synthesis and nonlinear optical absorption properties of two new conjugated ferrocene-bridge-pyridinium compounds. *Tetrahedron* **2007,** *63* (37), 9188-9194.

30. Higuchi, H.; Ishikura, T.; Mori, K.; Takayama, Y.; Yamamoto, K.; Tani, K.; Miyabayashi, K.; Miyake, M., Synthesis and properties of head-to-head, head-to-tail, and tail-to-tail orientational isomers of extended dihexylbithiophene-octaethylporphyrin system OEP-(DHBT)(n)-OEP connected with 1,3-butadiyne linkages (vol 74, pg 889, 2001). *Bulletin of the Chemical Society of Japan* **2001,** *74* (12), 2467-2467.

31. Capobianco, M. L.; Cazzato, A.; Alesi, S.; Barbarella, G., Oligothiophene-5-Labeled Deoxyuridines for the Detection of Single Nucleotide Polymorphisms. *Bioconjugate Chemistry* **2007,** *19* (1), 171-177.

32. Cui, M.-C.; Li, Z.-J.; Tang, R.-K.; Liu, B.-L., Synthesis and evaluation of novel benzothiazole derivatives based on the bithiophene structure as potential radiotracers for [beta]-amyloid plaques in Alzheimer's disease. *Bioorganic & Medicinal Chemistry* **2010,** *18* (7), 2777-2784.

33. (a) Gupta, I.; Ravikanth, M., Spectroscopic properties of meso-thienylporphyrins with different porphyrin cores. *Journal of Photochemistry and Photobiology A: Chemistry* **2006,** *177* (2-3), 156-163; (b) Bruckner, C.; Foss, P. C. D.; Sullivan, J. O.; Pelto, R.; Zeller, M.; Birge, R. R.; Crundwell, G., Origin of the bathochromically shifted optical spectra of meso-tetrathien-2[prime or minute]- and 3[prime or minute]-ylporphyrins as compared to meso-tetraphenylporphyrin. *Phys Chem Chem Phys* **2006,** *8* (20), 2402-2412.

34. Bhyrappa, P.; Sankar, M.; Varghese, B.; Bhavana, P., meso-Tetrathienylporphyrins: Steady-state emission and structural properties. *Journal of Chemical Sciences* **2006,** *118* (5), 393-397.

35. Rochford, J.; Botchway, S.; McGarvey, J. J.; Rooney, A. D.; Pryce, M. T., Photophysical and Electrochemical Properties of meso-Substituted Thien-2-yl Zn(II) Porphyrins. *The Journal of Physical Chemistry A* **2008,** *112* (46), 11611-11618.

36. Lakowicz, J. R., *Principles of fluorescence spectroscopy*. 3rd ed.; Springer: New York, 2006; p xxvi, 954 p.

37. Kim, D.; Holten, D.; Gouterman, M., Evidence from picosecond transient absorption and kinetic studies of charge-transfer states in copper(II) porphyrins. *Journal of the American Chemical Society* **1984,** *106* (10), 2793-2798.

CHAPTER 3: CARBORANYL FUNCTIONALIZED THIOPHENES FOR ELECTROPOLYMERIZATION AND BNCT

3.1 Introduction

Since prehistoric time, polymers have been used by Man in the form of skin, wood, bone, and fibers. Today, synthetic polymers represent the most widely used material in our day to day life. The development of polymeric science dates back to the 20th century, and since then, a lot of research has been carried out in this field. It is important to note that polymers were essentially designed to be insulators. We have materials such as plastics, rubber tubings, live wire plastic coatings, and anti-rusting materials. The list goes on and on. This was the case until 1976, when American scientists Heeger and MacDiarmid and their Japanese colleague Shirakawa discovered that when doped with iodine, polyacetylene developed metal-like properties with an increase in conductivity; this marked the beginning of modern development of conducting polymers[1]. Since then, many other conducting polymers have been synthesized including polypyrrole[2], polyaniline[3], poly(isothianaphthene)[4] and poly(phenylenevinylene)[5](see examples in Figure 3-1).

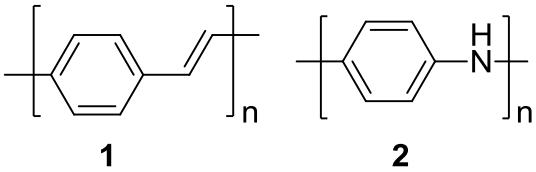

1 **2**

Figure 3-1: Structures of poly(phenylenevinylene) **1** and polyaniline **2**

In our research, we are interested in one group of conducting polymers, heterocyclic conjugated polymers. These polymers can be viewed as sp^2p_x chains whereby the structure similar to that of cis-$(CH)_x$ is stabilized by a heteroatom[6] (Figure 3-2). Since their discovery, heterocyclic

conjugated polymers have found a wide range of applications including in sensors[7], electronics[8], energy storage[9] and catalysis[10].

Figure 3-2: Structure of *cis*-$(CH)_x$ and heterocyclic conjugated polymers stabilized by a heteratom

3.2 Polythiophene Synthesis

Polythiophenes in particular have attracted a lot of interest in the research world and they have fast become the most frequently used π-conjugated materials. The main reason for this is that thiophenes can be easily functionalized to make a wide range of compounds. They can also be used as building blocks to make π-conjugated systems using transition metal-catalyzed cross-coupling reactions that are well developed. Another reason is that they have unique redox, optical and electronic properties, as well as the ability to self-assemble on solid surfaces[11]. There are two main routes by which polythiophenes (PTs) can be synthesized, i.e. the chemical route and the electrochemical route. Since their first synthesis in the 1980's, many PTs have been prepared by chemical synthesis. There has been a lot of interest in this field especially with the marked improvements in solubility of the PTs. The major drawback, however, is that polymers produced by this method contain significant regiochemical defects. This in turn leads to a loss of effective conjugation, and hence reduced conductivity levels. McCullough et al.[12] and Rieke et al.[13] have both designed syntheses that help overcome this problem (see Scheme 3-1). As a result, the polymers obtained have shown improved conductivity levels[6, 14].

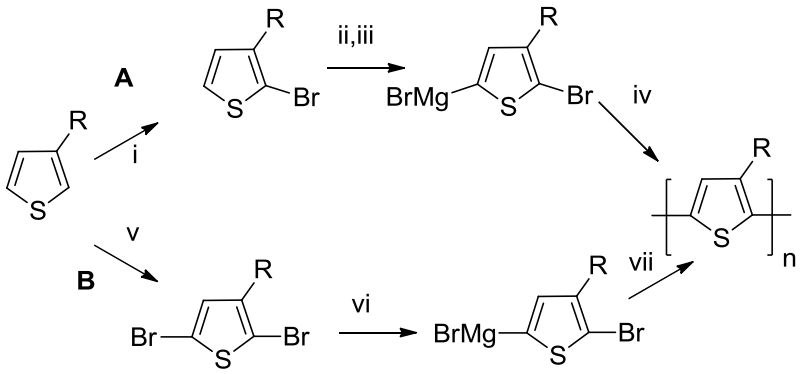

Reagents and conditions: i) Br_2/AcOH; ii) LDA/THF; iii), $MgBr_2.OEt_2$; iv), Ni(dppp)Cl_2; v) Br_2/$CHCl_3$; vi), Zn/THF; vii), Ni(dppe)Cl_2

Scheme 3-1: Two synthetic routes for preparing polythiophenes[14]

The second type of polymer synthesis, electropolymerization, also helps overcome this problem of regio-irregularity. In 1979, it was shown that polypyrrole could be produced by electropolymerization of pyrrole[15]. This process has since been extended to other aromatic compounds, including, polyaniline[16], furan[17], indole[18], benzene[19], and thiophene[18]. Synthesis of polythiophenes via electropolymerization has proved to be a challenge due to the so called "polythiophene paradox". This phenomenon refers to the overoxidation of polythiophenes whereby it competes with polymerization and oxidation of the monomer leading to the physical and chemical degradation of the polymer[20]. The mechanism of electrochemical formation of conducting polymers is characterized by the deposition of charged species produced by oxidation of the neutral monomer at the anode surface (Scheme 3-2).

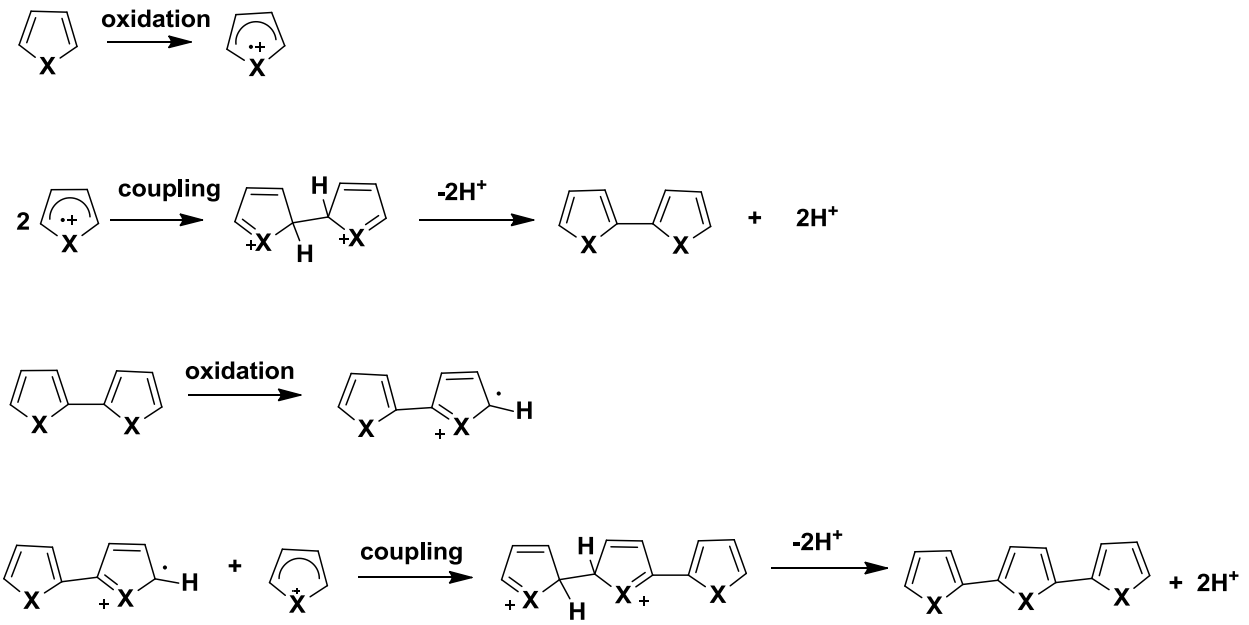

Scheme 3-2: Mechanism of electrochemical formation of conducting polymers[6]

The control of structure and properties of PTs has been pursued through the modification of the monomer structure. This can be achieved by the use of oligothiophenes as the monomeric unit[6]. The motivation behind this approach is based on two major reasons. First, the lower oxidation potentials of oligothiophenes[21] facilitate electropolymerization under mild conditions, i.e. at less positive potentials[22]. This will in turn limit the occurrence of side reactions or overoxidation of the deposited polymer. Secondly, using oligomers might reduce the α-β' defects in the polymer, since the oligomer is α-α' linked in the starting molecule[23]. The drawback with this method is that with an increase in conjugation in the starting monomer, there is a decrease in the reactivity of the corresponding cation radical. This inhibits the electropolymerization process, which affords low molecular weight polymers, and low conductivities[24]. However, even with these limits in mind, the use of oligomers provides the advantage of designing sophisticated structures which can be used to synthesize polymers with unique properties.

The structure of a monomer can be modified by functionalization of the monomers with electron-withdrawing groups. For example, it has been shown that introduction of an electron withdrawing group at the 3- and/or 4- position of a thiophene significantly decreases the polymerization potential and in turn increasing the photovoltaic polymer performance[20a, 23b, 25]. Functionalization of monomers with organoborane groups in particular is attractive due to their electron deficient nature[20b,22]. However, despite the remarkable properties associated with electron-deficient boron, organometallic polymers containing boron, have not been well established. This is due in part to the hydrolytic and oxidative sensitivity of many boron-containing molecules, thereby making the incorporation of boron into polymers synthetically difficult. Recent studies however show that not only can boron-containing polymers be obtained in high molecular weight, but also the polymers obtained are remarkably stable over long periods of time. This can be attributed to the development of new synthetic approaches to the synthesis of these polymers, as well as new methods of stabilization of the polymers. Organoborane polymers can be classified into three main categories, depending on the chemical structure of the organoborane polymer[26]; main-chain functionalized conjugated polymers, side-chain functionalized conjugated polymers and side-chain functionalized polyolefins, as shown in Figure 3-3.

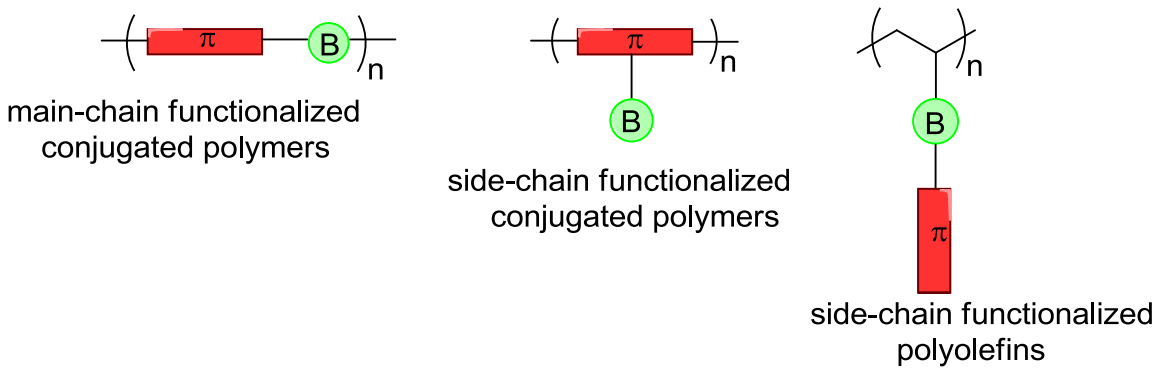

Figure 3-3: Three main categories of organoborane polymers[26].

One of the most recent advancement in the synthesis of polymeric organoboranes is the introduction of carboranes into the polymeric system. Carboranes refer to boron clusters which can either be neutral or anionic (see Figure 3-4). As a result of their three dimensional aromatic character, carboranes in both neutral and anionic forms have unique properties which include, low nucleophilicity, high hydrophobic character, as well as high chemical, thermal and optical stability[27]. Studies have shown that treatment of the closo carborane with a base readily removes a boron to form the nido ion[28]. Complexation of these open carborane cages with metals such as Ni, Co and Fe, leads to sandwich-type complexes that are highly stable. The overall charge of these complexes will vary from neutral to charged with the overall charge of -1 or -2, depending on the oxidation of the metal ion[28c]. These complexes have found practical uses in various fields, including in Boron Neutron Capture Therapy (BNCT) of tumors [29], molecular recognition[30], in construction of molecular rotors[31] and in solvent extraction of radionuclides[32].

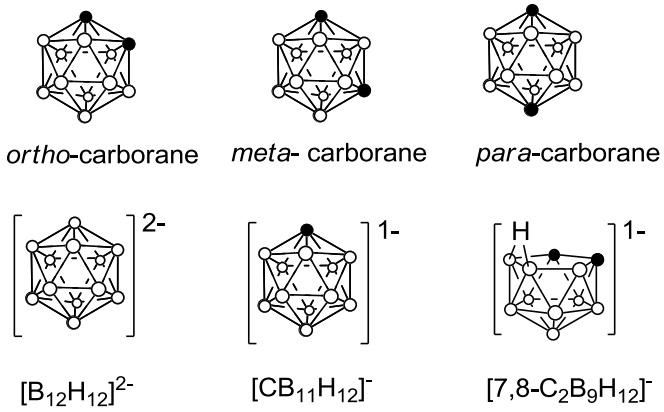

Figure 3-4: Structures of carborane cages.

We are therefore interested in the preparation of carborane substituted oligothiophenes. These compounds incorporate the desirable properties of oligothiophenes as well as those of carboranes. We expect the resulting compounds to have remarkable photophysical properties and

high stability compared to oligothiophenes without the carboranes groups. We will carry out the polymerization (chemical and electrochemical) of the cobaltabis(dicarbollide) oligothiophenes and study the physical properties of the resulting polymers. The major challenge in the polymerization of the oligothiophenes is the "polythiophene paradox" as mentioned earlier. We hope to overcome this problem with the incorporation of the electron deficient carborane into the monomeric oligothiophenes.

3.3 Results and Discussion

Synthesis of the oligothiophenes was started by Dr. Erhong Hao in our group, and we used procedures that he developed to reproduce the compounds and carry out the photophysical studies. We began by synthesis of **3** from 2-ethynylthiophene and decaborane in 56% yield as shown in Scheme 3-3. Treatment of the carborane with TBAF gave **4** in quantitative yield as a NBu_4 salt. Compound **5** was then synthesized by reacting **4** with ^tBuOK and $Co(OAc)_2$ in DME. Compound **5** was obtained after air oxidation in 70% overall yield.

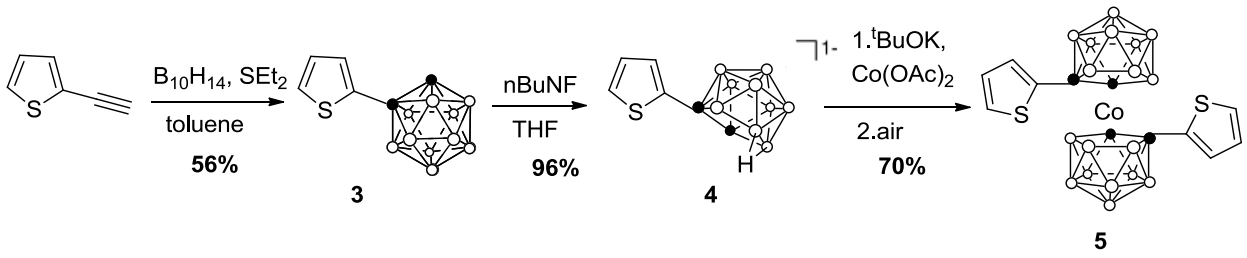

Scheme 3-3: Synthesis of thiophene-disubstituted cobaltabis(dicarbollide) **5**

The UV-Vis and fluorescence emissions of **3** and **4** were studied in DCM, MeOH and DMF. Compound **4** showed an absorption maximum that is higher than **3** in all solvents. In DCM, for example, **4** showed a maximum absorption peak at 271 nm, while **3** showed a maximum absorption at 250 nm as shown in Figure 3-5. Next we prepared the bithiophene analogue. We

started with 5-bromo-2,2'-bithiophene, which was subjected to Sonogashira coupling using trimethylsilyl acetylene, followed by deprotection of the trimethylsilane using K_2CO_3 to afford 80% of **7** after flash chromatography as shown in Scheme 3-4. Deprotection using K_2CO_3 was preferred over using 0.1M TBAF, which yielded a product that was difficult to purify, and consequently led to low yields. Compound **7** was then reacted with $B_{10}H_{14}$ to yield 70% of **8.** This was then followed by degradation using TBAF to give **9** in quantitative yields. Reaction of **9** with ^{t}BuOK and $Co(OAc)_2$ followed by air oxidation afforded 58% of compound **10**.

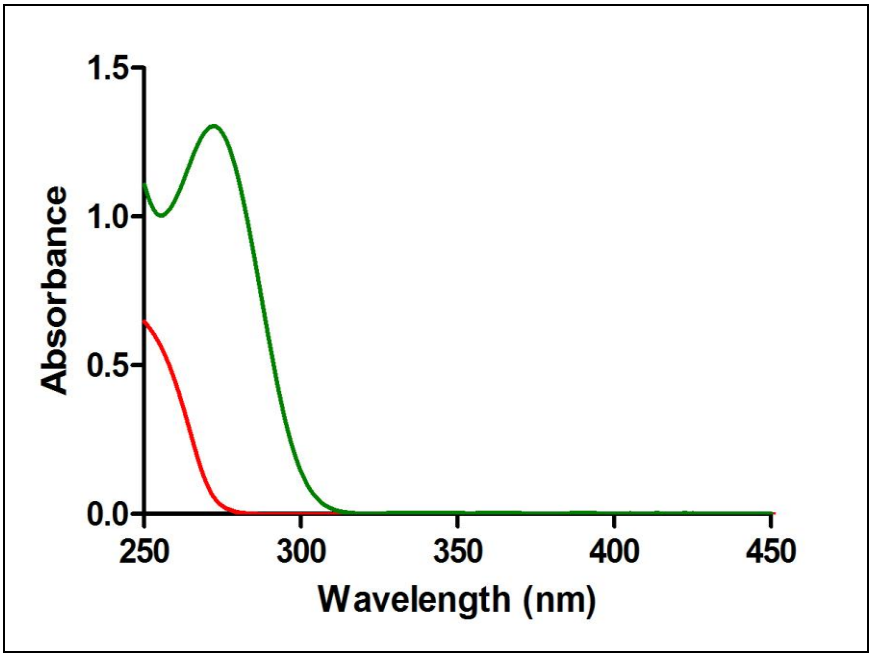

Figure 3-5: UV-vis absorption spectra of **3** (red) and **4** (green) in DCM at 25^{o}C

The UV-vis of **8** and **9** were studied in DCM, MeOH and DMF at room temperature. Just like compounds **3** and **4**, compound **9** showed a maximum absorption peak at a longer wavelength at 329 nm, compared to the maximum absorption peak at 316 nm for compound **8** in DCM as shown in Figure 3-6.

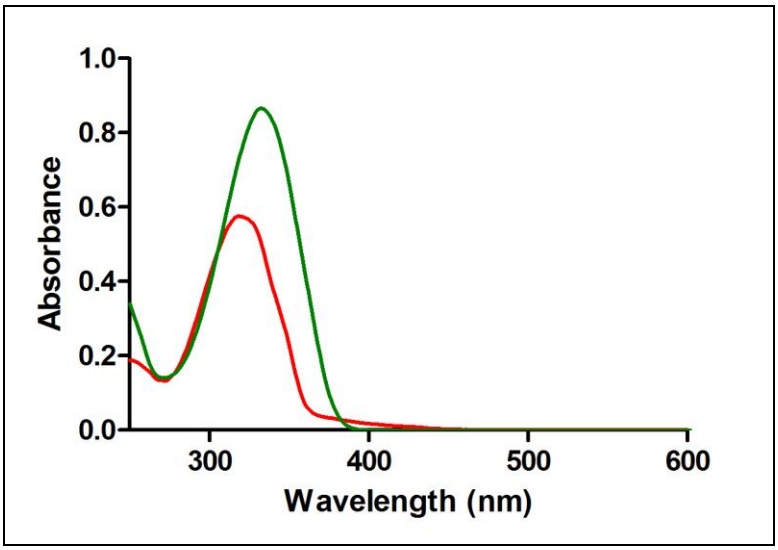

Figure 3-6: Uv-vis apsorption spectra of **8** (red) and **9** (green) in DCM at 25°C

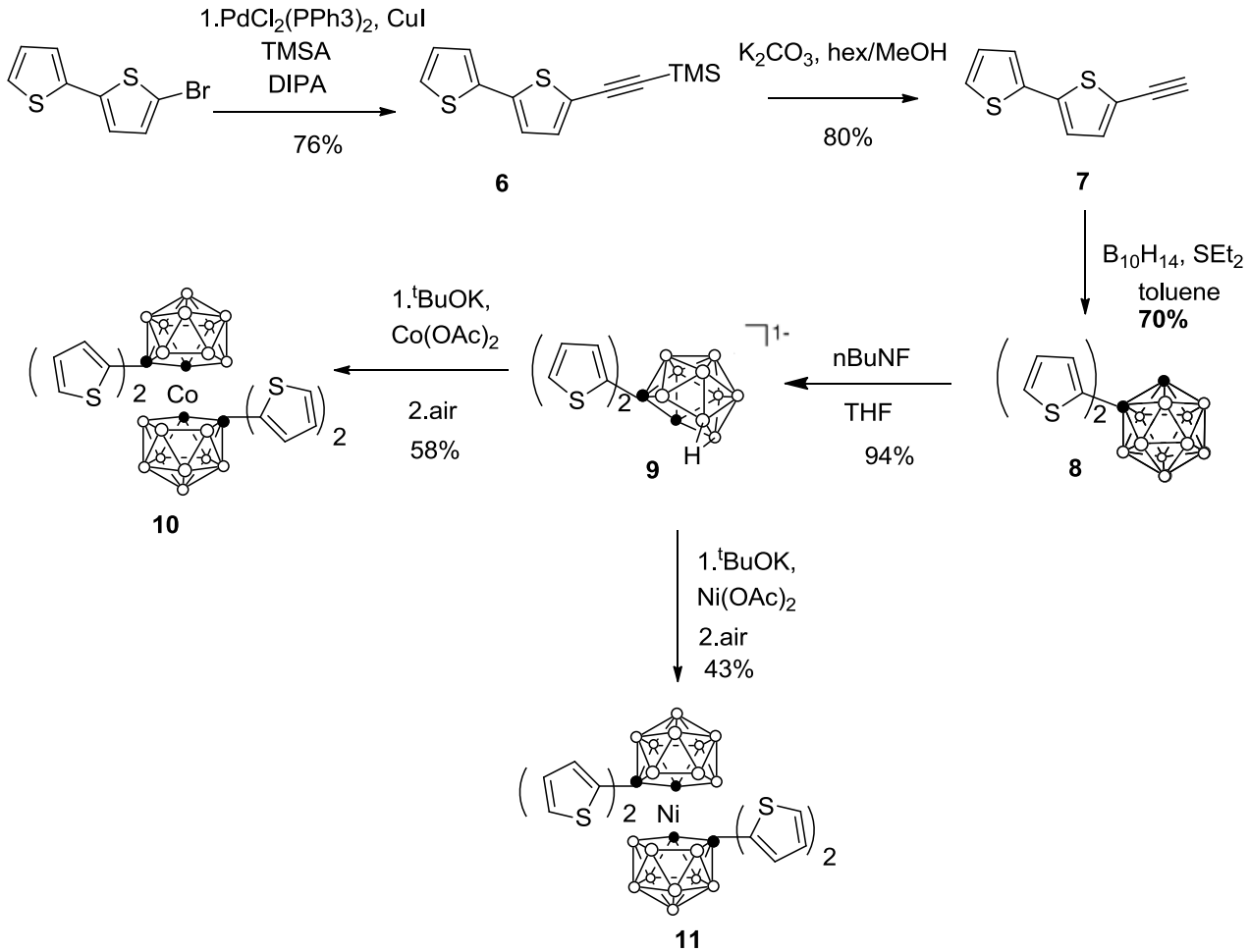

Scheme 3-4: Synthesis of bithiophene-disubstituted Co- and Ni-bis(dicarbollide) **10** and **11**

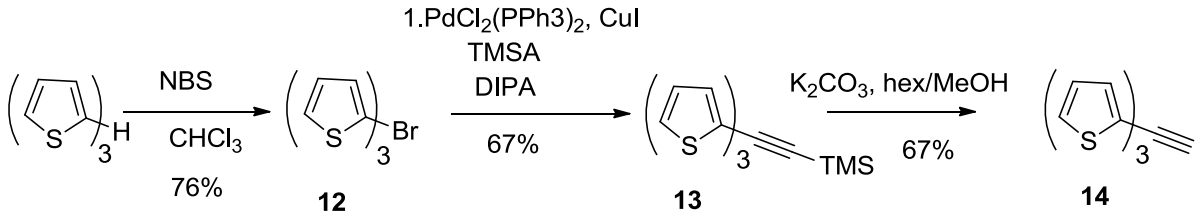

Scheme 3-5: Synthesis of 5-ethynyl-2,2':5',2"-terthiophene, **14**.

Our next step was the synthesis of the terthiophene analogue. We started the synthesis by brominating 2,2':5',2"-terthiophene using NBS to afford **12** in 76% yield as shown in Scheme 3-5. This was followed by a Sonogashira coupling reaction with **12** and TMSA. Deprotection of the trimethylsilane group was carried out using K_2CO_3 to afford 67% yield of compound **14**. Reaction of **14** with $B_{10}H_{14}$ afforded **15** in 50% yield. Treatment with base afforded **16** in quantitative yield. Finally, the reaction of **16** with ^{t}BuOK and $Co(OAc)_2$ and $Ni(OAc)_2$ afforded **17** and **18** in 60 and 43% yield respectively.

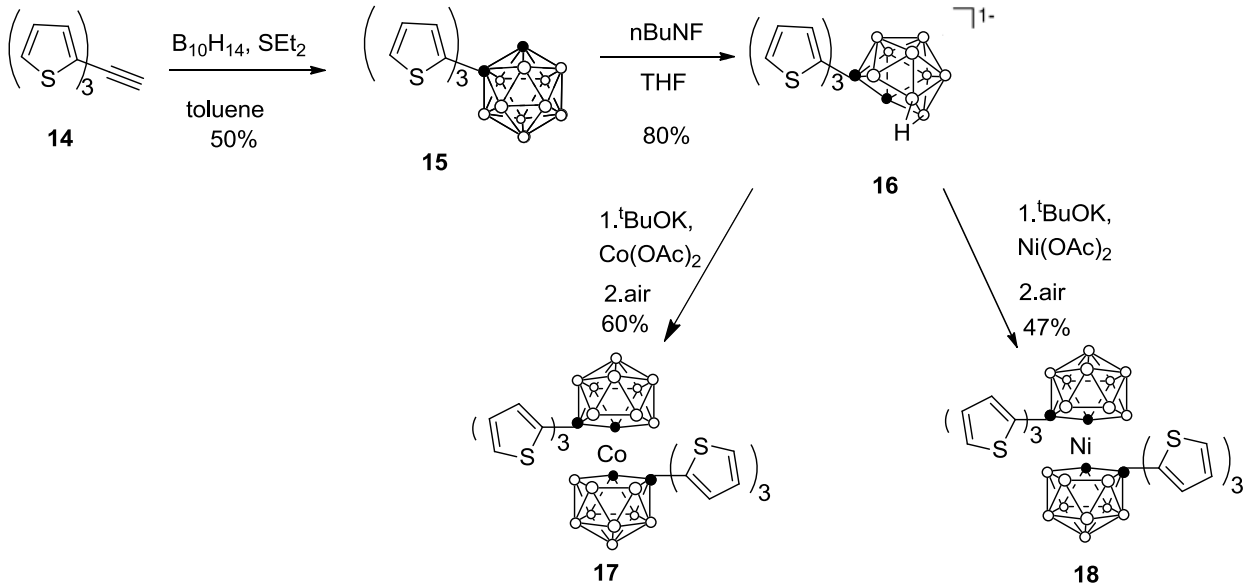

Scheme 3-6: Synthesis of terthiophene-disubstituted Co- and Ni-bis(dicarbollide) **17** and **18**.

The UV-vis of **15** and **16** studied in DCM showed that compound **16** had a maximum absorption peak at a longer wavelength than compound **15**. Compound **16** has a maximum absorption peak at 369 nm, while **15** has a maximum absorption peak at 360 nm in DCM as shown in Figure (3-7).

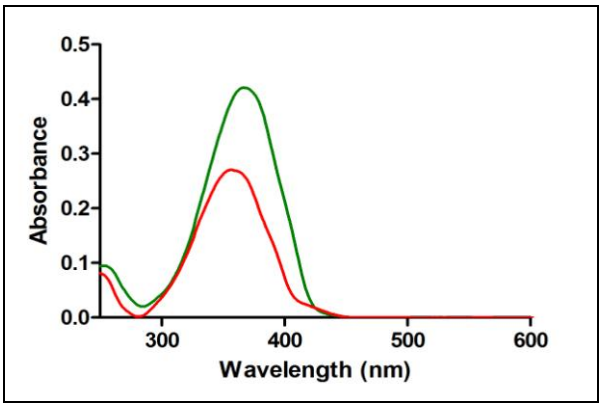

Figure 3-7: UV-vis spectra for **15** (red) and **16** (green) in DCM at 25^{o}C

An attempt to synthesize the quaterthiophene-disubstituted metallabisdicarbollides proved to be futile (see Scheme 3-7). This was as a result of the highly insoluble quaterthiophene compounds in regular organic solvents.

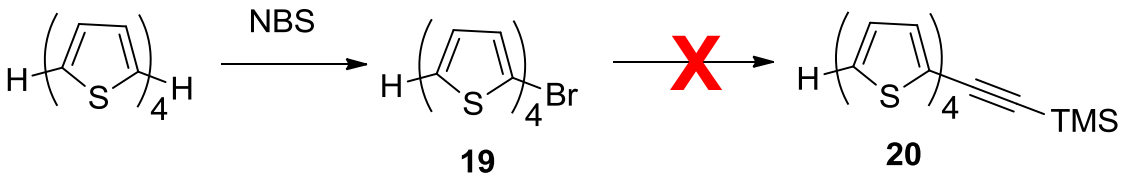

Scheme 3-7: Synthesis of ([2,2':5',2":5",2"'-quaterthiophen]-5-ylethynyl)trimethylsilane, **20**

3.4 Electropolymerization of the Cobalt(III)bisdicarbollide Complexes

Electropolymerization of the cobalt(III)bisdicarbollide complexes was carried out by our collaborator, Dr. Bruno Fabre from Université de Rennes 1, France. Both the bis(bithienyl) and bis(terthienyl) cobalt(III)bisdicarbollide complexes, **10** and **17**, yielded conducting metallopolymers. The bis(thiophene) cobalt(III)bisdicarbollide **5** however, did not electropolymerize. This can be attributed to the fact that with an increase in the length of the oligothiophene substituents, there is a decrease in the oxidative potential. This is supported by DFT calculations which indicate that as the length of the oligothiophene substituents increase, there is a drastic decrease in the metallic and dicarbollide cage carbon atom contributions, so that the HOMOs can be considered almost purely oligothiophene based (see Figure 3-8).

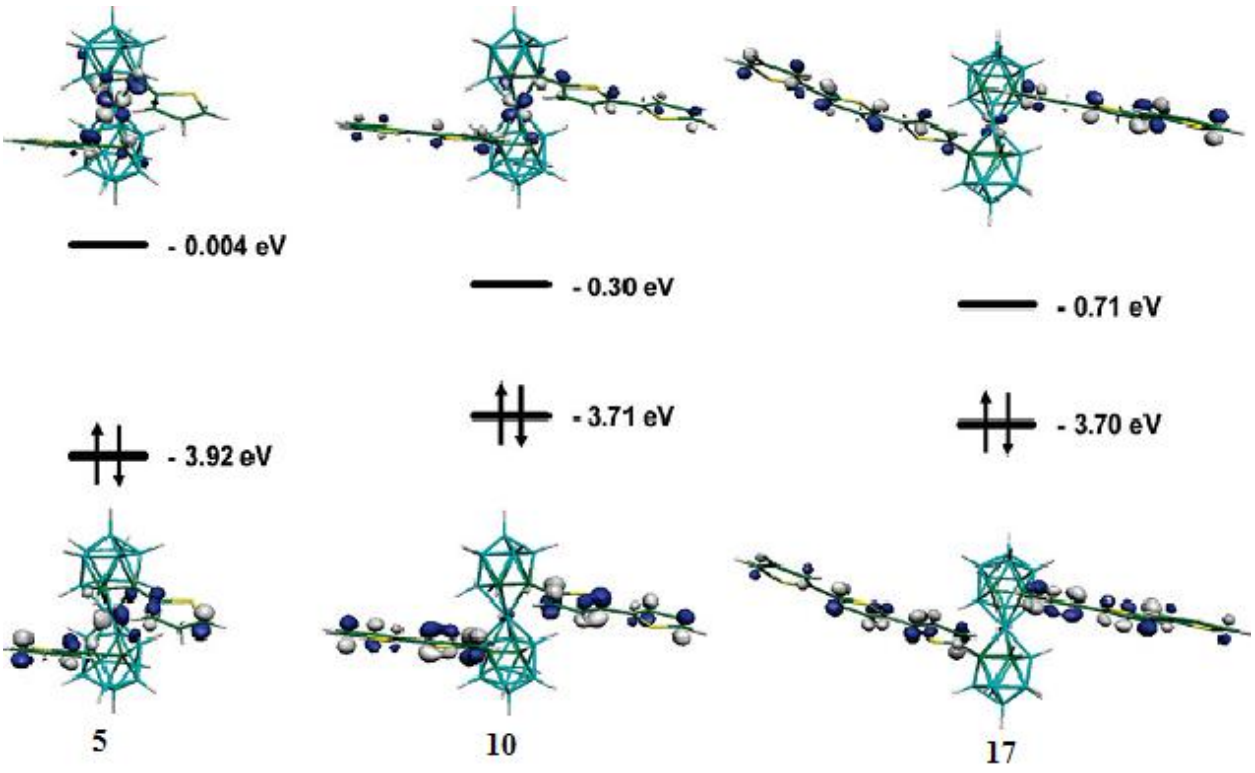

Figure 3-8: HOMOs and LUMOs of **5, 10** and **17** from DFT calculations[28c]

To help understand the properties of the polymers further, a UV-Vis spectroscopic analysis was performed on poly(**10**) and poly(**17**). The UV-Vis spectrum was carried out in DCM. For compounds **5, 10** and **17**, the bands that appeared between 260-280 nm and 460-500 nm can be attributed to the cobaltabisdicarbillide center, with the weaker one being due to d-d transition in the Co metal. **5, 10** and **17** had λ_{max} values of 250, 325 and 375 nm respectively. The polymers poly(**10**) and poly(**17**) showed absorption maximum at 410 and 448 nm respectively, which was expected since poly(**17**) assimilates the more conjugated sexithiophene compared to poly(**10)** which assimilates the quaterthiophene components (see Figure 3-9).

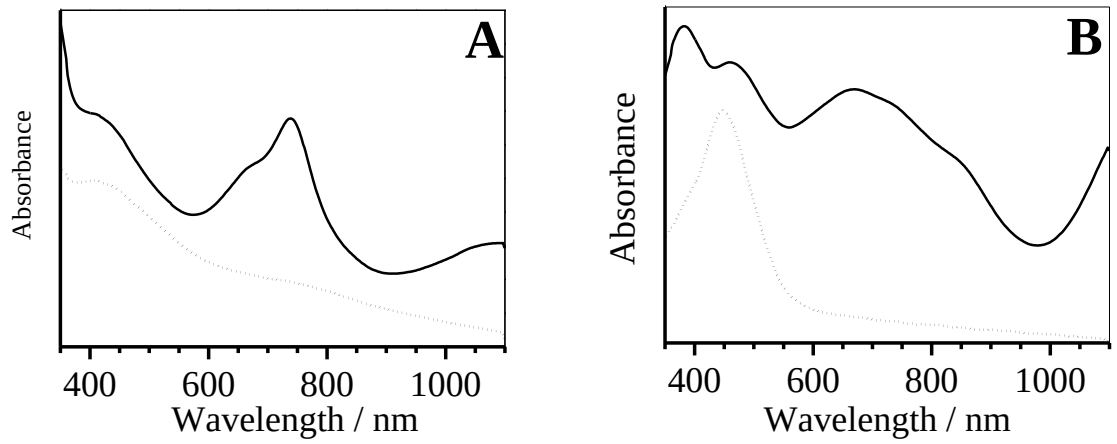

Figure 3-9: Solid-state UV-vis spectra of (A) poly(**10**) and (B) poly(**17**) in their doped (solid line) and reduced (dotted line) states[28c].

Studies on the surface morphologies of the polymers were carried out by Dr. Zorabel M. LeJeune and Dr. Jayne Garno in the Department of Chemistry at LSU. Samples of the doped and undoped films of the polymers were characterized using tapping-mode AFM. It was concluded that the undoped samples of poly(**10**) and poly(**17**) were more compressed and less rugged, compared to the doped samples (see Figure 3-10). Furthermore, a study of the polymer conductivity was

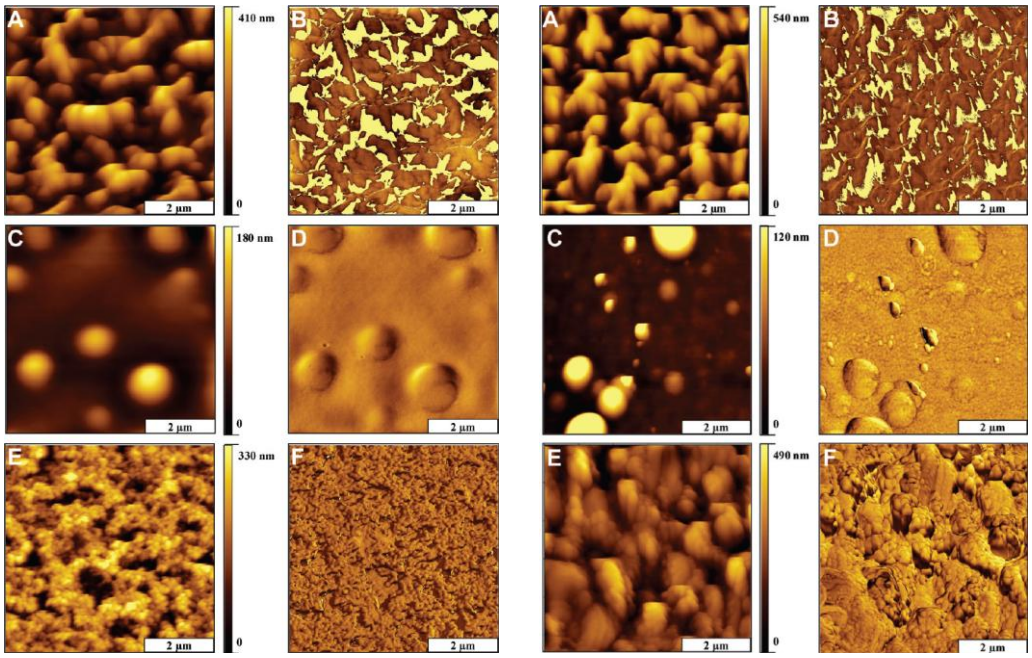

Figure 3-10: (A,C,E) Tapping-mode AFM topographs and (B,D,F) corresponding phase topographs of neutral undoped (**I**) and p-doped (**II**) (A,B) poly(**5**), (C,D) poly(**10**) and (E,F) poly(**17**). Scan size for all topographs: 5 x 5µm^{2} [28c]

carried out using conductive probe AFM. This was done by measuring the current (*I*) flowing through the polymer/gold surface junction against an applied voltage (*V*). From the profiles, it can be seen that the more conjugated poly(**17**) is more conducting than poly(**10**) as shown in Figure 3-11.

3.5 Photophysical Studies of Oligothiophenes

The effect of carboranes on the photophysical properties of the oligothiophenes was studied by comparing the absorption and emission of the carborane containing oligothiophenes with those of free oligothiophenes. We also compared the quantum yield of the different oligothiophenes as well as the solvent effects on quantum yields.

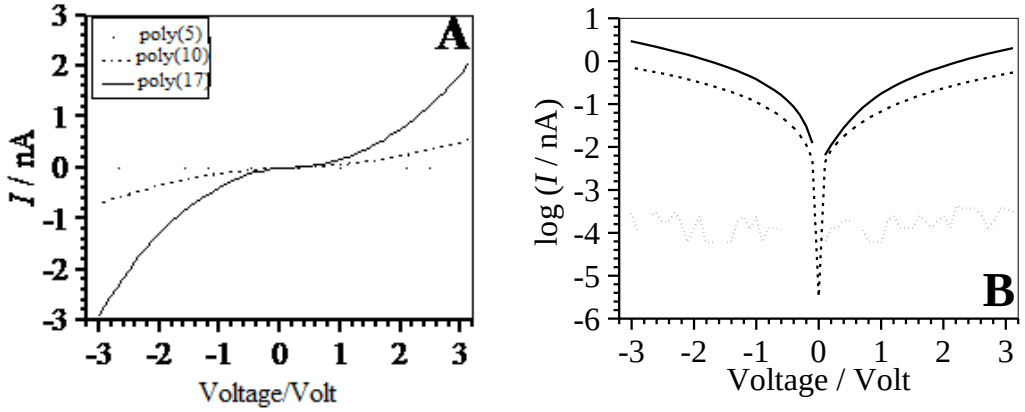

Figure 3-11: Current-voltage curves (A) and corresponding semilog plots (B) for as-grown doped poly(**5**), poly(**10**) and poly(**17**), acquired under ambient conditions[28c].

Table 3-1: Photophysical Data of oligothiophenes in DCM

Compound	Absorbance λ_{max} (nm)	Emission λ_{max} (nm)	Stoke's Shift (nm)	Quantum Yield Φ_F	Log Ɛ (M^{-1} cm^{-1})
21	-	-	-	-	-
3	250	352	102	0.006	5.0
4	271	342	71	0.07	3.8
22	303	362	59	0.018	4.0
8	317	394, 463	77, 146	0.161	3.8
9	328	399, 482	71, 154	0.254	4.3
23	354	407,426	53, 72	0.210	4.1
15	360	434	74	0.416	4.5
16	369	437	68	0.569	5.2

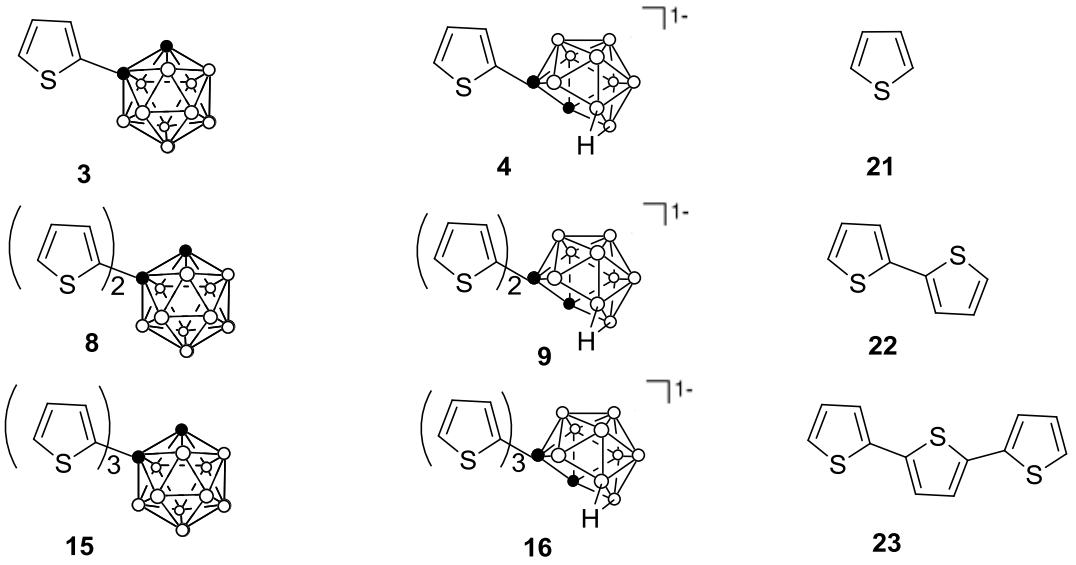

Figure 3-12: Structures of oligothiophenes studied

Table 3-2: Photophysical data of oligothiophenes in MeOH

Compound	Absorbance λ_{max} (nm)	Emission λ_{max} (nm)	Stoke's Shift (nm)	Quantum Yield Φ_F	Log Ɛ (M^{-1} cm^{-1})
21	-	-	-	-	-
3	238	362	124	4.6×10^{-5}	3.8
4	268	322	54	4.6×10^{-3}	3.8
22	301	370	69	0.031	4.2
8	316	427	111	0.068	3.8
9	354	403, 423	49, 69	0.069	4.3
23	351	403, 424	52, 73	0.063	4.1
15	371	461	90	0.086	4.3
16	355	404, 424	49,69	0.085	4.9

Table 3-3: Photophysical data of oligothiophenes in DMF

Compound	Absorbance λ_{max} (nm)	Emission λ_{max} (nm)	Stoke's Shift (nm)	Quantum Yield Φ_F	Log Ɛ (M^{-1} cm^{-1})
21	-	-	-	-	-
3	267	306	39	0.05	3.3
4	273	391	118	9.24×10^{-3}	3.4
22	305	369	64	0.06	4.0
8	323	423	100	0.13	3.7
9	358	408, 430	50, 72	0.10	4.2
23	356	409, 430	53, 74	0.088	4.5
15	375	459	84	0.151	4.3
16	358	410, 429	52, 71	0.105	4.9

From the absorption spectra shown in Table 3-1 and Table 3-2, it was evident that the compounds absorbed at longer wavelengths with increase in the number of thiophene rings. In addition to this, introduction of a carborane to the system led to a red shift in absorption. This can be attributed to the fact that carborane cages are aromatic 3-D structures, therefore, there is an increase in conjugation of the system. We also studied the quantum yields of the oligothiophenes in different solvents. As a common practice, the determination of quantum yields of an unknown is performed by comparing with a standard of known fluorescence[33]. In our case, the quantum yields were measured at 298K, using 3-chloro-7-methoxy-4-methylcoumarin (Φ_F = 0.12 in cyclohexane) as a standard[34]. The general trend for the quantum yields in DCM and MeOH was that there was an increase in quantum yield with an increase in number of thiophene rings, and also both the *closo*- and *nido*- carboranes enhanced the quantum yields. Interestingly, the trend was not observed with DMF as the solvent. In this case, the *closo*-

carborane was observed to enhance the quantum yield, while the *nido*-carborane dimished it. Studies have shown that in some solvents, the nido-carborane does indeed diminish the quantum yield[33]. A number of factors can be responsible for this observation. The first reason is the presence of photoinduced electron transfer in polar solvents which lead to low fluorescence yields[33, 35]. Secondly, presence of hydrogen bonding in polar solvents reduces quantum yields by enhancing the non-radiative decay[33, 36].

3.6 Biological Studies

In collaboration with Dr. Xiaoke Hu, we performed *in vitro* studies on these compounds to determine whether they were viable candidates for PDT and/or BNCT. The reasoning behind this was based on the fact that thiophenes are known to have many desirable properties, including their stability, and of course their photophysical properties, which have led to their being used in many optical devices[11]. Furthermore, the presence of the boron cage substituent makes these compounds promising candidates for boron delivery in BNCT applications. In addition to this, the small size of the molecules will hopefully make it easy for them to cross the BBB in the treatment of brain tumors.

The phototoxicity study on both the closo- and nido- containing oligothiophenes. This study was important because the uptake of electronic energy of a photon by a UV-absorbing molecule initiates photochemically damaging processes in the cells[37]. When a molecule absorbs a photon, it moves from the stable singlet ground state to either a singlet excited state or a triplet excited state. The triplet excited states have longer lifetimes than singlet excited states and hence, can take part in various chemical reactions. An alternative route for this triplet excited state is the transfer of triplet energy to oxygen to form singlet oxygen, $^1O_2$, which in the case of PDT destroys tumor cells. It is therefore important for the photosensitizer to not only be phototoxic,

but low concentrations of the compounds are required to bring about the necessary cancerous cell destruction. In our case, the phototoxicity assays for all the oligothiophenes were carried out *in vitro* using human carcinoma HEp2 cells. After incubating the cells for 20-24 h, the cells were exposed to low light dose (1 J cm^{-1}), and none of the oligothiophenes were found to be cytotoxic (see Figure 3-13). It is important for a compound that is a potential PDT photosensitizer to have low dark toxicity, but be cytotoxic in presence of light. For the dark toxicity test, the assays for all the oligothiophenes were carried out *in vitro* using human carcinoma HEp2 cells. They were then incubated for 20-24 h. At concentrations of 10μM, all compounds were found to be non-toxic to the cells in the dark as shown in Figure 3-14. These results indicated that despite the compounds not being potential candidates for PDT, they could potentially be used in BNCT. From cellular uptake experiments conducted over 24 h, compound **15** was found to accumulate faster and at a higher extent than all other compounds that were tested as shown in Figure 3-15.

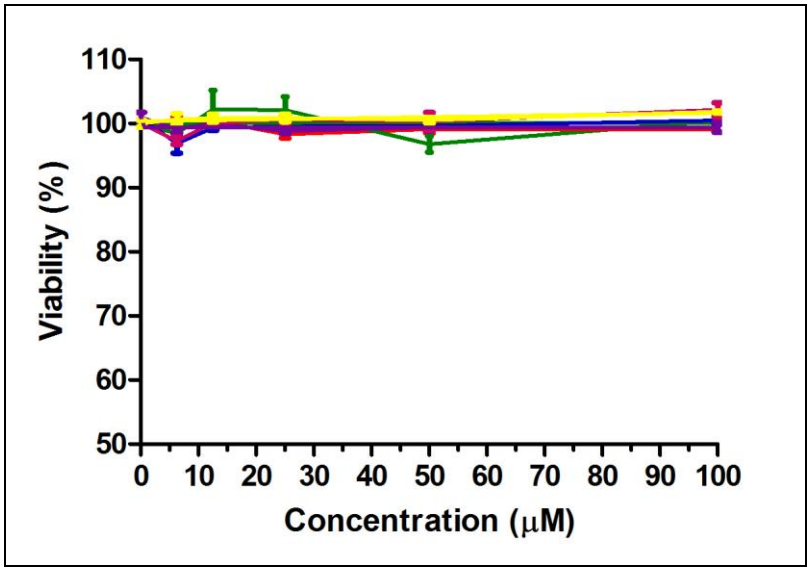

Figure 3-13: Phototoxicities of Oligothiophenes **3** (red)**, 4** (green)**, 8** (blue)**, 9** (purple)**, 15** (maroon) and **16** (yellow) toward HEp2 cells using 1 J cm^{-1} dose light.

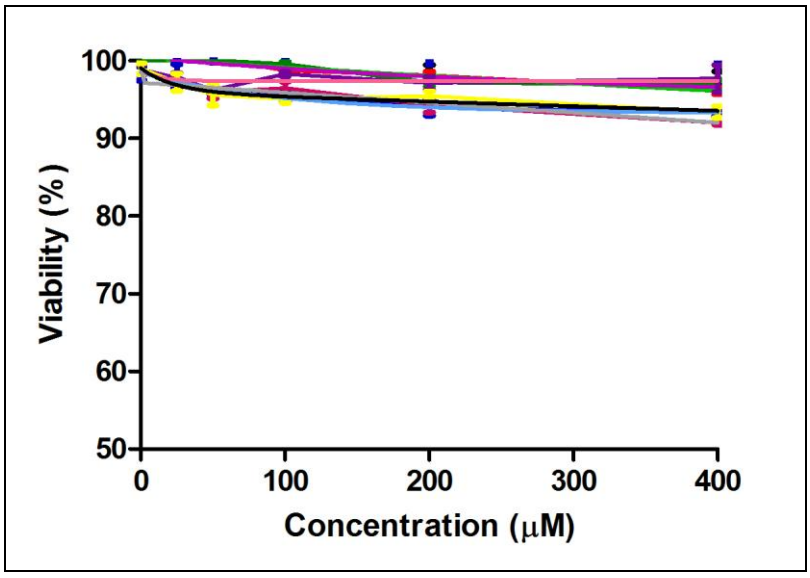

Figure 3-14: Dark Toxicity of Oligothiophenes **3** (red), **4** (green), **8** (blue), **9** (purple), **15** (maroon) and **16** (yellow) toward HEp2 cells using Titer Blue assay.

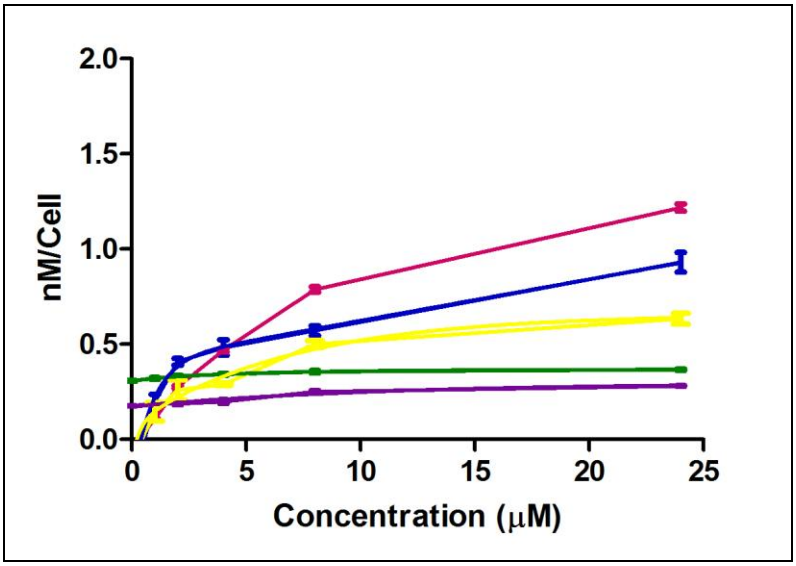

Figure 3-15: Time-dependent uptake for oligothiophenes **4** (green), **8** (blue), **9** (purple), **15** (maroon) and **16** (yellow) at 10μM by HEp2 cells.

It is important to study the intracellular localization of compounds to evaluate their potential for tumor destruction. In our study, the subcellular localization of compounds **3**, **4**, **8**, **9**, **14**, and **15**

in HEp2 cells was studied. At concentrations of 10 μM, the compounds were allowed to incubate overnight and thereafter evaluated by fluorescent microscopy (see Figures 3-16, 3-17 and 3-18).

Table 3-4: Summary of subcellular localization sites of oligothiophenes

Compound	Media/solvent	Sub-cellular localization
3	DMSO/Cremophor	Mitochondria, Golgi, Lysosome
4	DMSO/Cremophor	Mitochondria, Golgi, Lysosome
8	DMSO/Cremophor	ER (small part), Lysosome (small part), Mitochondria, Golgi
9	DMSO/Cremophor	Mitochondria, Lysosome, Golgi
15	DMSO/Cremophor	ER (small part), Golgi, Lysosome, Mitochondria
16	DMSO/Cremophor	Mitochondria, Golgi, Lysosome (part)

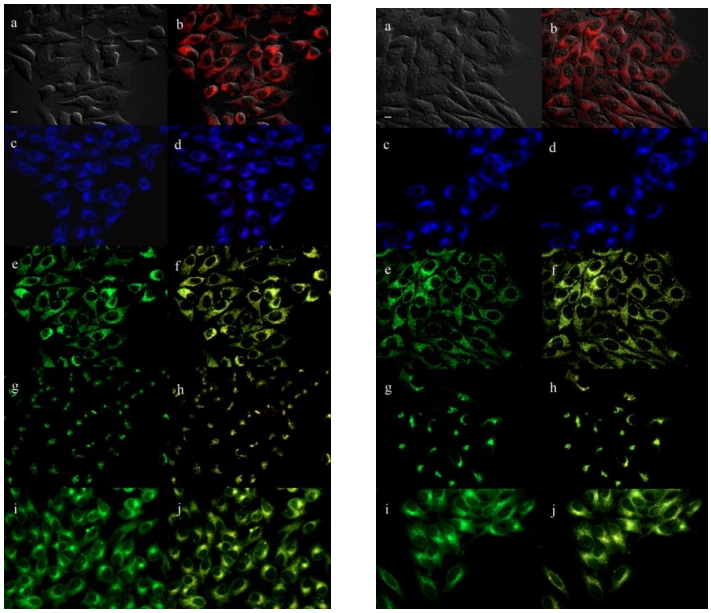

3 **4**

Figure 3-16: Subcellular localization of **3** and **4** in HEp2 cells at 10μM for 24 h. (a) Phase contrast, (b) overlay of **3** and **4** and phase contrast, (c) ER-tracker green fluorescence (e) MitoTracker Green Fluorescence (g) LysoSensor Green fluorescence, (i) BODIPY Ceramide fluorescence, (d), (f), (j) overlays of organelle tracers with **3** and **4**. Scale bar: 10 μM.

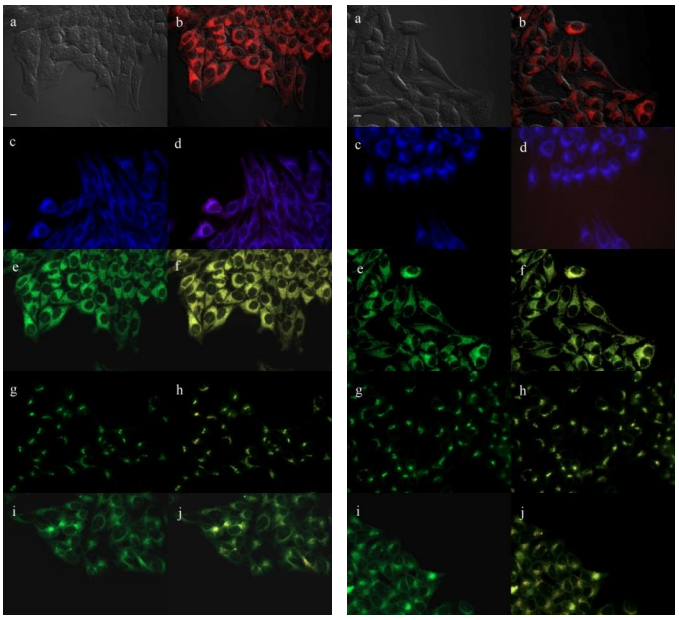

8 **9**

Figure 3-17: Subcellular localization of **8** and **9** in HEp2 cells at 10μM for 24 h. (a) Phase contrast, (b) overlay of **8** and **9** and phase contrast, (c) ER-tracker green fluorescence (e) MitoTracker Green Fluorescence (g) LysoSensor Green fluorescence, (i) BODIPY Ceramide fluorescence, (d), (f), (j) overlays of organelle tracers with **8** and **9**. Scale bar: 10 μM.

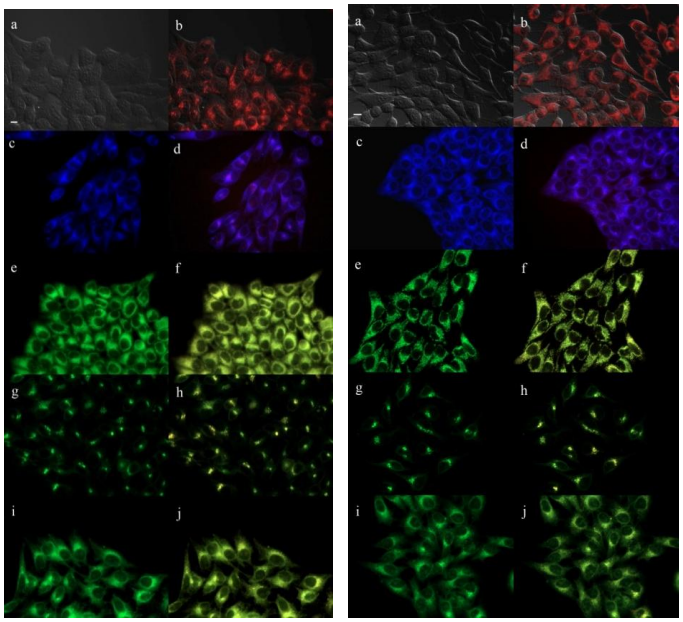

15 **16**

Figure 3-18: Subcellular localization of **15** and **16** in HEp2 cells at 10μM for 24 h. (a) Phase contrast, (b) overlay of **15** and **16** and phase contrast, (c) ER-tracker green fluorescence (e) MitoTracker Green Fluorescence (g) LysoSensor Green fluorescence, (i) BODIPY Ceramide fluorescence, (d), (f), (j) overlays of organelle tracers with **15** and **16**. Scale bar: 10 μM.

As previously discussed, all oligothiophenes were foud to emit at wavelengths between 322 and 459, as shown in Tables 3-1, 3-2 and 3-3. However, when carrying out the sub-cellular localization studies, it was observed that all the studied oligothiophenes emitted at wavelengths > 500 nm. A possible explanation for this observation could be that in cell media, these oligothiophenes undergo some form of polymerization so that they form more conjugated systems, which emit at longer wavelengths than the corresponding oligothiophenes. Further studies are currently going on to establish the reason behind this behavior.

3.7 Conclusions

Synthesis of various caboranyl-substituted oligothiophenes was successfully carried out. The compoundss were purified using silica gel chromatography and obtained in good yields. Complexation of the open cage carborane derivatives with Co and Ni afforded the highly stable Co- and Ni- bis(dicarbollide) compounds respectively. A study on the photophysical properties of the oligothiophenes revealed that the wavelength of absorption increases with an increase in the number of thiophene rings. In addition it was observed that the nido-carborane containing oligothiophene absorbed at longer wavelength and recorded higher quantum yields than the closo-carborane containing oligothiophenes. However, the effects of solvent polarity on the quantum yields was observed when DMF was used. It was observed that in DMF, the nido-carborane containing oligothiophenes recorded lower quantum yields than their corresponding closo-caborane containing oligothiophenes. From the biological data obtained, we noted that the synthesized oligothiophenes were potential candidates for use in BNCT. Further work is being carried out by our group to help us understand why the oligothiophenes emit at longer wavelengths in cells as observed during *in vitro* cell studies.

3.8 Experimental

General Procedure

All reactions were monitored by thin layer chromatography (TLC) using 0.25mm silica gel plates purchased from Sorbent technologies, with or without UV indicator (60F-254). All column chromatographies were run using silica gel, 32-63μm from Sorbent Technologies. ^{1}H and ^{13}C NMR spectra were obtained either on a DPX-250 or AV-400 Bruker spectrometer. Chemical shifts (δ) are given in ppm relative to $CDCl_3$ (7.26ppm, ^{1}H; 77.2ppm, ^{13}C), or acetone-d_6 (2.05ppm, ^{1}H; 54.0ppm ^{13}C). MALDI-TOF mass spectra were obtained on a Bruker OmniFLEX MALDI-TOF mass spectrometer. ESI-TOF was obtained on Agilent 6210. Reagents and solvents were obtained from either Sigma-Aldrich or Fischer Scientific, and were used without further purification. Decaborane was obtained from Katchem, Inc. (Czech Republic) and all other reagents were obtained from Sigma-Aldrich and used without further purification.

UV-Visible Spectroelectrochemistry

UV-visible absorption spectra were recorded on a Shimadzu Multispec-1501 spectrophotometer (190-1100 nm scan range) using quartz SUPRASIL cells (1 cm). The polymer films were grown on an indium tin oxide (ITO)-coated glass slide electrode.

Computational Analysis

Density functional theory (DFT) calculations and performed with the hybrid Becke three-parameter exchange functional and the Lee-Yang-Parr nonlocal correlation functional (B3LYP)

implemented in the Gaussian 03 (Revision D.02), program suite using the LanL2DZ basis set. The figures were generated with MOLEKEL 4.3[28c].

Conducting Probe Atomic Force Microscopy (AFM)

Samples of doped and undoped cobaltabisdicarbollide-functionalized polythiophene films were prepared on gold surfaces on glass using controlled potential electropolymerization. The substrates have a gold coating (1000 Å) on a 50 Å layer of Cr formed on glass. Surface characterizations were accomplished in ambient conditions using a model 5500 scanning probe microscope (SPM). Characterizations of the surface morphology were carried out using tapping mode atomic force microscopy (AFM). Monolithic silicon probes (PPP-NCL) were used for tapping mode experiments. A multipurpose SPM scanner with was used for imaging, with interchangeable nose cones for either tapping mode or conductive probe AFM experiments. For current imaging and *I-V* measurements, a preamp is integrated within the nose cone. Conductive probe AFM experiments were carried out using a V-shaped conductive AFM tip (CSC11/Ti-Pt, coated with 10 nm Pt layer on a sublayer of 20 nm Ti.

Cell Culture

All tissue culture media and reagents were obtained from Invitrogen. HEp2 cells were plated on LabTek II two chamber coverslips. They were allowed to grow for a duration of 24-48h. Compounds being investigated were then added at 10μM and incubated overnight. This was then followed by the addition of the tracers, which were added concurrently with the compound for the remainder of the incubation period. The tracers used were: BODIPY Ceramide, ERTracker Green, LysoSensor Green and MitoTracker Green. Distribution of the compound was determined

using a Zeiss AxioVert 200M inverted fluorescent microscope fitted with standard texas Red, FITC, DAPI and Cy5LP filter sets.

Phototoxicity

The HEp2 cells were placed at 7500 per well in costar 96-well plate and allowed to grow overnight. Compounds were diluted to 100μM in medium, and then diluted to the final working concentrations of 6.25μM. (If DMSO was required to dissolve the compound, a 1% DMSO concentration was maintained throughout the experiment and dilutions by replacing the growth medium with medium plus 1% DMSO before making dilutions) The cells were then incubated overnight (20-24h). The loading medium was then removed and the cells were fed medium containing 50mM HEPES pH 7.4. The plate was placed on ice. It was then exposed to a 610nm LP filtered light from a halogen lamp for 20 minutes (~1 Jcm^{-2}). IR radiation was filtered using a 10nm water layer contained in a petri dish placed on top of the 96 well plate. The medium was removed and cells fed medium containing 20μL CellTiter Blue per 100μL medium and then incubated for 4 hours. This was followed by conversion of the substrate by viable cells which was measured by fluorescence..

Dark Toxicity

HEp2 cells were plated at 7500 cells per well in Costar 96-well plates and allowed to grow for 48h. Compounds were diluted to 100μM in medium, and then diluted to 6.5μM.(If DMSO was required to dissolve the compound, a 1% DMSO concentration was maintained throughout the experiment and dilutions by replacing the growth medium with medium plus 1% DMSO before making dilutions) The cells were incubated overnight (20-24h). Loading medium was then removed and cells were fed medium containing 20μL CellTiter Blue per 100μL medium and

then incubated for 4h. This was followed by conversion of the substrate by viable cells which was measured by fluorescence at 570/615nm.

Time Dependent Cellular Uptake

HEp2 cells were plated at 7500 per well on Costar 96-well dish and allowed to grow for 48h. Compounds were diluted to a 20μM stock in medium. Equal volume of the stock was added in triplicate wells containing cells (100μL) to give a final concentration of 10μM. The cells were exposed to the compounds for 1h, 2h, 4h, 8h and 24h. At the end of the incubation time, the medium was removed and the cells washed with 200μL of PBS. After removal of PBS, the cells and compounds were then solubilized using 100μL of 0.25% Triton X-100 in PNS. To determine the compound concentration, fluorescence emission was read using FLUOstar plate reader using excitation/emission wavelengths appropriate for the compound under study. The cell numbers were quantified using the CyQuant cell proliferation assay reagent.

Synthesis of Thiophene-2-*o*-carborane (3)

Decarborane (2.6g, 21.26 mmol) was dissolved in 30 mL dry toluene. To this solution was added diethylsulfide (4.22g, 46.78 mmol) and the reaction mixture allowed to stir at 40oC for 3 h, and then at 60oC for 2h. 2-ethynylthiophene (2.3g, 21.26 mmol) was dissolved in 30 mL dry toluene and this solution added to the decarborane solution. The final reaction mixture was allowed to reflux for 48h. After the 48h, it was allowed to cool to room temperature, after which the solvent was evaporated under vacuum. The resulting residue was purified by column chromatography using 2:8 DCM/Hexane as eluent. The product was obtained as white crystals in 56% yield. ^{1}H NMR ($CDCl_3$, 250 MHz) δ 7.25-7.27 (1H, m), 7.20-7.21 (1H, m), 6.90-6.92 (1H, m), 3.86 (1H, s), 1.50-3.50 (br, 10H). ^{13}C NMR ($CDCl_3$, 63 MHz) 137.2, 130.4, 128.3, 127.7, 72.4, 63.7. ^{11}B

NMR ($CDCl_3$, 128 MHz, $BF_3.OEt_2$)δ -3.3 (d, ^1J(B,H)) 146 Hz, 1B) -6.6 (d, ^1J(B,H)) 147 Hz, 1B), -10.0 to -16.0 (br m, 8B). MALDI-TOF [M + H]+ 226.3. HRMS(ESI) *m/z* calcd for $C_6H_{13}B_{10}S$, 226.1739; found, 226.1746.

Synthesis of Tetrabutylammonium Thiophene-2-*o*-nido-carborane (4)

Thiophene-2-o-carborane (0.23g, 1.02 mmol) was dissolved in 10 mL dry THF. To this solution, 2.04 mL of TBAF (1.0M in THF) was added under a nitrogen atmosphere. The reaction mixture was stirred at 60^{o}C for 2h and the reaction monitored by TLC to make sure no more starting material was present. It was then poured into 50mL water and extracted with EtOAc. The organic layers were dried over anhydrous Na_2SO_4. It was then filtered, and the solvent removed under vacuum. The final residue was purified by passing through a pad of silica gel using EtOAc as eluent. The product was obtained as a white solid in 96% yield. ^{1}H NMR (acetone-d_6, 250 MHz) δ 6.95 (1H, m), 6.74 (1H, m), 6.65 (1H, m), 3.37 (8H, m), 3.35 (1H, br),1.75 (8H, m), 1.50-3.50 (br, 9H, BH), 1.37 (8H, m, CH_2), 0.91 (12H, m, CH_3), -2.03-2.50 (1H, br,BH). ^{13}C NMR ($CDCl_3$, 100 MHz) 150.9, 126.3, 121.9, 121.5,60.3, 59.0, 24.0, 21.0, 19.7, 13.6. ^{11}B NMR ($CDCl_3$, 128 MHz,$BF_3.OEt_2$) δ -10.0 to -16.0 (br m, 3B), -18.0 to -20.0 (br m,3B), -24.6 (d, ^1J (B,H)) 149 Hz, 1B), -34.7(dd, ^1J (B,H)) 43.8Hz, ^1J (B,H)) 43.7 Hz, 1B), -37.6 (d, ^1J(B,H)) 138 Hz, 1B).HRMS (ESI) [M-NBu_4]-*m*/*z* calcd for $C_6H_{14}B_9S$, 214.1657; found,214.1664.

Synthesis of Tetrabutylammonium Cobalt(III) Bis-(thiophene-2-*o*-nido-carborane) (5)

Tetrabutylammonium thiophene-2-*o*-nido-carborane (0.46g, 1.00mmol), anhydrous $CoCl_2$ (1.35g, 10.00 mmol) and *t*BuOK (1.12 g, 10.0 mmol), were dissolved in 10 mL of anhydrous dimethoxyethane. The reaction was placed under nitrogen atmosphere and allowed to reflux for 30 h. It was then cooled to room temperature and the precipitate that formed filtered off. The

filtrate was diluted using 50 mL dichloromethane and washed with *n*-Bu_4NHSO_4 aqueous solution. The organic layers were dried over anhydrous Na_2SO_4 and dried under a vacuum. The final residue was purified by column chromatography using DCM as the eluent. The product was obtained as a yellow powder 0.25g ,70 % yield. ^{1}H NMR (acetone-d_6, 250 MHz) δ 7.23 (1H,m), 7.14 (1H, m), 6.89 (2H, m),6.76 (1H, m), 6.64 (1H, m), 4.26 (1H, s), 3.42 (8H, m), 3.23 (1H, s), 1.77 (8H,m), 1.53-3.40 (18H, br), 1.38 (8H, m), 0.95-1.01 (12H, m). ^{13}C NMR ($CDCl_3$, 100 MHz) 125.7,125.8, 123.2, 59.1, 30.9, 24.1, 19.7, 13.7. ^{11}B NMR ($CDCl_3$, 128 MHz, $BF_3.OEt_2$) δ 9.0-30.0 (br m, max at 5.9, -0.5, -8.8 and -30.8, 18B) ppm. HRMS (ESI) $[M\text{-}NBu_4]^-$ *m*/*z* calcd for $C_{12}H_{26}B_{18}S_2Co$, 488.26; found, 488.2628.

Synthesis of ([2,2'-bithiophen]-5-ylethynyl)trimethylsilane (6)

To a mixture of 5-bromo-2,2'-bithiophene (1.0g, 4.1mmol), PdCl2(PPh3)2 (0.143g, 0.204mmol), CuI (0.039g, 0.204mmol) in DIPA (60ml) was added TMSA (1.41ml, 10.2mmol) dropwise under argon atmosphere. The mixture was stirred at room temperature for 6h. The reaction was quenched by pouring into water and extracting with ethyl acetate. The organic layers were concentrated under reduced pressure and the residue purified by column chromatography using 20%DCM in hexanes to produce 76% product as a yellow solid. ^{1}H NMR ($CDCl_3$, 400MHz) δ 7.24 (1H, d, *J*= 5Hz, ArH), 7.18 (1H, d, *J*= 4Hz, ArH), 7.13 (1H, d, *J*= 4Hz, ArH), 7.02 (2H, t, J^1= 5Hz, J^2= 4Hz, ArH), 0.26 (9H, s, CH_3).

Synthesis of 5-ethynyl-2,2'-bithiophene (7)

Protecting group was removed from ([2,2'-bithiophen]-5-ylethynyl)trimethylsilane, **6**, (0.71g, 2.71mmol) by reacting it with K_2CO_3 (1.12g, 8.13mmol) at room temperature for 2h. The reaction was quenched by addition of water. This was diluted with Et_2O and washed with water.

The organic layer was dried over Na_2SO_4 and evaporated under pressure. The residue was purified using column chromatography using 20%DCM in hexanes to produce 80% product as a yellow solid. ^{1}H NMR ($CDCl_3$, 400MHz) δ 7.25 (1H, d, *J*= 1Hz, ArH), 7.19 (2H, m, ArH), 7.03 (2H, d, *J*= 4Hz, ArH), 3.41 (1H, s, CH).

Synthesis of 2,2′-Bithiophene-5-*o*-carborane (8)

Decarborane (0.072g, 0.57mmol), 2-ethynylbithiophene (0.062g, 0.33mmol), and dry CH_3CN (0.5ml) were dissolved in dry toluene (1.5ml). The reaction mixture was stirred at 80^{o}C under nitrogen atmosphere for 24h. It was then cooled to room temperature, and methanol (1.0ml) added to the reaction mixture. It was then stirred for 30 min followed by drying under vacuum. The final residue was purified by column chromatography using 10% DCM in hexanes as eluent. The title compound was obtained as a light brown solid, in 70% yield. ^{1}H NMR ($CDCl_3$, 250 MHz) *δ* 7.27 (1H, d, *J*) 5.10 Hz, ArH), 7.18 (1H, d, *J*) 3.00 Hz, ArH), 7.09 (1H, d, *J*) 3.73 Hz, ArH), 7.03 (1H, t, *J*) 4.48 Hz, ArH), 6.94 (1H, d, *J*) 3.71 Hz, ArH), 3.86 (1H, s, CH), 1.50-3.50 (br, 10H, BH).^{13}C NMR ($CDCl_3$, 63 MHz) 140.4, 136.0, 135.2, 131.1, 128.5, 126.2, 125.3, 123.8, 72.4, 63.8. ^{11}B NMR ($CDCl_3$, 128 MHz, $BF_3.OEt_2$)*δ* -3.4 (d, ^1J(B,H)) 145 Hz, 1B), -6.5 (d, ^1J(B,H)) 141 Hz, 1B), -10.0 to -16.0 (br m, 8B). MALDI-TOF [M +H]+ 309.5. HRMS (ESI) *m/z* calcd for $C_{10}H_{15}B_{10}S_2$, 307.1630;found, 307.1623.

Synthesis of Tetrabutylammonium 2,2′-Bithiophene-5-*o*-nido-carborane (9)

2,2′-Bithiophene-5-*o*-carborane (0.50g, 1.62 mmol) was dissolved in 20 mL dry THF. To this solution, 3.24 mL of TBAF (1.0M in THF) was added under a nitrogen atmosphere. The reaction mixture was stirred at 60^{o}C for 2h and the reaction monitored by TLC to make sure no more starting material was present. It was then poured into 100 mL water and extracted with EtOAc.

The organic layers were dried over anhydrous Na_2SO_4. It was then filtered, and the solvent removed under vacuum. The final residue was purified by passing through a pad of silica gel using EtOAc as eluent. The product was obtained as a yellow solid, in 94% yield. ^{1}H NMR (acetone-d_6, 250 MHz) δ 7.27(1H, dd, *J*) 1.11 Hz, *J*) 4.02 Hz, ArH), 7.08 (1H, dd, *J*) 1.07Hz, *J*) 2.50 Hz, ArH), 6.98 (1H, dd, *J*)5.04 Hz, *J*)1.43 Hz,ArH), 6.88 (1H, d, *J*) 3.69 Hz, ArH), 6.58 (1H, d, *J*) 3.73 Hz,ArH), 3.36-3.43 (8H, m, CH_2), 2.87 (1H, br s, CH), 1.73-1.83(8H, m, CH_2), 1.50-3.50 (br, 9H, BH), 1.35-1.46 (8H, m, CH_2),0.91-1.00 (12H, m, CH_3), -2.51 (br, 1H, BH).^{13}C NMR (acetone-d_6,63 MHz) 152.1, 138.8, 133.5, 128.6, 124.3, 123.7, 123.2,122.9, 80.5, 77.1, 59.2, 24.3, 20.3, 13.8. ^{11}B NMR ($CDCl_3$, 128MHz, $BF_3.OEt_2$) δ -10.0 to -16.0 (br m, 3B), -18.0 to -20.0(br m, 3B), -24.6 (d, ^1J (B,H)) 149 Hz, 1B), -34.7 (dd, ^1J (B,H)) 43.8 Hz, ^1J (B,H)) 43.7 Hz, 1B), -37.6 (d, ^1J(B,H)) 138 Hz,1B). HRMS (ESI) [M-NBu_4]- *m*/*z* calcd for $C_{10}H_{16}B_9S_2$, 298.1582;found, 298.1586.

Synthesis of Tetrabutylammonium Cobalt(III) Bis(2,2′-bithiophene-5-*o*-nido-carborane) (10)

Tetrabutylammonium 2,2′-Bithiophene-5-*o*-nido-carborane (0.022g, 0.07mmol), anhydrous $CoCl_2$ (0.095g, 0.73 mmol) and *t*BuOK (0.082 g, 0.73 mmol), were dissolved in 0.5 mL of anhydrous dimethoxyethane. The reaction was placed under nitrogen atmosphere and allowed to reflux for 30 h. It was then cooled to room temperature and the precipitate that formed filtered off. The filtrate was diluted using 10 mL dichloromethane and washed with *n*-Bu_4NHSO_4 aqueous solution. The organic layers were dried over anhydrous Na_2SO_4 and dried under a vacuum. The final residue was purified by column chromatography using DCM as the eluent. Product was obtained as a dark yellow solid in 58% yield. ^{1}H NMR (acetone-d_6, 250 MHz) δ 7.19 (3H, m), 7.06 (2H, m), 6.98 (2H, m), 6.79 (2H, br s), 6.41 (1H, br s), 4.17 (1H, br s),3.32

(1H, br s), 3.07 (8H, m), 1.60 (8H,m), 1.50-3.50 (18H, br, BH), 1.37 (8H, m),1.01 (12H, m). ^{13}C NMR ($CDCl_3$, 100 MHz) 127.8, 127.5, 124.5, 123.7, 123.0, 122.9, 59.0, 43.4, 24.2, 19.6, 13.5.^{11}B NMR ($CDCl_3$, 128 MHz, $BF_3.OEt_2$) δ 9.0-30.0 (br m, max at 5.9, -0.5, -8.8 and -30.8, 18B) ppm. HRMS (ESI) $[M\text{-}NBu_4]^-$ *m/z* calcd for $C_{20}H_{30}B_{18}S_4Co$, 652.2346; found, 652.2362.

Synthesis of Tetrabutylammonium Nickel(III) Bis(2,2′-bithiophene-5-*o*-nido-carborane) (11)

Procedure similar to synthesis of **10**. ^{1}H NMR (acetone-d_6, 400MHz) δ 7.28 (3H, m), 7.07 (2H, m), 7.02 (2H, m), 6.67 (2H, br s), 6.39 (1H, br s), 4.15 (1H, br s), 3.28 (1H, br s), 3.10 (8H, m), 1.59 (8H, m), 1.60-3.33 (18H, br), 1.29 (8H, m), 1.04 (12H, m).

Synthesis of 5-bromo-2,2':5',2''-terthiophene (12)

2,2':5',2"-Terthiophene (2.0g, 8.0mmol) was dissolved in CCL_4 (80ml) and NBS (1.41g, 8.0mmol) was added to the solution. The solution was stirred for 48 h at room temperature. The solution was then filtered through cotton wool to remove the imide. The filtrate was dried under pressure, and resulting residue purified by column chromatography using 20% DCM in hexanes to afford product in 76% yield as a yellow solid. 1H NMR (CDCl3, 400MHz) δ 7.28 (2H, m, ArH), 7.18 (2H, m, ArH), 7.12 (1H, d, *J*= 4Hz, ArH), 7.03 (1H, t, J^1= 4Hz, J^2= 5Hz, ArH), 6.93 (IH, d, *J*= 4Hz, ArH).

Synthesis of ([2,2':5',2''-terthiophen]-5-ylethynyl)trimethylsilane (13)

To a mixture of 5-bromo-2,2':5',2"-terthiophene (2.0g, 6.11mmol), $PdCl_2(PPh_3)_2$ (0.21g, 0.31mmol), CuI (0.06, 0.31mmol) in DIPA (120ml) was added TMSA (2.12ml, 15.28mmol) dropwise under argon atmosphere. The mixture was stirred at room temperature for 6 h. The reaction was quenched by pouring into water and extracted with EtOAc and dried under reduced

pressure. Product was purified by column chromatography using 20% DCM in hexanes to afford 67% of product as a yellow solid. 1H NMR (CDCl3, 400MHz) δ 7.26 (2H, m), 7.15 (2H, m), 7.09 (1H, d, J= 4Hz), 7.01 (1H, t, J^1= 4Hz, J^2= 5Hz), 6.93 (1H, d, J= 4Hz), 0.23 (9H, s)

Synthesis of 5-ethynyl-2,2':5',2''-terthiophene (14)

Protecting group was removed from ([2,2':5',2"-terthiophen]-5-ylethynyl)trimethylsilane (0.5g, 1.45mmol) by reacting it with K_2CO_3 (0.6g, 4.35mmol) at room temperature for 2h. The reaction was quenched by addition of water. This was diluted with Et_2O and washed with water. The organic layer was dried over Na_2SO_4 and evaporated under pressure. The residue was purified using column chromatography using 20%DCM in hexanes to produce 67% product as a yellow solid. ^{1}H NMR ($CDCl_3$, 400MHz) δ 7.23 (1H, m), 7.18 (1H, m), 7.07 (1H, m), 7.02 (2H, m), 6.98 (1H, d, *J* = 4Hz), 6.92 (1H, d, *J* = 4Hz), 3.42 (1H, s)

Synthesis of 2,2′,5′,2′′-Terthiophene-5-*o*-carborane (15)

Decarborane (0.12g, 0.97mmol), 5-ethynyl-2,2':5',2"-terthiophene (0.148g, 0.54mmol), and dry CH_3CN (1.48 ml) were dissolved in dry toluene (6.4 ml). The reaction mixture was stirred at 80^{o}C under nitrogen atmosphere for 24h. It was then cooled to room temperature, and methanol (1.0ml) added to the reaction mixture. It was then stirred for 30 min followed by drying under vacuum. The final residue was purified by column chromatography using 10% DCM in hexanes as eluent. Product was obtained as a yellow solid in 50% yield. ^{1}H NMR (CD_2Cl_2, 300 MHz) δ 7.29 (1H, br s), 7.22 (1H, br s), 7.07 (4H, m), 6.97 (1H, br s), 3.90 (1H, s), 1.47-3.50 (br, 10H, BH).^{13}C NMR (CD_2Cl_2, 63 MHz) 140.0, 138.8, 136.7, 135.0, 134.7, 131.0, 128.2, 125.7, 125.2, 125.0, 124.8, 123.6, 72.7, 64.2. ^{11}B NMR ($CDCl_3$, 128 MHz, $BF_3.OEt_2$) δ -3.2 (d, ^1J(B,H)) 143

Hz, 1B), -6.4 (d, ^{1}J(B,H)) 148 Hz, 1B), -10.0 to -16.0 (br m, 8B). MALDI-TOF [M + H]+ 391.3. HRMS(ESI) *m/z* calcd for $C_{14}H_{17}B_{10}S_3$, 390.1468; found, 390.1475.

Synthesis of Tetrabutylammonium 2,2′,5′,2′′-Terthiophene-5-*o*-nido-carborane (16)

2,2′:5′,2′′-Terthiophene-5-*o*-carborane (0.042g, 0.108 mmol) was dissolved in 1.8 mL dry THF. To this solution, 0.22 mL of TBAF (1.0M in THF) was added under a nitrogen atmosphere. The reaction mixture was stirred at 60^{o}C for 2h and the reaction monitored by TLC to make sure no more starting material was present. It was then poured into 1.8 mL water and extracted with EtOAc. The organic layers were dried over anhydrous Na_2SO_4. It was then filtered, and the solvent removed under vacuum. The final residue was purified by passing through a pad of silica gel using EtOAc as eluent. The product was obtained as a yellow solid in 80% yield. ^{1}H NMR (acetone-d_6, 250 MHz) δ 7.43 (1H,d, *J*= 4.91 Hz), 7.25 (1H, d, *J* = 3.41 Hz), 7.16 (1H,d, *J* = 3.71 Hz), 7.05-7.08 (2H, m), 6.95 (1H, d, *J* =3.61 Hz), 6.59 (1H, d, *J* = 3.64 Hz), 3.40-3.47 (8H,m,), 3.02 (1H, br s), 1.76 (8H, m), 1.52-3.50(br, 9H), 1.39 (8H, m), 0.96 (12H, m),-2.40 (br, 1H, BH).^{13}C NMR (acetone-d_6, 63 MHz) 152.1, 137.2,137.1, 135.2, 132.6, 128.6, 125.3, 124.9, 124.1, 123.7, 123.6,122.8, 80.8, 67.7, 59.0, 24.2, 20.0, 13.6. ^{11}B NMR ($CDCl_3$,128MHz, $BF_3.OEt_2$) δ -10.0 to -16.0 (br m, 3B), -18.0 to -20.0(br m, 3B), -24.6 (d, ^{1}J (B,H)) 149 Hz, 1B), -34.7 (dd, ^{1}J (B,H)) 43.8 Hz, ^{1}J (B,H)) 43.7 Hz, 1B), -37.6 (d, ^{1}J(B,H)) 138 Hz,1B). HRMS (ESI) $[M\text{-}NBu_4]^-$ *m*/*z* calcd for $C_{14}H_{18}B_9S_3$, 380.1462; found, 380.1466.

Synthesis of Tetrabutylammonium Cobalt(III) Bis-(2,2′,5′,2′′-terthiophene-5-*o*-nido-carborane) (17)

Tetrabutylammonium 2,2′,5′,2′′-Terthiophene-5-*o*-nido-carborane (0.005g, 0.013mmol), anhydrous $CoCl_2$ (0.0095g, 0.073 mmol) and *t*BuOK (0.0082 g, 0.073 mmol), were dissolved in 0.1 mL of anhydrous dimethoxyethane. The reaction was placed under nitrogen atmosphere and

allowed to reflux for 30 h. It was then cooled to room temperature and the precipitate that formed filtered off. The filtrate was diluted using 10 mL dichloromethane and washed with *n*-Bu_4NHSO_4 aqueous solution. The organic layers were dried over anhydrous Na_2SO_4 and dried under a vacuum. The final residue was purified by column chromatography using DCM as the eluent. Product was obtained as a dark yellow solid in 60% yield. ^{1}H NMR (acetone-d_6, 250MHz) δ 7.41 (2H, m), 7.26 (2H, m), 7.18 (2H, m), 7.05 (4H, m), 6.86 (2H, m), 6.55 (2H, m), 3.62 (1H, br s), 3.44 (8H, m), 3.10 (1H, br s), 1.76 (8H, m), 1.52-3.48 (18H, br), 1.39 (8H, m), 0.97 (12H, m). ^{13}C-NMR ($CDCl_3$, 100 MHz) 138.1, 137.9, 135.1, 132.5, 127.5, 126.2, 124.8, 123.9, 123.5,122.7, 68.7, 58.9, 42.6, 24.2, 20.0, 13.6. ^{11}B NMR ($CDCl_3$, 128 MHz,$BF_3.OEt_2$) δ 9.0-30.0 (br m, max at 5.9, -0.5, -8.8 and -30.8,18B) ppm. HRMS (ESI) $[M\text{-}NBu_4]^-$ *m*/*z* calcd for $C_{28}H_{34}B_{18}S_6Co$, 816.2129; found, 816.2115.

Synthesis of Tetrabutylammonium Nickel(III) Bis-(2,2′,5′,2″-terthiophene-5-*o*-nido-carborane) (18)

Procedure similar to synthesis of compound **17**. 47% yield. ^{1}H NMR ($CDCl_3$, 400MHz) δ 7.39 (2H, m), 7.23 (2H, m), 7.17 (2H, m), 7.07 (4H, m), 6.92 (2H, m), 6.55 (2H, m), 3.57 (1H, br s), 3.34-3.41 (8H, m), 3.07 (1H, br s), 1.69-1.78 (8H, m), 1.47-3.46 (18H, br), 1.33-1.41 (8H, m), 0.92-0.98 (12H, m). MALDI-TOF calcd for for $C_{28}H_{34}B_{18}S_6Ni$, 816.21; found 816.706.

3.9 References

1. (a) Heeger, A. J., Nobel Lecture: Semiconducting and metallic polymers: The fourth generation of polymeric materials. *Rev Mod Phys* **2001,** *73* (3), 681-700; (b) MacDiarmid, A. G., "Synthetic metals": A novel role for organic polymers (Nobel lecture). *Angew Chem Int Edit* **2001,** *40* (14), 2581-2590; (c) Shirakawa, H., Nobel Lecture: The discovery of polyacetylene film - the dawning of an era of conducting polymers. *Rev Mod Phys* **2001,** *73* (3), 713-718.

2. Patil, A. O.; Heeger, A. J.; Wudl, F., Optical properties of conducting polymers. *Chem Rev* **1988,** *88* (1), 183-200.

3. Stejskal, J.; Gilbert, R. G., Polyaniline. Preparation of a conducting polymer (IUPAC technical report). *Pure and Applied Chemistry* **2002,** *74* (5), 857-867.

4. (a) Wudl, F.; Kobayashi, M.; Heeger, A. J., Poly(isothianaphthene). *The Journal of Organic Chemistry* **1984,** *49* (18), 3382-3384; (b) Kobayashi, M.; Colaneri, N.; Boysel, M.; Wudl, F.; Heeger, A. J., The Electronic and Electrochemical Properties of Poly(isothianaphthene). *J Chem Phys* **1985,** *82* (12), 5717-5723; (c) Colaneri, N.; Kobayashi, M.; Heeger, A. J.; Wudl, F., Electrochemical and opto-electrochemical properties of poly(isothianaphthene). *Synthetic Met* **1986,** *14* (1-2), 45-52.

5. Marsella, M. J.; Fu, D.-K.; Swager, T. M., Synthesis of regioregular poly(methyl pyridinium vinylene): An isoelectronic analogue to poly(phenylene vinylene). *Adv Mater* **1995,** *7* (2), 145-147.

6. Roncali, J., Conjugated poly(thiophenes): synthesis, functionalization, and applications. *Chem Rev* **1992,** *92* (4), 711-738.

7. (a) Josowicz, M.; Janata, J., Suspended gate field effect transistors modified with polypyrrole as alcohol sensor. *Analytical Chemistry* **1986,** *58* (3), 514-517; (b) Kuwabata, S.; Martin, C. R., Mechanism of the Amperometric Response of a Proposed Glucose Sensor Based on a Polypyrrole-Tubule-Impregnated Membrane. *Analytical Chemistry* **1994,** *66* (17), 2757-2762.

8. (a) Burroughes, J. H.; Jones, C. A.; Friend, R. H., New semiconductor device physics in polymer diodes and transistors. *Nature* **1988,** *335* (6186), 137-141; (b) Gustafsson, G.; Cao, Y.; Treacy, G. M.; Klavetter, F.; Colaneri, N.; Heeger, A. J., Flexible light-emitting diodes made from soluble conducting polymers. *Nature* **1992,** *357* (6378), 477-479; (c) Zhang, C.; Hoger, S.; Pakbaz, K.; Wudl, F.; Heeger, A., Improved efficiency in green polymer light-emitting diodes with air-stable electrodes. *Journal of Electronic Materials* **1994,** *23* (5), 453-458.

9. Conway, B. E., Transition from ``Supercapacitor" to ``Battery" Behavior in Electrochemical Energy Storage. *Journal of The Electrochemical Society* **1991,** *138* (6), 1539-1548.

10. (a) Hable, C. T.; Wrighton, M. S., Electrocatalytic oxidation of methanol and ethanol: a comparison of platinum-tin and platinum-ruthenium catalyst particles in a conducting polyaniline matrix. *Langmuir* **1993,** *9* (11), 3284-3290; (b) Bull, R. A.; Fan, F.-R.; Bard, A. J., Polymer Films on Electrodes. *Journal of The Electrochemical Society* **1983,** *130* (7), 1636-1638.

11. Mishra, A.; Ma, C.-Q.; Bäuerle, P., Functional Oligothiophenes: Molecular Design for Multidimensional Nanoarchitectures and Their Applications†. *Chem Rev* **2009,** *109* (3), 1141-1276.

12. (a) McCullogh, R. D.; Williams, S. P.; Tristam-Nagle, S.; Jayaraman, M.; Ewbank, P. C.; Miller, L., The first synthesis and new properties of regioregular, head-to-tail coupled polythiophenes. *Synthetic Met* **1995,** *69* (1-3), 279-282; (b) McCullough, R. D.; Lowe, R. D., Enhanced electrical conductivity in regioselectively synthesized poly(3-alkylthiophenes). *Journal of the Chemical Society, Chemical Communications* **1992,** (1), 70-72.

13. Chen, T. A.; Rieke, R. D., The first regioregular head-to-tail poly(3-hexylthiophene-2,5-diyl) and a regiorandom isopolymer: nickel versus palladium catalysis of 2(5)-bromo-5(2)-(bromozincio)-3-hexylthiophene polymerization. *Journal of the American Chemical Society* **1992,** *114* (25), 10087-10088.

14. Roncali, J., Synthetic Principles for Bandgap Control in Linear π-Conjugated Systems. *Chem Rev* **1997,** *97* (1), 173-206.

15. Sadki, S.; Schottland, P.; Brodie, N.; Sabouraud, G., The mechanisms of pyrrole electropolymerization. *Chem Soc Rev* **2000,** *29* (5), 283-293.

16. Carswell, A. D. W.; O'Rea, E. A.; Grady, B. P., Adsorbed Surfactants as Templates for the Synthesis of Morphologically Controlled Polyaniline and Polypyrrole Nanostructures on Flat Surfaces: From Spheres to Wires to Flat Films. *Journal of the American Chemical Society* **2003,** *125* (48), 14793-14800.

17. Glenis, S.; Benz, M.; LeGoff, E.; Schindler, J. L.; Kannewurf, C. R.; Kanatzidis, M. G., Polyfuran: a new synthetic approach and electronic properties. *Journal of the American Chemical Society* **1993,** *115* (26), 12519-12525.

18. Tourillon, G.; Garnier, F., New electrochemically generated organic conducting polymers. *Journal of Electroanalytical Chemistry and Interfacial Electrochemistry* **1982,** *135* (1), 173-178.

19. Delamar, M.; Lacaze, P. C.; Dumousseau, J. Y.; Dubois, J. E., Electrochemical oxidation of benzene and biphenyl in liquid sulfur dioxide: formation of conductive deposits. *Electrochimica Acta* **1982,** *27* (1), 61-65.

20. (a) Hao, E.; Fabre, B.; Fronczek, F. R.; Vicente, M. G. H., Syntheses and Electropolymerization of Carboranyl-Functionalized Pyrroles and Thiophenes. *Chem Mater* **2007,** *19* (25), 6195-6205; (b) Gratzl, M.; Hsu, D. F.; Riley, A. M.; Janata, J., Electrochemically deposited polythiophene. 1. Ohmic drop compensation and the polythiophene paradox. *The Journal of Physical Chemistry* **1990,** *94* (15), 5973-5981.

21. (a) Cunningham, D. D.; Laguren-Davidson, L.; Mark, H. B.; Van Pham, C.; Zimmer, H., Synthesis of oligomeric 2,5-thienylenes; their u.v. spectra and oxidation potentials. *Journal of the Chemical Society, Chemical Communications* **1987,** (13), 1021-1023; (b) Diaz, A. F.; Crowley, J.; Bargon, J.; Gardini, G. P.; Torrance, J. B., Electrooxidation of aromatic oligomers and conducting polymers. *Journal of Electroanalytical Chemistry and Interfacial Electrochemistry* **1981,** *121*, 355-361; (c) Galal, A.; Lewis, E. T.; Ataman, O. Y.; Zimmer, H.; Mark, H. B., Electrochemical synthesis of conducting polymers from oligomers containing thiophene and furan rings. *Journal of Polymer Science Part A: Polymer Chemistry* **1989,** *27* (6), 1891-1896.

22. (a) Heinze, J.; Mortensen, J.; Hinkelmann, K., Some new Electrochemical Results on the Properties of Conducting Polymers. *Synthetic Met* **1987,** *21* (2), 209-214; (b) Eales, R. M.; Hillman, A. R., Polymerisation of terthiophene at controlled doping level. *Journal of Electroanalytical Chemistry and Interfacial Electrochemistry* **1988,** *250* (1), 219-223.

23. (a) Zotti, G.; Marin, R. A.; Gallazzi, M. C., Electrochemical Polymerization of Mixed Alkyl−Alkoxybithiophenes and -terthiophenes. Substitution-Driven Polymerization from Thiophene Hexamers to Long-Chain Polymers. *Chem Mater* **1997,** *9* (12), 2945-2950; (b) Cutler, C. A.; Burrell, A. K.; Collis, G. E.; Dastoor, P. C.; Officer, D. L.; Too, C. O.; Wallace, G. G., Photoelectrochemical cells based on polymers and copolymers from terthiophene and nitrostyrylterthiophene. *Synthetic Met* **2001,** *123* (2), 225-237; (c) Garnier, F., Organic-Based Electronics à la Carte. *Accounts Chem Res* **1999,** *32* (3), 209-215; (d) Roncali, J., Electrogenerated functional conjugated polymers as advanced electrode materials. *J Mater Chem* **1999,** *9* (9), 1875-1893.

24. (a) Yumoto, Y.; Yoshimura, S., Synthesis and electrical properties of a new conducting polythiophene prepared by electrochemical polymerization of [alpha]-terthienyl. *Synthetic Met* **1986,** *13* (1-3), 185-191; (b) Waltman, R. J.; Bargon, J.; Diaz, A. F., Electrochemical studies of some conducting polythiophene films. *The Journal of Physical Chemistry* **1983,** *87* (8), 1459-1463.

25. (a) Li, H.; Sundararaman, A.; Venkatasubbaiah, K.; Jäkle, F., Organoborane Acceptor-Substituted Polythiophene via Side-Group Borylation. *Journal of the American Chemical Society* **2007,** *129* (18), 5792-5793; (b) Zhao, C.-H.; Wakamiya, A.; Inukai, Y.; Yamaguchi, S., Highly Emissive Organic Solids Containing 2,5-Diboryl-1,4-phenylene Unit. *Journal of the American Chemical Society* **2006,** *128* (50), 15934-15935; (c) Shirota, Y.; Kinoshita, M.; Noda, T.; Okumoto, K.; Ohara, T., A Novel Class of Emitting Amorphous Molecular Materials as Bipolar Radical Formants: 2-{4-[Bis(4-methylphenyl)amino]phenyl}- 5-(dimesitylboryl)thiophene and 2-{4-[Bis(9,9-dimethylfluorenyl)amino]phenyl}- 5-(dimesitylboryl)thiophene. *Journal of the American Chemical Society* **2000,** *122* (44), 11021-11022; (d) Noda, T.; Shirota, Y., 5,5‘-Bis(dimesitylboryl)-2,2‘-bithiophene and 5,5‘‘-Bis(dimesitylboryl)-2,2‘:5‘,2‘‘-terthiophene as a Novel Family of Electron-Transporting Amorphous Molecular Materials. *Journal of the American Chemical Society* **1998,** *120* (37), 9714-9715.

26. Jäkle, F., Advances in the Synthesis of Organoborane Polymers for Optical, Electronic, and Sensory Applications. *Chem Rev* **2010,** *110* (7), 3985-4022.

27. (a) Fabre, B.; Clark, J. C.; Vicente, M. G. H., Synthesis and Electrochemistry of Carboranylpyrroles. Toward the Preparation of Electrochemically and Thermally Resistant Conjugated Polymers. *Macromolecules* **2005,** *39* (1), 112-119; (b) Fabre, B.; Chayer, S.; Vicente, M. G. H., First conducting polymer functionalized with covalently linked carborane units. *Electrochemistry Communications* **2003,** *5* (5), 431-434.

28. (a) Hawthorne, M. F.; Young, D. C.; Andrews, T. D.; Howe, D. V.; Pilling, R. L.; Pitts, A. D.; Reintjes, M.; Warren, L. F.; Wegner, P. A., .pi.-Dicarbollyl derivatives of the transition metals. Metallocene analogs. *Journal of the American Chemical Society* **1968,** *90* (4), 879-896; (b) Wiesboeck, R. A.; Hawthorne, M. F., Dicarbaundecaborane(13) and Derivatives. *Journal of the American Chemical Society* **1964,** *86* (8), 1642-1643; (c) Fabre, B.; Hao, E. H.; LeJeune, Z. M.; Amuhaya, E. K.; Barriere, F.; Garno, J. C.; Vicente, M. G. H., Polythiophenes Containing In-Chain Cobaltabisdicarbollide Centers. *Acs Applied Materials & Interfaces* **2010,** *2* (3), 691-702.

29. Hao, E.; Zhang, M.; E, W.; Kadish, K. M.; Fronczek, F. R.; Courtney, B. H.; Vicente, M. G. a. H., Synthesis and Spectroelectrochemistry of N-Cobaltacarborane Porphyrin Conjugates. *Bioconjugate Chemistry* **2008,** *19* (11), 2171-2181.

30. Rojo, I.; Teixidor, F.; Viñas, C.; Kivekäs, R.; Sillanpää, R., Synthesis and Coordinating Ability of an Anionic Cobaltabisdicarbollide Ligand Geometrically Analogous to BINAP. *Chemistry – A European Journal* **2004,** *10* (21), 5376-5385.

31. Hawthorne, M. F.; Ramachandran, B. M.; Kennedy, R. D.; Knobler, C. B., Approaches to rotary molecular motors. *Pure and Applied Chemistry* **2006,** *78* (7), 1299-1304.

32. Gruner, B.; Plesek, J.; Baca, J.; Cisarova, I.; Dozol, J. F.; Rouquette, H.; Vinas, C.; Selucky, P.; Rais, J., Cobalt bis(dicarbollide) ions with covalently bonded CMPO groups as selective extraction agents for lanthanide and actinide cations from highly acidic nuclear waste solutions. *New J Chem* **2002,** *26* (10), 1519-1527.

33. Dash, B. P.; Satapathy, R.; Gaillard, E. R.; Maguire, J. A.; Hosmane, N. S., Synthesis and Properties of Carborane-Appended C-3-Symmetrical Extended pi Systems. *Journal of the American Chemical Society* **2010,** *132* (18), 6578-6587.

34. (a) Becker, R. S.; deMelo, J. S.; Macanita, A. L.; Elisei, F., Comprehensive evaluation of the absorption, photophysical, energy transfer, structural, and theoretical properties of alpha-oligothiophenes with one to seven rings. *Journal of Physical Chemistry* **1996,** *100* (48), 18683-18695; (b) Oh, J. K.; Stoeva, V.; Rademacher, J.; Farwaha, R.; Winnik, M. A., Synthesis, characterization, and emulsion polymerization of polymerizable coumarin derivatives. *Journal of Polymer Science Part a-Polymer Chemistry* **2004,** *42* (14), 3479-3489.

35. Lor, M.; Thielemans, J.; Viaene, L.; Cotlet, M.; Hofkens, J.; Weil, T.; Hampel, C.; Mullen, K.; Verhoeven, J. W.; Van der Auweraer, M.; De Schryver, F. C., Photoinduced electron transfer in a rigid first generation triphenylamine core dendrimer substituted with a peryleneimide acceptor. *Journal of the American Chemical Society* **2002,** *124* (33), 9918-9925.

36. (a) Bigger, S. W.; Ghiggino, K. P.; Meilak, G. A.; Verity, B., Illustration of the principles of fluorimetry. An apparatus and experiments specially designed for the teaching laboratory. *Journal of Chemical Education* **1992,** *69* (8), 675-null; (b) Lakowicz, J. R., *Principles of fluorescence spectroscopy*. 3rd ed.; Springer: New York, 2006; p xxvi, 954 p.

37. DeRosa, M. C.; Crutchley, R. J., Photosensitized singlet oxygen and its applications. *Coordination Chemistry Reviews* **2002,** *233-234*, 351-371.

CHAPTER 4: SYNTHESIS OF TETRABENZOPORPHYRINS CONJUGATED WITH POLYAMINES FOR PDT

4.1 Introduction

Porphyrins and pthalocyanines (see Figure 4-1) represent two of the most studied classes of conjugated systems[1]. Because of their unique optical chemical, and photophysical properties, these compounds have been used widely in material science[2], sensing[2a, 3], biomedical imaging[2a], and in medicine[4]. PDT and BNCT are two relatively new bimodal therapies, which require the use of sensitizers for the treatment of cancer.

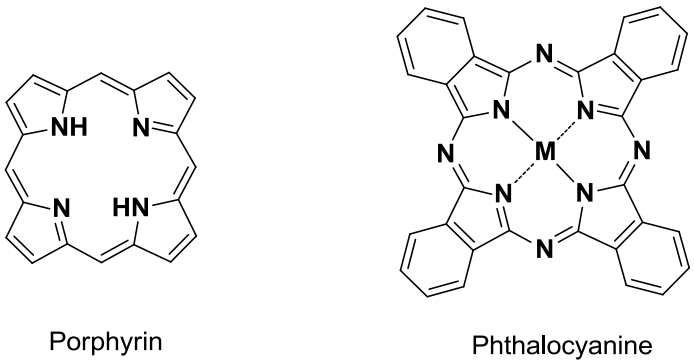

Figure 4-1: Structures of porphyrin and phthalocyanine

Studies have shown that not only can porphyrins act as photosensitizers, but they also have been found to have a high affinity for tumor cells[5]. The drawback for the use of porphyrins is that at the wavelengths at which they absorb, bodily tissues also strongly absorb light, and this limits their clinical use[1]. Because of this, there have been many attempts to modify the core of the porphyrin chromophore so as to shift their absorption to the red and near IR regions. This has led to synthesis and investigation of new classes of porphyrins which include porphyrins isomers, expanded porphyrins, hydroporphyrins, and π-extended porphyrins. Π-extended porphyrins make up a class of porphyrinoid chromophores, most of which contain fused aromatic rings via the β-

carbon atoms, as well as π-extended porphyrins at the *meso*-position. Examples of the π-extended porphyrins can be seen in Figure 4-2.

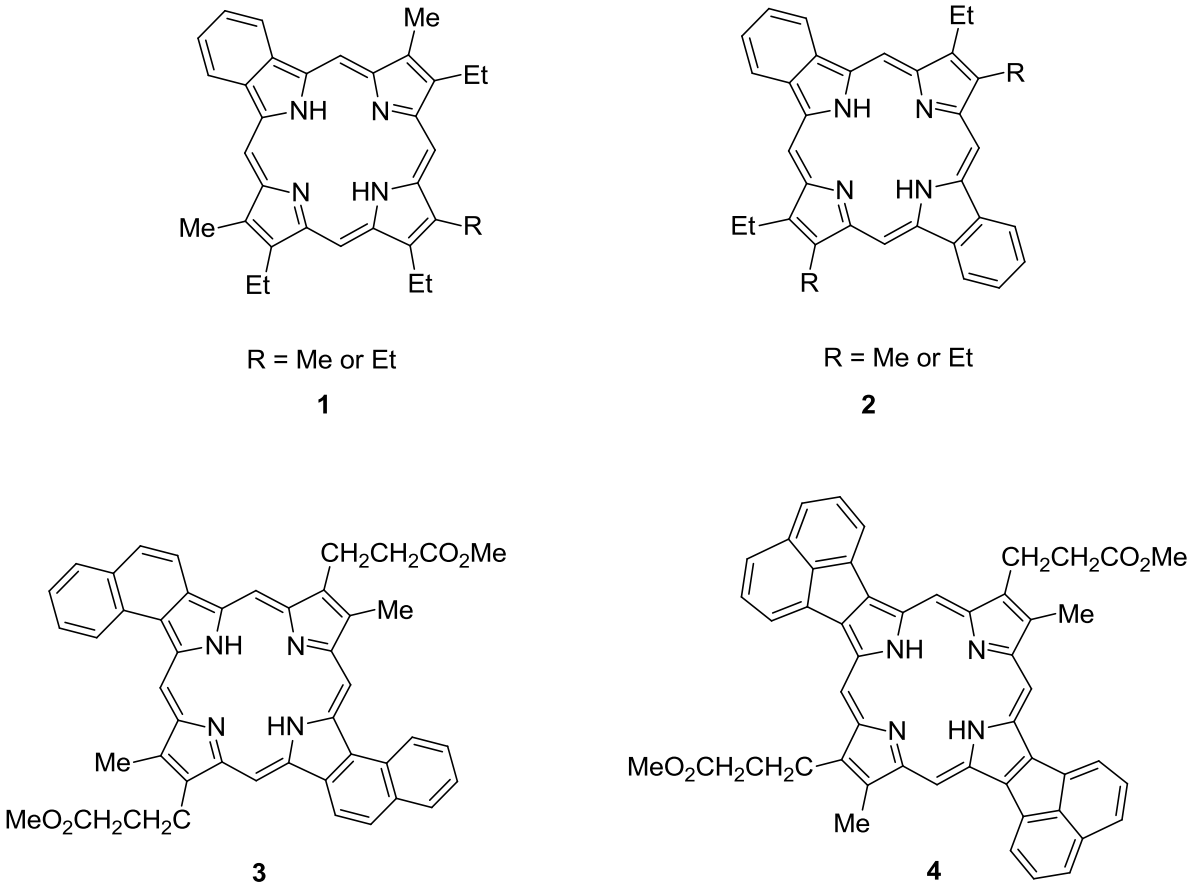

Figure 4-2: Examples of π-extended porphyrins[1]

Among the π-extended porphyrins, tetrabenzoporphyrin (TBP) has received a lot of interest. As its name indicates, TBP contains four β,β'-fused benzene rings onto a porphyrin macrocycle. Incorporation of these benzene rings leads to extension of the π-conjugation, which in turn leads to a bathochromic shift in the absorption[1]. These optical properties make TBP promising candidates for PDT, as well as in electronic devices and sensors. The first ZnTBP, **5**, was synthesized by Helberger and co-workers (see Scheme 4-1). They reacted *o*-cyanoacetophenone

with different phthalimidines to accomplish this[6]. Because of its physicochemical properties, TBP drew a lot of attention in the research world, as different groups came up with different procedures for synthesizing them. Linstead and co-workers prepared ZnTBP **5** from o-cyanocinnamic acid and also from 3-carboxymethylphthalimidine[7]. Vogler and Kunkely later came up with a different procedure for the same TBP which required reaction of 2-acetylbenzoic acid, **6**, with zinc acetate in aqueous ammonia in the presence of molecular sieves at 400^{o}C[8]. Remy also prepared **5** by reacting isoindole **7** with formaldehyde at 375^{o}C[9]. One thing all these procedures have in common is the fact that they all require harsh conditions, of heating at 300^{o}C often in the presence of an acid. This made the synthesis of functionalized TBPs challenging and also led to low yields.

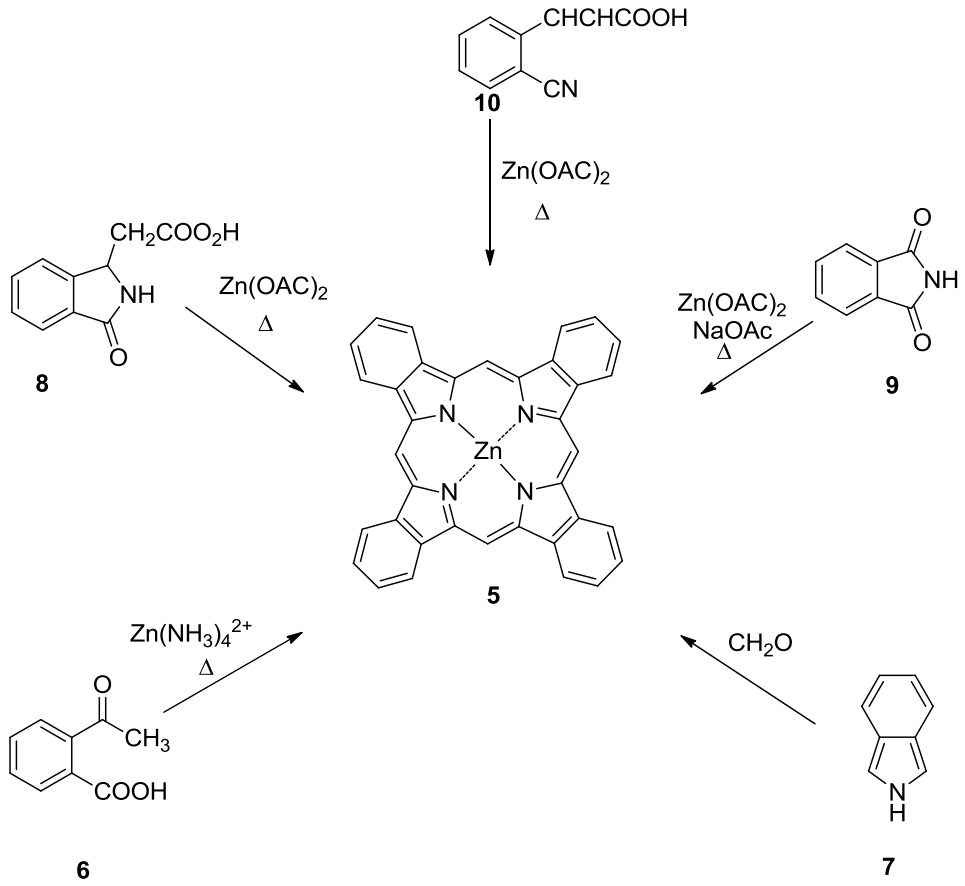

Scheme 4-1: Different synthetic routes to ZnTBP, **5**

Milder synthetic methods have since been explored[10]. Recently, Beletskaya and co-workers came up with a method for the synthesis of TBP from 4,7-dihydroisoindole[11]. Using standard Barton-Zard chemistry, 4,7-dihydroisoindole[11] was synthesized from (trimethylsilyl)acetylene, tosylacetylene and 1,3-butadiene. It was then successfully used in the preparation of TBPs using standard Lindsey protocol[11] as shown in Scheme 4-2.

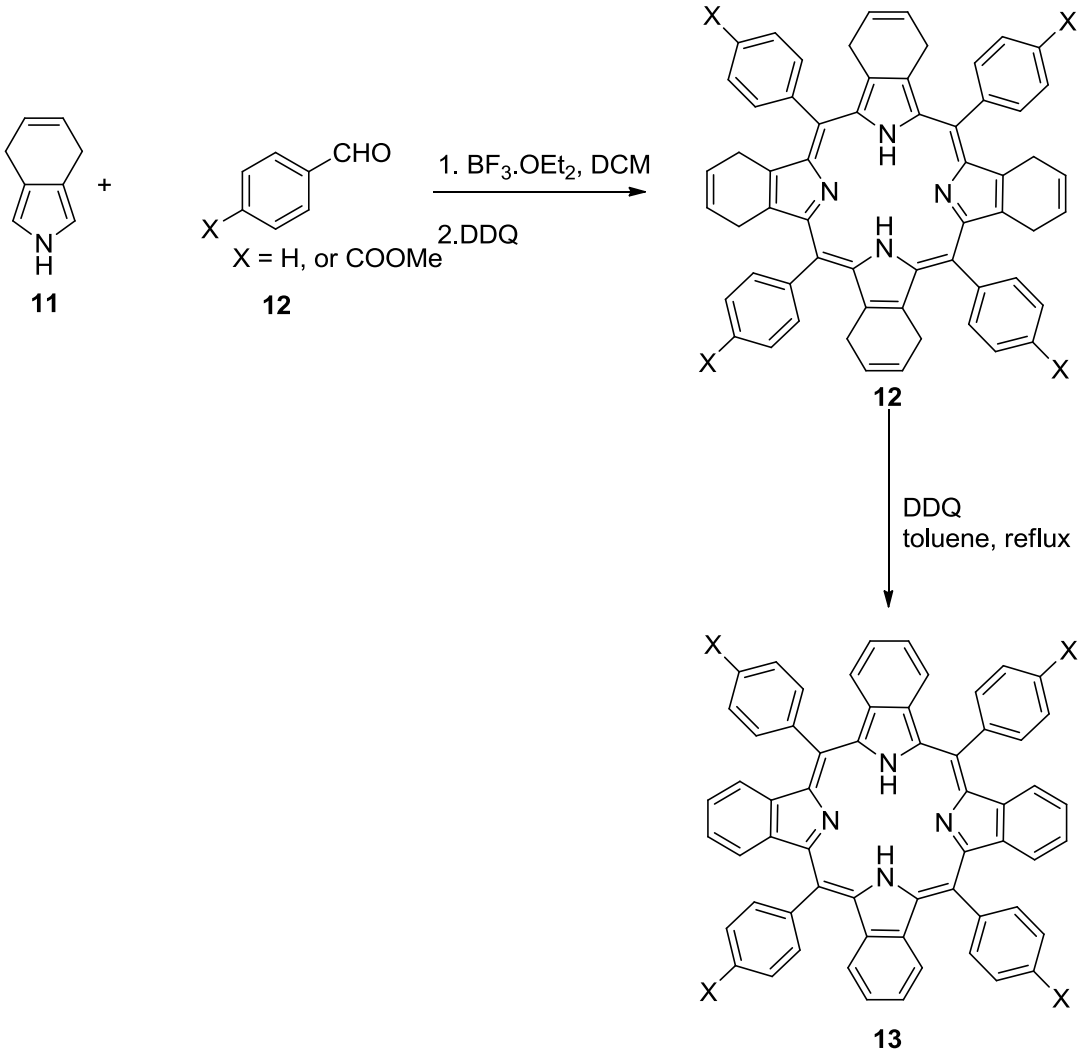

Scheme 4-2: Mild synthetic route of synthesizing TBPs[11]

One of the main areas of concern has been the low solubility of the TBPs. These compounds, for example **5**, have been found to be insoluble in most organic solvents, which has further led to problems with their purification. One way in which this problem can be overcome is by introduction of substituents to increase solubility[12].

4.2 Polyamine Conjugated TBPs in PDT

PDT is a bimodial treatment which combines the applications of a photosensitizer and visible light to destroy cancerous cells[13]. It is based on two biological properties of PDT drugs; their selective accumulation into cancer cells and the photoactivation of the photosensitizer by visible light in the presence of oxygen. The singlet oxygen that is generated kills the abnormal tissues[14], while sparing the normal adjacent cells[15]. Photofrin®, a first generation photosensitizer has been used in several countries to treat various cancers[15]. It however suffers several drawbacks, which include poor selectivity, leading to death of the surrounding normal cells and also photosensitivity of the skin due to slow clearance rate of the photosensitizer, which may last for several weeks after treatment[16]. Other drugs that have been developed and approved in different countries are Foscan®, which is used in treatment of head and neck cancer[14a] and Visudyne® which was approved for the treatment of age related macular degeneration[13]. To improve the efficiency of PDT, it is crucial to develop drugs with improved selectivity for tumor cells. Porphyrin polyamine conjugates present a promising way to overcome this problem[15].

4.2.1 Functions of Polyamines

Polyamines are components of all cells that are required for cell growth and survival. Because they play a critical role in cell proliferation, agents that interfere with polyamine metabolism have been developed and studied as potential anti-tumor drugs[17]. Interrupting the polyamine metabolic pathway leads to either cessation of cell growth or cell destruction[18]. In mammalian

cells, the polyamines spermine, spermidine and putrescene (see Figure 4-3), together with Mg^{2+} are the main cations in cells. The polyamine levels in cells are regulated by biosynthesis, degradation and transport[19]. Uptake of polyamines increases in rapidly proliferating cells[16a]. Therefore, tumor cells whereby the polyamine requirements surpass their biosynthetic abilities, use the polyamine transport system (PAT) to fulfill their needs. PAT displays a high affinity for polyamines and at the same time a low specificity for them. It therefore affords selective accumulation of polyamine analogues in cancerous tissue, and in turn presenting attractive anti-cancer chemotherapeutic strategies[14a, 16a].

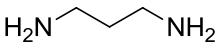

putrescine

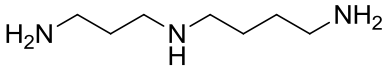

spermidine

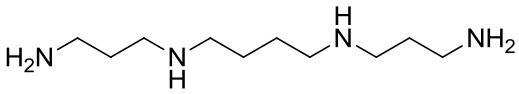

spermine

Figure 4-3: Polyamines found in mammalian cells

Various research groups have shown that polyamine conjugation can be utilized to convey cytotoxic drugs into rapidly growing cells[14a, 20]. Cohen and co-workers showed that chlorambucil-spermidine conjugate showed greater anti-tumor activity both *in vivo* and *in vitro* than chlorambucil on its own[20a]. Papadopoulou and co-workers also demonstrated that nitroimidazole-based polyamine derivatives could be of great interest as cytotoxins and radiosensitizers for their selective uptake by tumor cells through PAT[20c]. Sol and co-workers

have also done extensive research on porphyrin-polyamine conjugates for PDT and DNA cleavage. Their studies further indicated the importance of amphiphilicity for photodynamic activity by the porphyrin-polyamine conjugates[14a].

In our research, we focus on the synthesis of TBP. As mentioned before, these compounds are known to absorb and emit at longer wavelengths than regular porphyrins. This is critical in the development of a photosensitizer that will be used in PDT. We employed a mixed condensation strategy in the preparation of mono- and di-substituted TBPs. In addition, we conjugated the TBPs to the polyamines spermine and spermidine, using a short and flexible carbon chain spacer. We carried out in vitro studies of these conjugates, and also studied their photophysical properties.

4.3 Results and Discussion

From the preliminary results obtained by Dr. Martha Sibrian-Vasquez, it was observed that the mono-substituted TBP-spermine conjugate recorded low dark toxicity (See Appendix). In addition, when exposed to light, it was found to be highly phototoxic, with an IC_{50} value of 1.95μM at 1 J/cm light dose. Furthermore, the mono-substituted TBP-spermine conjugate recorded the fastest and highest cellular uptake of all conjugates tested. So with this in mind, we set out to synthesize the di-substituted TBP-spermine conjugates to establish whether it would show even better *in vitro* results.

We began the synthesis with the preparation of the polyamines. We started with the protection of spermine using Boc-ON in the presence of triethylamine. Three equivalents of protecting group were used to ensure only the terminal amines and one secondary amine reacted leaving one secondary amine unreacted. This afforded compound **14** in 92% yield as shown in Scheme 4-3.

The next step was introduction of the flexible spacer using N-(4-bromobutyl)phthalimide in the presence of base. The target compound **16**, was obtained after cleaving the phthalimide-protected amine group using hydrazine monohydrate.

The synthesis of porphyrins **17**-**19** was carried out by a former group member, Dr. Martha Sibrian-Vasquez. After carrying out a condensation reaction using Lindsey's method, using butanopyrrole, benzaldehyde and methyl 4-formylbenzoate, she obtained the mono-substituted product **17**, and a mixture of the di-substituted products **18** and **19** (See Scheme 4-4).

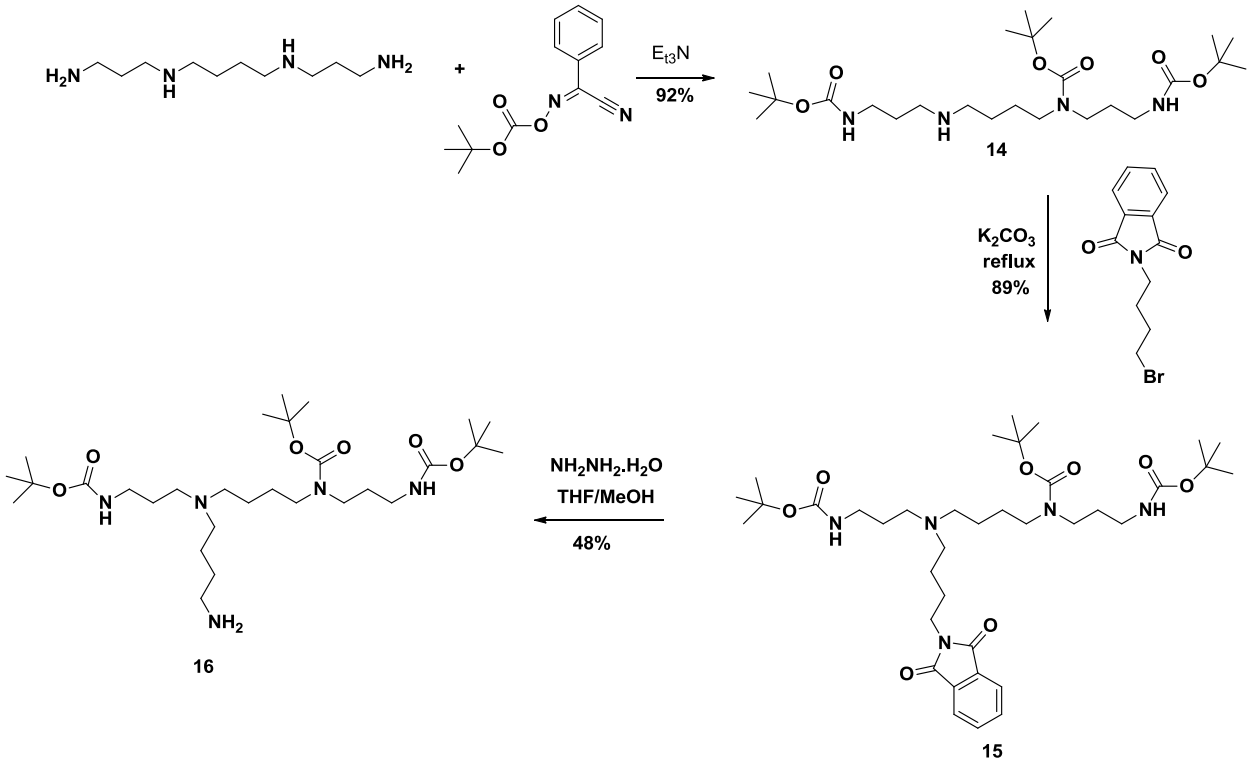

Scheme 4-3: Synthesis of Boc-protected spermine **16**

Starting with the mixture of substituted products, **18** and **19**, we attempted to separate the two isomers using column chromatography. This proved to be futile, as the two isomers have similar R_f values. We therefore decided to take the mixture of isomers to the next step. We carried out

the oxidation of the macrocycle, using DDQ, to give the fully conjugated TBPs, **20** and **21**. At this stage, it was then possible to separate the two isomers using silica gel chromatography to afford the two isomers **20** and **21** (see Scheme 4-5). The next step was the removal of Cu metal. This was achieved by dissolving the TBPs in concentrated H_2SO_4, and allowing the solution to stir for 10 minutes. The use of H_2SO_4 in this case was based on the fact that these TBP-Cu complexes belong to the class I porphyrins that are considered to be extremely stable, and therefore require a strong acid to remove the Cu metal. Purification of **22** and **23** involved filtration of the precipitate, and washing it with a large amount of water.

The next step was the hydrolysis of the ester groups. This was carried out by refluxing the TBP in NaOH solution to afford the final TBPs, **24** and **25**, in quantitative yields.

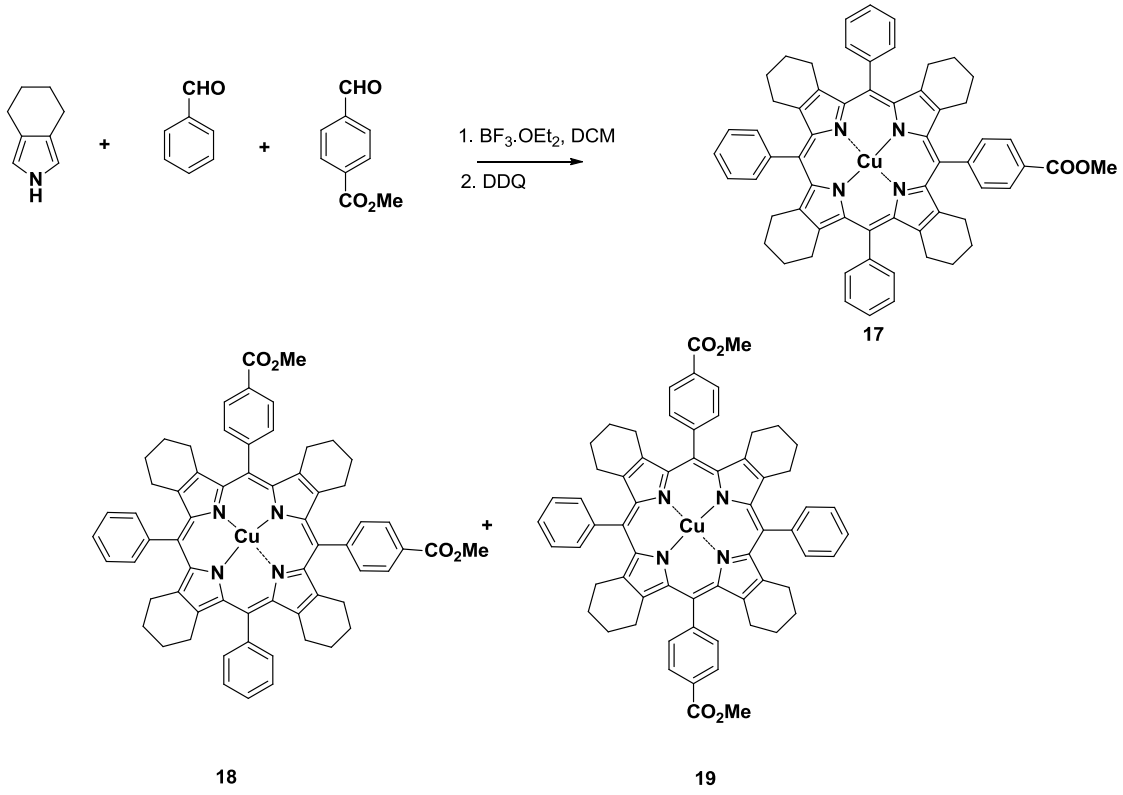

Scheme 4-4: Synthesis of mono- and di-substituted TBP precursors.

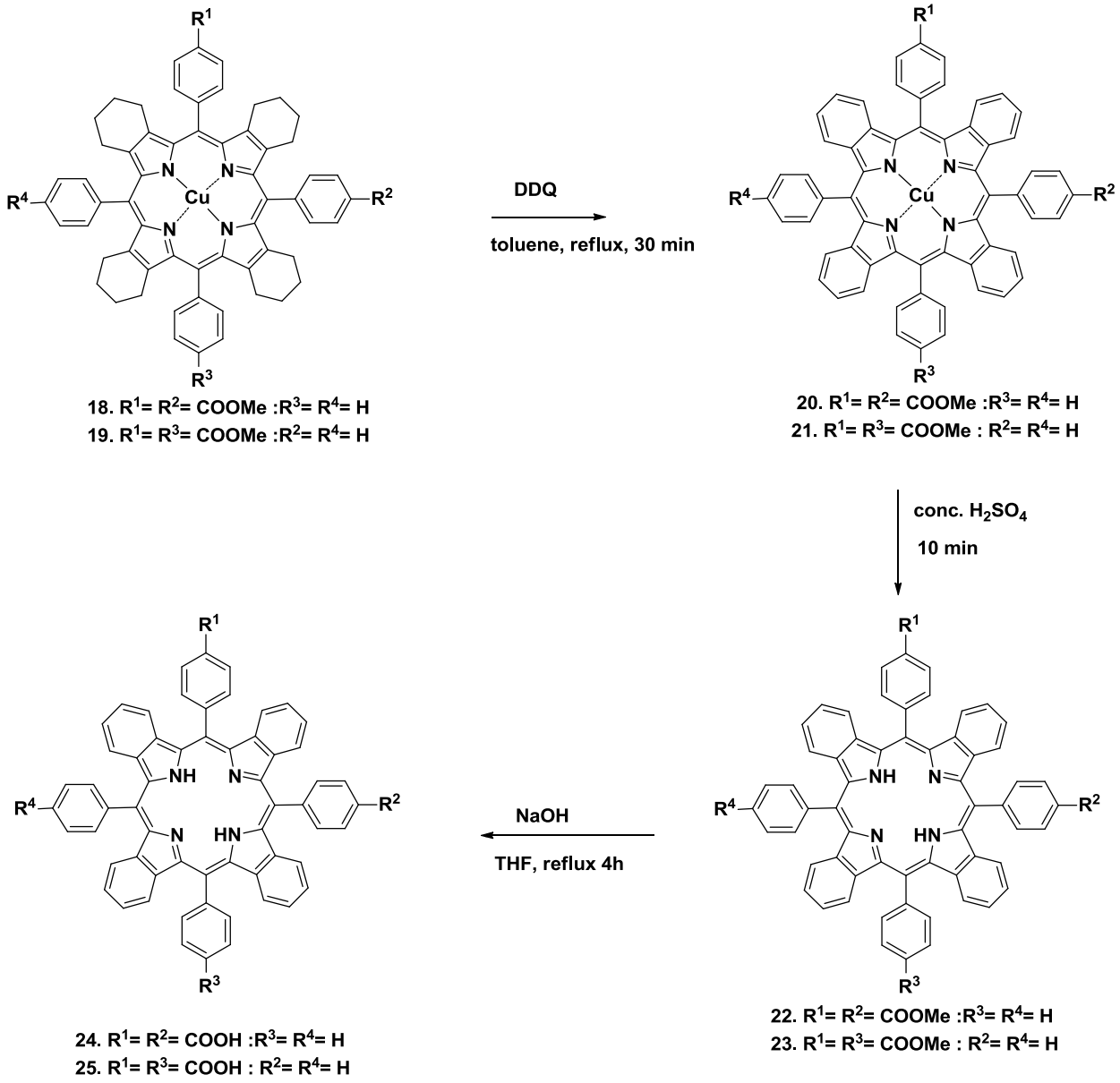

Scheme 4-5: Synthesis of di-substituted TBPs **24** and **25**.

Several attempts were made to conjugate the Boc-protected spermine to TBPs **24** and **25**. In the first attempt, we carried out the conjugation reaction in the presence of DIEA, HOBt, and TBTU,

with DMF as the reaction solvent. Unfortunately, we did not get the target compounds, and we could not correctly assign the product from NMR or MS (see Scheme 4-6).

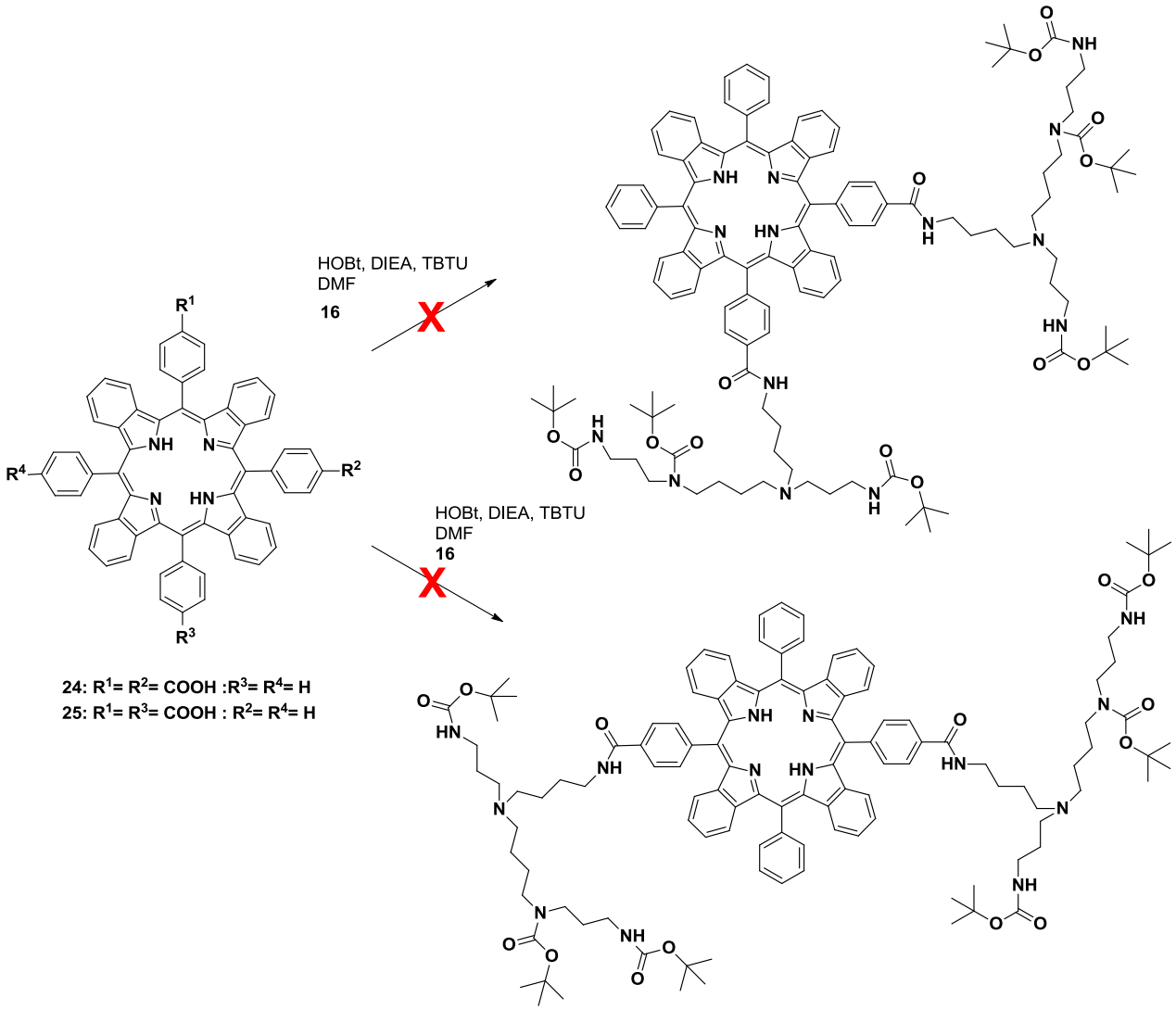

Scheme 4-6: First Attempt Synthesis of TBP-polyamine conjugates

In order to facilitate the coupling reaction, we decided to introduce a glycine spacer (see Scheme 4-7). We started by reacting the TBPs with Boc-protected glycine in the presence of DIEA,

HOBt, TBTU and with DMF as the reaction solvent. Unfortunately, purification of the product proved to be difficult because of presence of DIEA which was difficult to separate.

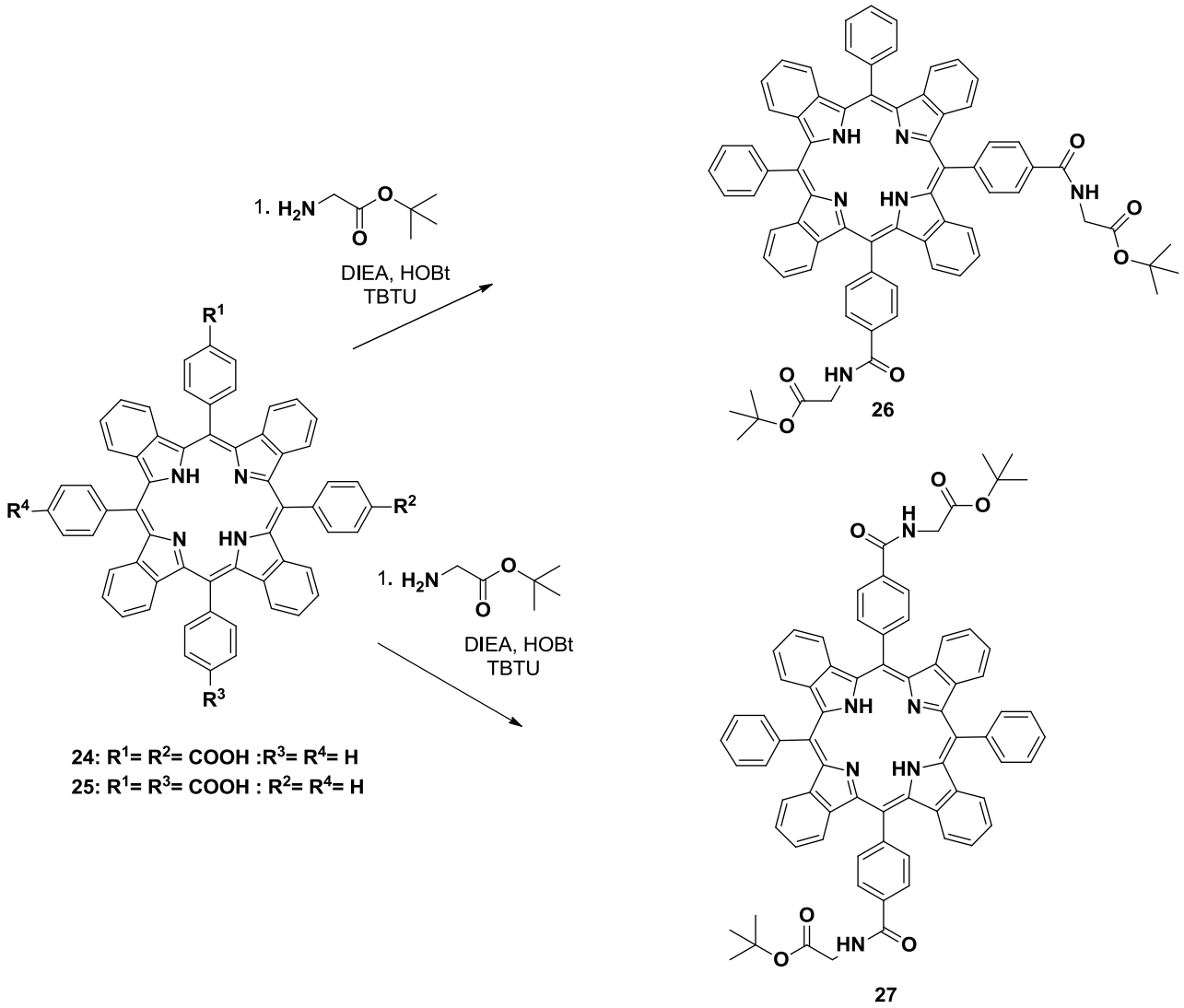

Scheme 4-7: Synthesis of TBP-Boc-protected glycine conjugates **26** and **27**

We are currently trying to purify **26** and **27**. After we obtain the pure compounds, we will deprotect the Boc groups using TFA. This will be followed by conjugation of the TBPs with the

already synthesized Boc-protected spermine **16**. Finally, we will deprotect the Boc- groups to obtain the final compounds **28** and **29**, as shown in Scheme 4-8.

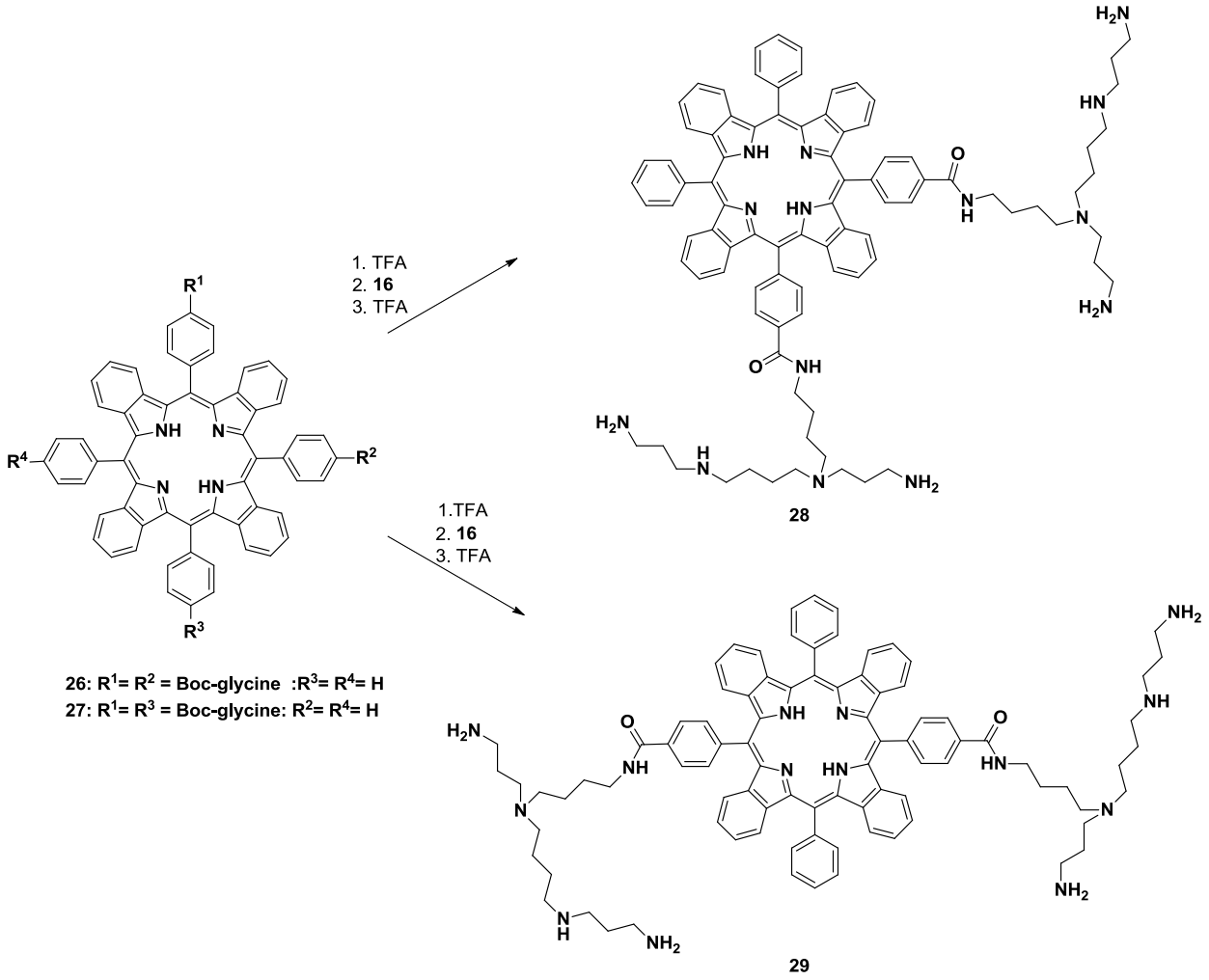

Scheme 4-8: Synthesis of conjugates **28** and **29**.

We decided to prepare the TBPs using a different synthetic route[11]. Our objective was to determine whether we could get better yields than before. In addition, we anticipate that we will get fewer products, which will make the isolation and purification of the desired products easier. It will still be a mixed condensation but starting with 4,7-dihydro-2H-isoindole, rather than butanopyrrole as in Scheme 4-4. We began the synthesis by preparing acetylene sulfone **28**[21] (see

Scheme 4-9). This was done by deprotecting the trimethylsilane group using NaF at room temperature, to afford **30** at 47% yield. Studies have shown that tosylacetylene is a strong dienophile, that readily reacts with electron-rich dienes[11, 22]. The next step was a Diels- Alder reaction, which involved reaction of the highly reactive acetyl sulfone with 1,3-butadiene at room temperature for 48 h, to afford the cyclohexadiene, **31**, in 80% yield[11]. We are still working on completing the synthesis. In the next step of the synthesis we will use standard Barton-Zard chemistry, using compound **31** for the preparation of **32** (see Scheme 4-10). Compound **32** will then be used for the preparation of 4,7-dihydroisoindole **33**, which will finally be used in the synthesis of TBP **22** and **23** using standard Lindsey protocol.

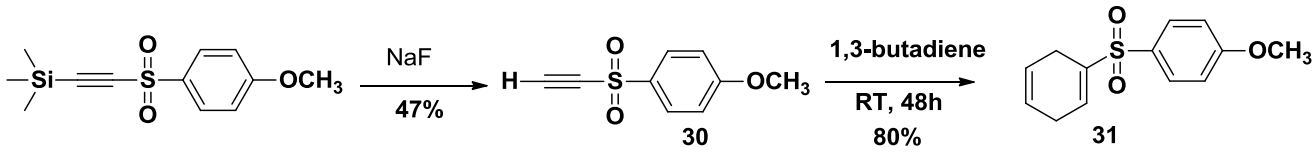

Scheme 4-9: Synthesis of 1-(cyclohexa-1,4-dien-1-ylsulfonyl)-4-methoxybenzene, **29**

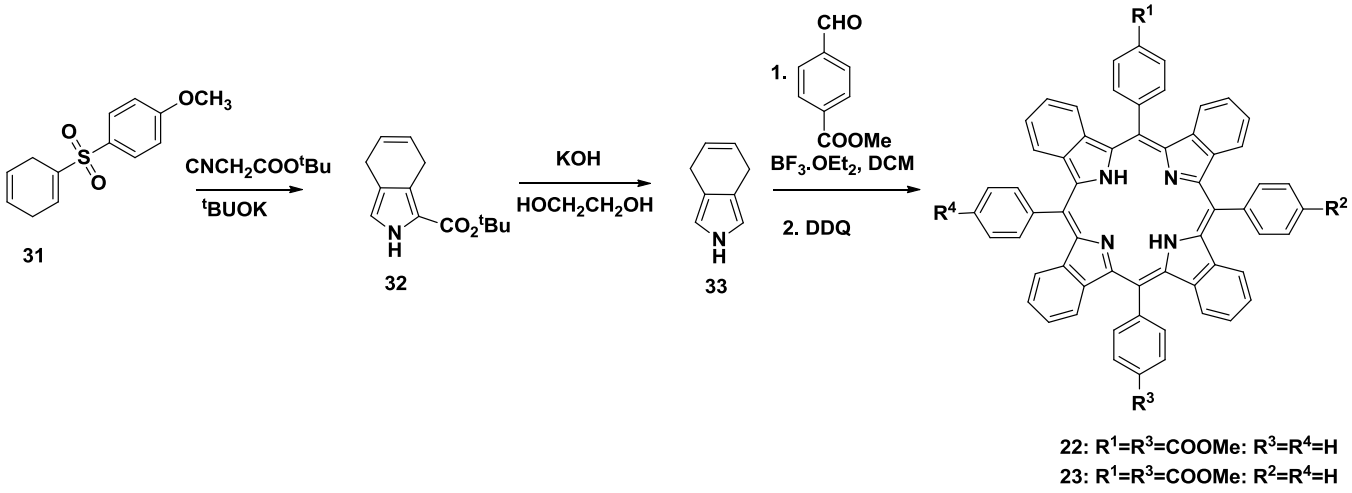

Scheme 4-10: Synthesis of TBPs **22** and **23**.

4.4 Conclusions

Synthesis of the Boc-protected spermine **16** was carried out successfully. Purification of the intermediate steps was easily achieved using silica gel chromatography and the target compound obtained in good yields. In addition, synthesis of the di-substituted TBP isomers **24** and **25** was successfully carried out. Similarly, purification involved silica gel chromatography using differemt EtOAc/Hexane solvent systems for elution. Future work which entails completion of TBP synthesis using the alternative route is currently underway. Furthermore, optimization of reaction conditions to obtain the TBP-spermine conjugates is also underway.

4.5 Experimental

General Procedure

All reactions were monitored by use of thin layer chromatography (TLC) using 0.25mm silica gel plates purchased from Sorbent technologies, with or without UV indicator (60F-254). All column chromatographies were run using silica gel, 32-63μm from Sorbent Technologies. ^{1}H and ^{13}C NMR spectra were obtained either on a DPX-250 or AV-400 Bruker spectrometer. Chemical shifts (δ) are given in ppm relative to $CDCl_3$ (7.26ppm, ^{1}H; 77.2ppm, ^{13}C), or acetone-d_6 (2.05ppm, ^{1}H; 54.0ppm ^{13}C). MALDI-TOF mass spectra were obtained on a Bruker OmniFLEX MALDI-TOF mass spectrometer. ESI-TOF was obtained on Agilent 6210. Reagents and solvents were obtained from either Sigma-Aldrich or Fischer Scientific, and were used without further purification.

Synthesis of Compound 14

Spermine (1.0g, 4.94 mmol) was dissolved in anhydrous THF (40 mL). The solution was then cooled to $0^{o}C$. Boc-ON (3.7g, 14.8 mmol) was dissolved in THF (40 mL) and the solution added

dropwise to the spermine solution, under argon. Et_3N (2.0g, 19.8 mmol) was added in one portion and the reaction mixture stirred for 20h at 0^oC. After 20h the solvent was evaporated under vacuum and the residue dissolved in DCM. The resulting solution was then washed twice with 5% NaOH, and then water. The organic phase was dried over Na_2SO_4, filtered and the product purified by flash chromatography, using 20%$CHCl_3$/Hexane. Yield 2.3g, 92%. ^1H NMR ($CDCl_3$, 400MHz) δ 5.24 (2H, br s), 3.67 (4H, m), 3.12 (4H, m), 2.52 (4H, m), 1.81 (4H, m), 1.58 (4H, m), 1.27 (27H, s). ^{13}C NMR (acetone-d_6, 100MHz) 168.0, 78.5, 77.6, 53.2, 51.7, 46.8, 44.6, 38.8, 37.4, 36.8, 34.2, 26.5, 23.9, 23.5. ESI-TOF calcd for $C_{25}H_{50}N_4O_6$ 502.69, found 503.38.

Synthesis of Compound 15

Boc-protected spermine (2.0g, 3.98 mmol) and N-(4-bromobutyl)phthalimide (1.35g, 4.78 mmol) were dissolved in anhydrous CH_3CN (100 mL) and the reaction mixture put under argon. K_2CO_3 (5.6g, 19.9 mmol) was then added to the reaction mixture in one portion, after which the reaction mixture was refluxed for 24h. The reaction mixture was then allowed to cool to room temperature, followed by solvent removal under vacuum. The solid residue was dissolved in DCM and then washed twice with saturated $NaHCO_3$, then water, and finally dried over Na_2SO_4. The solvent was evaporated under vacuum, after which the product was purified by column chromatography using 20%$CHCl_3$/Hexane to afford 89% yield. ^1H NMR ($CDCl_3$, 400MHz) δ 7.78 (2H, d, J= 3.5Hz), 7.66 (2H, dd, J= 3.5Hz, J= 3.5 Hz), 5.33 (2H, br s), 3.65 (4H, m), 3.38 (2H, t), 3.2 (2H, br s), 3.09 (4H, m), 2.35 (4H, m), 1.83 (4H, m), 1.60 (8H, m), 1.38 (27H, s). ^{13}C NMR (acetone-d_6, 100MHz) 168.0, 155.7, 134.1, 132.3, 122.9, 78.5, 77.5, 58.6, 52.9, 51.5, 46.7, 44.4, 43.9, 37.3, 36.6, 33.2, 27.8, 25.7, 25.4. ESI-TOF calcd for $C_{38}H_{62}N_4O_8$, 703.46, found 704.46.

Synthesis of Compound 16

Compound **15** (1.0g, 1.42 mmol) and hydrazine monohydrate (3.56g, 71.0 mmol) were dissolved in 25 mL of a mixture of THF/MeOH (8:2). The reaction mixture was stirred under a nitrogen atmosphere at 90^{o}C for 5 h, and then at 50^{o}C for 18 h. The reaction mixture was allowed to cool to roon temperature, and the solvent was evaporated under vacuum and the residue dissolved in CH_2Cl_2. The organic phase was washed with 5% aqueous NaOH (3 x 100 mL), H_2O (3 x 100 mL), and finally dried over Na_2SO_4. The solvent was evaporated under vacuum and the product purified by column chromatography on silica gel using 3% NH_4OH/MeOH. Yield 0.39g, 48%%. 1H NMR ($CDCl_3$, 400MHz) δ 5.32 (2H, br s), 5.30 (1H, br s), 3.58 (4H, m), 3.24 (2H, t), 3.18 (2H, br s), 3.04(4H, m), 2.24 (4H, m), 1.80 (4H, m), 1.58 (8H, m), 1.37 (27H, s).

Synthesis of Compound 20 and 21

The mixture of isomers (0.26g, 0.258 mmol) was dissolved in 32 mL anhydrous toluene. DDQ (0.59g, 2.58 mmol) was added to this solution and the resulting mixture refluxed for 30 minutes. The reaction mixture was then allowed to cool to room temperature, and diluted with $CHCl_3$. It was then washed with saturated $NaHCO_3$, water and finally dried over Na_2SO_4. The solvent was removed under vacuum, and the resulting product purified by column chromatography using $CHCl_3$, to afford 0.05g and 0.086g of **20** and **21** respectively.. HRMS m/z calcd for $C_{64}H_{40}CuN_4O_4$ 991.2340, found 991.2325 and 991.2340 respectively.

Synthesis of Compound 22

Compound **20** (0.075g) was dissolved in concentrated H_2SO_4 (5 mL). The solution was allowed to stir at room temperature for 10 minutes. It was then poured in ice/water. The resulting mixture was extracted with $CHCl_3$, dried over Na_2SO_4, and dried under reduced pressure. The final product was purified using flash chromatography using $CHCl_3$ to afford 80% yield. ^{1}H NMR

($CDCl_3$, 400MHz) δ 8.67 (4H, m), 8.47 (6H, m), 8.03 (4H, m), 7.85 (4H, m), 7.45 (8H, m), 7.33 (8H, m), 4.12 (6H, s). 13C NMR 167.5, 136.2, 135.9, 131.6, 131.2, 130.3, 129.5, 129.3, 124.2, 52.0. HRMS m/z calcd for $C_{64}H_{42}N_4O_4$ 931.3279, found 931.3271.

Synthesis of Compound 23

Procedure similar for Compound **22**. Starting with compound **21** (0.086g), Yield 73% ^{1}H NMR ($CDCl_3$, 400MHz) δ 8.59 (4H, m), 8.42 (6H, m), 8.00 (4H, m), 7.90 (4H, m), 7.46 (8H, m), 7.30 (8H, m), 3.90 (6H, s). HRMS m/z calcd for $C_{64}H_{42}N_4O_4$ 931.3279, found 931.3259.

Synthesis of Compound 24

Compound **22** (0.050mg, 0.054 mmol) was dissolved in 8 mL of a mixture of 1:1 2M NaOH/THF. The mixture was refluxed for 4h. It was then allowed to cool to room temperature and 1N HCl used to acidify the reaction mixture to pH 4-5. The precipitate that formed was filtered and washed with water until pH was neutral. Yield 92%. ^{1}H NMR (acetone-d6, 400MHz) δ 10.8 (2H, s), 8.45 (4H, m), 8.03 (6H, m), 7.56 (4H, m), 7.23 (4H, m), 7.18 (8H, m), 7.10 (8H, m). HRMS m/z calcd for $C_{62}H_{38}N_4O_4$ 903.2966, found 903.2970.

Synthesis of Compound 25

Procedure similar Compound **24**. Starting with compound **23** (0.070g, 0.075mmol), Yield 93%. ^{1}H NMR (acetone-d6, 400MHz) δ 10.7 (2H, s), 8.52 (4H, m), 8.05 (6H, m), 7.58 (4H, m), 7.27 (4H, m), 7.22 (8H, m), 7.13 (8H, m). HRMS m/z calcd for $C_{62}H_{38}N_4O_4$ 903.2966, found 903.2961.

Synthesis of Tosylacetylene (30)

p-Tolyl-2-(trimethylsilyl)ethynyl sulfone (0.9g, 3.56 mmol) was dissolved in EtOH (18 mL) and the solution cooled to 0^{o}C. A chilled solution of NaF (0.45g, 10.7 mmol) in 6.75 mL water was then added dropwise to the sulfone solution. The reaction was then allowed to warm to room

temperature. It was allowed to stir for 3h. It was then extracted with hexane to afford the title compound in 47% yield. ^{1}H NMR ($CDCl_3$, 400MHz), δ 7.90 (2H, d, J= 8Hz), 7.40 (2H, d, J= 8Hz), 3.44 (1H, s), 2.48 (3H, s).

Synthesis of 1-(cyclohexa-1,4-dien-1-ylsulfonyl)-4-methoxybenzene (31)

A heavy walled pressure tube was placed in an ice/salt bath, and the temperature maintained at -10^{o}C. 1,3-butadiene (5ml, 59.22 mmol) was the added to the flask. tolylacetylene (0.2g, 1.02 mmol) was then added to the reaction vessel, and the pressure tube sealed tight. The reaction mixture was allowed to warm to room temperature, after which it was allowed to stir for 48h. The reaction vessel was then cooled to -10^{o}C for the excess 1,3-butadiene to condense back to liquid form. It was then evaporated slowly, and the residue purified by column chromatography using 1/10 EtOAc/hexane to afford the title compound in 80% yield. 1H NMR 7.75 (2H, d, J= 8Hz), 7.43 (2H, d, J= 8Hz), 6.99 (1H, s), 5.67 (2H, d, J= 11Hz), 2.95 (2H, s), 2.76 (2H, d, J= 8Hz), 2.42 (3H, s).

4.6 References

1. Kadish, K. M.; Smith, K. M.; Guilard, R., *The porphyrin handbook*. Academic Press: San Diego, 2000.

2. (a) Astruc, D.; Boisselier, E.; Ornelas, C. t., Dendrimers Designed for Functions: From Physical, Photophysical, and Supramolecular Properties to Applications in Sensing, Catalysis, Molecular Electronics, Photonics, and Nanomedicine. *Chem Rev* **2010,** *110* (4), 1857-1959; (b) Drain, C. M.; Varotto, A.; Radivojevic, I., Self-Organized Porphyrinic Materials. *Chem Rev* **2009,** *109* (5), 1630-1658.

3. Leznoff, C. C.; Lever, A. B. P., *Phthalocyanines : properties and applications*. VCH: New York, NY, 1989.

4. McMillin, D. R.; McNett, K. M., Photoprocesses of Copper Complexes That Bind to DNA. *Chem Rev* **1998,** *98* (3), 1201-1220.

5. (a) Soloway, A. H.; Tjarks, W.; Barnum, B. A.; Rong, F.-G.; Barth, R. F.; Codogni, I. M.; Wilson, J. G., The Chemistry of Neutron Capture Therapy. *Chem Rev* **1998,** *98* (4), 1515-1562; (b) Hao, E.; Jensen, T. J.; Courtney, B. H.; Vicente, M. G. H., Synthesis and Cellular Studies of

Porphyrin−Cobaltacarborane Conjugates. *Bioconjugate Chemistry* **2005,** *16* (6), 1495-1502; (c) Sibrian-Vazquez, M.; Nesterova, I. V.; Jensen, T. J.; Vicente, M. G. H., Mitochondria Targeting by Guanidine− and Biguanidine−Porphyrin Photosensitizers. *Bioconjugate Chemistry* **2008,** *19* (3), 705-713.

6. (a) Helberger, J. H., The impact of cupric-l-cyanide on the o-Halogen acetophenone. *Justus Liebigs Annalen Der Chemie* **1937,** *529*, 205-218; (b) Helberger, J. H.; von Rebay, A., The effect of copper-I-cyanide on o-halogenacetophenone II. *Justus Liebigs Annalen Der Chemie* **1937,** *531*, 279-287; (c) Helberger, J. H.; von Rebay, A.; Hever, D. B., The effect of metals on o-cyanacetophenone as well as on 3-methyl phtalimidine, synthesis of tetrabenzoporphin. *Justus Liebigs Annalen Der Chemie* **1938,** *533*, 197-215.

7. Barrett, P. A.; Linstead, R. P.; Rundall, F. G.; Tuey, G. A. P., Phthalocyanines and related compounds - Part XIX Tetrabenzporphin, tetrabenzmonazaporphin and their metallic derivatives. *Journal of the Chemical Society* **1940**, 1079-1092.

8. Vogler, A.; Kunkely, H., Simple Template Synthesis of Zinc Tetrabenzporphyrin. *Angewandte Chemie International Edition in English* **1978,** *17* (10), 760-760.

9. Remy, D. E., A versatile synthesis of tetrabenzporphyrins. *Tetrahedron Letters* **1983,** *24* (14), 1451-1454.

10. (a) Vicente, M. G. H.; Tomé, A. C.; Walter, A.; Cavaleiro, J. S., Synthesis and cycloaddition reactions of pyrrole-fused 3-sulfolenes: a new versatile route to tetrabenzoporphyrins. *Tetrahedron Letters* **1997,** *38* (20), 3639-3642; (b) Ito, S.; Murashima, T.; Ono, N.; Uno, H., A new synthesis of benzoporphyrins using 4,7-dihydro-4,7-ethano-2H-isoindole as a synthon of isoindole. *Chemical Communications* **1998,** (16), 1661-1662; (c) Ichimura, K.; Sakuragi, M.; Morii, H.; Yasuike, M.; Toba, Y.; Fukui, M.; Ohno, O., Formation of tetrabenzoporphine skeleton by the reactions of phthalimide with zinc carbonates. *Inorganica Chimica Acta* **1991,** *186* (1), 95-101.

11. Filatov, M. A.; Cheprakov, A. V.; Beletskaya, I. P., A Facile and Reliable Method for the Synthesis of Tetrabenzoporphyrin from 4,7-Dihydroisoindole. *European Journal of Organic Chemistry* **2007,** *2007* (21), 3468-3475.

12. (a) Mamardashvili, N. Z.; Semeikin, A. S.; Golubchikov, O. A., Synthesis of Tetrakis(4-tert-butylbenzo)porphine and its Metallocomplexes. *Zhurnal Organicheskoi Khimii* **1994,** *30* (5), 770-773; (b) Matsuzawa, Y.; Ichimura, K.; Kudo, K., Preparation of soluble tetrabenzoporphyrins with substituents at the peripheral positions. *Inorganica Chimica Acta* **1998,** *277* (2), 151-156.

13. Vicente, M. G., Porphyrin-based sensitizers in the detection and treatment of cancer: recent progress. *Curr Med Chem Anticancer Agents* **2001,** *1* (2), 175-94.

14. (a) Sol, V.; Lamarche, F.; Enache, M.; Garcia, G.; Granet, R.; Guilloton, M.; Blais, J. C.; Krausz, P., Polyamine conjugates of meso-tritolylporphyrin and protoporphyrin IX: Potential agents for photodynamic therapy of cancers. *Bioorganic & Medicinal Chemistry* **2006,** *14* (5), 1364-1377; (b) Songca, S. P., In-vitro activity and tissue distribution of new fluorinated meso-tetrahydroxyphenylporphyrin photosensitizers. *Journal of Pharmacy and Pharmacology* **2001,** *53* (11), 1469-1475.

15. Weimin, S.; Gen, Z.; Guifu, D.; Yunxiao, Z.; Jin, Z.; Jingchao, T., Synthesis and in vitro PDT activity of miscellaneous porphyrins with amino acid and uracil. *Bioorganic & Medicinal Chemistry* **2008,** *16* (10), 5665-5671.

16. (a) Garcia, G.; Sarrazy, V.; Sol, V.; Morvan, C. L.; Granet, R.; Alves, S.; Krausz, P., DNA photocleavage by porphyrin-polyamine conjugates. *Bioorganic & Medicinal Chemistry* **2009,** *17* (2), 767-776; (b) Chaleix, V.; Sol, V.; Guilloton, M.; Granet, R.; Krausz, P., Efficient synthesis of RGD-containing cyclic peptide-porphyrin conjugates by ring-closing metathesis on solid support. *Tetrahedron Letters* **2004,** *45* (27), 5295-5299.

17. (a) Cullis, P. M.; Green, R. E.; Merson-Davies, L.; Travis, N., Probing the mechanism of transport and compartmentalisation of polyamines in mammalian cells. *Chemistry & Biology* **1999,** *6* (10), 717-729; (b) Hahm, H. A.; Ettinger, D. S.; Bowling, K.; Hoker, B.; Chen, T. L.; Zabelina, Y.; Casero, R. A., Phase I Study of N1,N11-Diethylnorspermine in Patients with Non-Small Cell Lung Cancer. *Clinical Cancer Research* **2002,** *8* (3), 684-690.

18. Casero, R. A.; Woster, P. M., Terminally Alkylated Polyamine Analogues as Chemotherapeutic Agents. *Journal of Medicinal Chemistry* **2000,** *44* (1), 1-26.

19. Igarashi, K.; Ito, K.; Kashiwagi, K., Polyamine uptake systems in Escherichia coli. *Research in Microbiology 152* (3-4), 271-278.

20. (a) Holley, J. L.; Mather, A.; Wheelhouse, R. T.; Cullis, P. M.; Hartley, J. A.; Bingham, J. P.; Cohen, G. M., Targeting of Tumor Cells and DNA by a Chlorambucil-Spermidine Conjugate. *Cancer Research* **1992,** *52* (15), 4190-4195; (b) Ghaneolhosseini, H.; Tjarks, W.; Sjöberg, S., Synthesis of novel boronated acridines- and spermidines as possible agents for BNCT. *Tetrahedron* **1998,** *54* (15), 3877-3884; (c) Papadopoulou, M. V.; Rosenzweig, H. S.; Bloomer, W. D., Synthesis of a novel nitroimidazole-spermidine derivative as a tumor-targeted

hypoxia-selective cytotoxin. *Bioorganic & Medicinal Chemistry Letters* **2004,** *14* (6), 1519-1522.

21. (a) Otten, A.; Namyslo, J. C.; Stoermer, M.; Kaufmann, D. E., 2-(Het)aryl-Substituted 7-Azabicyclo[2.2.1]heptane Systems. *European Journal of Organic Chemistry* **1998,** *1998* (9), 1997-2001; (b) Eisch, J. J.; Shafii, B.; Odom, J. D.; Rheingold, A. L., Bora-aromatic systems. Part 10. Aromatic stabilization of the triarylborirene ring system by tricoordinate boron and facile ring-opening with tetracoordinate boron. *Journal of the American Chemical Society* **1990,** *112* (5), 1847-1853.

22. (a) Back, T. G., The chemistry of acetylenic and allenic sulfones. *Tetrahedron* **2001,** *57* (25), 5263-5301; (b) Chen, Z.; Trudell, M. L., A Simplified Method for the Preparation of Ethynyl P-Tolyl Sulfone and Ethynyl Phenyl Sulfone. *Synthetic Communications: An International Journal for Rapid Communication of Synthetic Organic Chemistry* **1994,** *24* (21), 3149 - 3155.

APPENDIX: PRELIMINARY RESULTS

Preliminary results obtained by Dr. Martha Sibrian-Vasquez

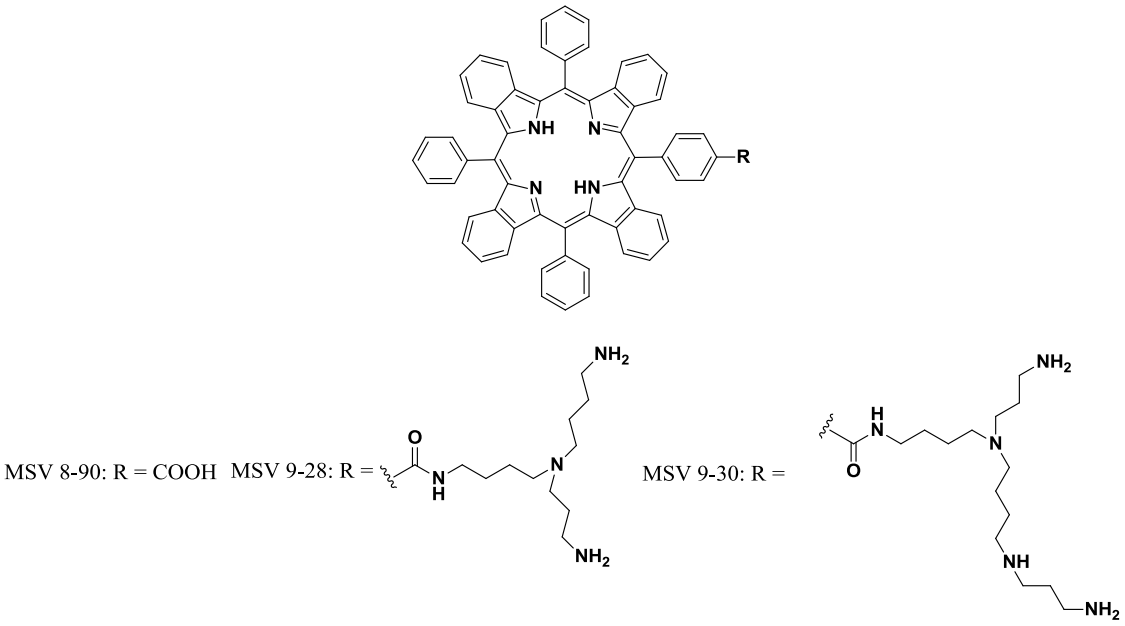

Figure 5-1: Structures of studied TBPs **MSV 8-90**, **MSV 9-28** and **MSV 9-30**

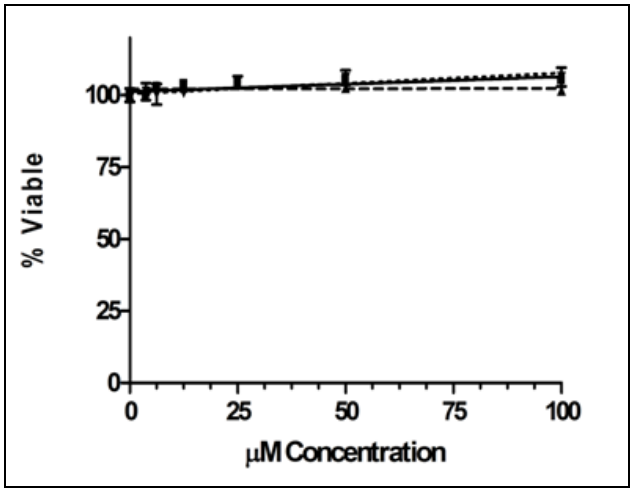

Figure 5-2: Phototoxicities of TBPs **MSV 8-90** (■), **MSV 9-28** (▲) and **MSV 9-30** (▼) toward HEp2 cells using 1 J/cm dose light.

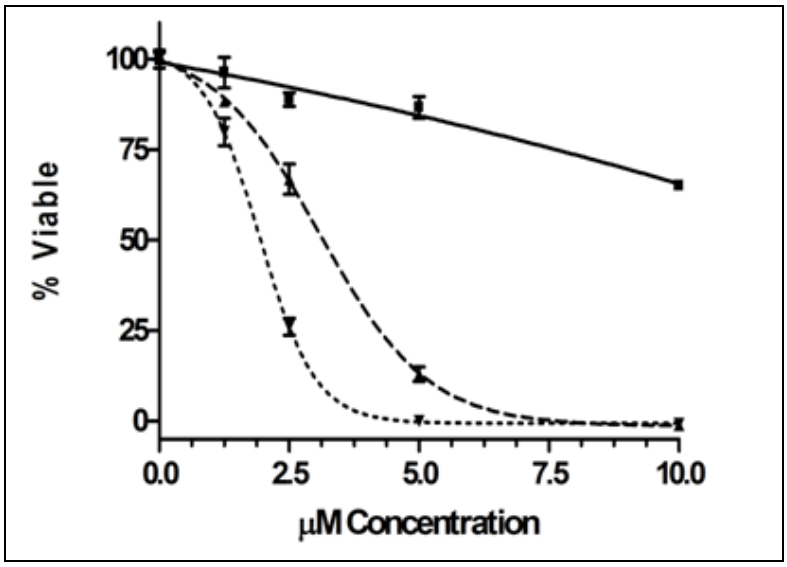

Figure 5-3: Dark Toxicity of TBPs **MSV 8-90** (■), **MSV 9-28** (▲) and **MSV 9-30** (▼) toward HEp2 cells using Titer Blue assay.

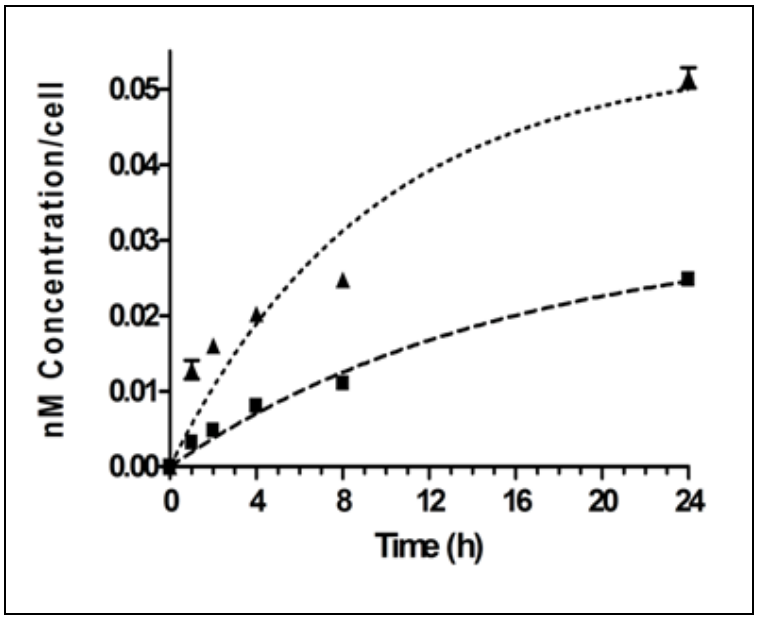

Figure 5-4: Time-dependent uptake for TBPs **MSV09-28** (■) and **MSV 09-30** (▲) at 10μM by HEp2 cells.

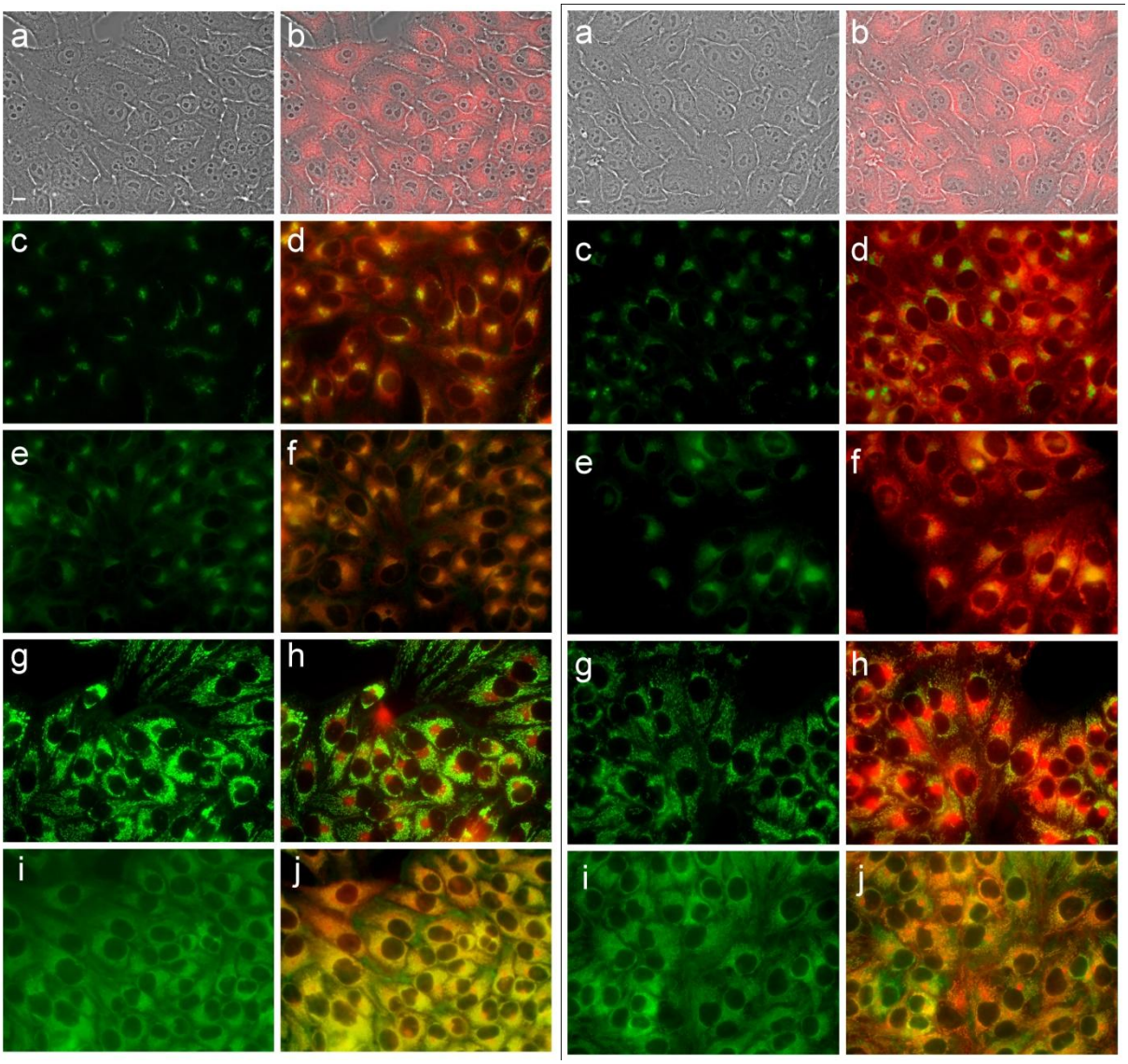

MSV8-90 **MSV 9-28**

Figure 5-5: Subcellular localization of **MSV 8-90** and **MSV 9-28** in HEp2 cells at 10μM for 24 h. (a) Phase contrast, (b) overlay of **MSV 8-90** and **MSV 9-28** and phase contrast, (c) ER-tracker green fluorescence (e) MitoTracker Green Fluorescence (g) LysoSensor Green fluorescence, (i) BODIPY Ceramide fluorescence, (d), (f), (j) overlays of organelle tracers with **MSV 8-90** and **MSV 9-28**. Scale bar: 10 μM.

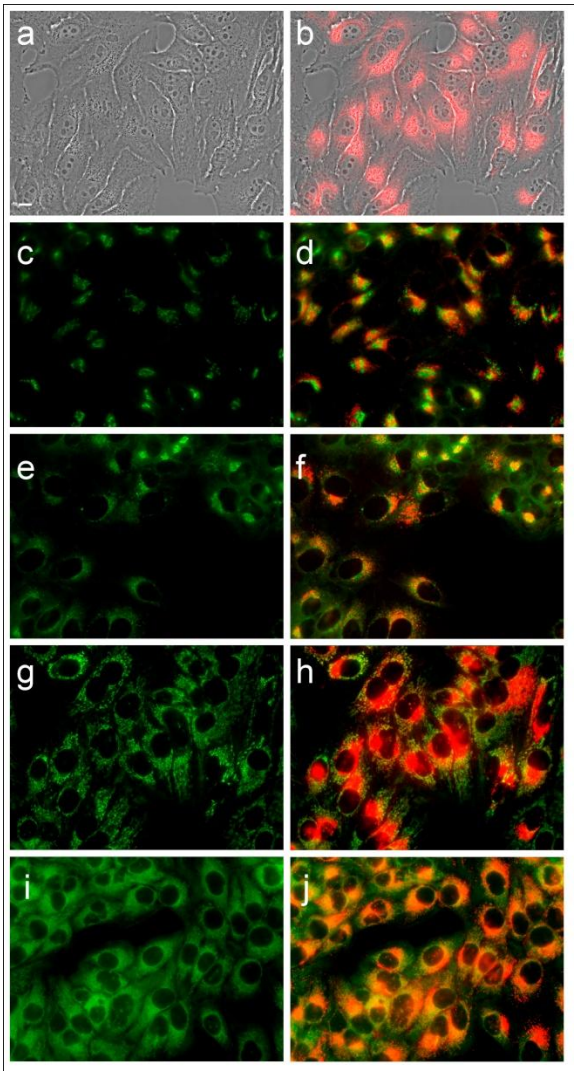

MSV 9-30

Figure 5-6: Subcellular localization of **MSV 9-30** in HEp2 cells at 10μM for 24 h. (a) Phase contrast, (b) overlay of **MSV 9-30** and phase contrast, (c) ER-tracker green fluorescence (e) MitoTracker Green Fluorescence (g) LysoSensor Green fluorescence, (i) BODIPY Ceramide fluorescence, (d), (f), (j) overlays of organelle tracers with **MSV 9-30**. Scale bar: 10 μM.

VITA

Edith Amuhaya was born in Nairobi, Kenya, to Margaret and Solomon Inyama on September 2nd 1980. She graduated from Pangani Girls School in 1998. In September 2000, she enrolled at The University of Nairobi, where she graduated with a Bachelor of Science in Chemistry, on March 11th 2005. In August 2005, she joined the chemistry department at LSU, and later joined Prof. M.Graça H. Vicente's research group to do her research work in porphyrin chemistry. During her free time, Edith loves to cook, read and go for long walks.